Distribution Agreement

In presenting this thesis or dissertation as a partial fulfillment of the requirements for an advanced degree from Emory University, I hereby grant to Emory University and its agents the non-exclusive license to archive, make accessible, and display my thesis or dissertation in whole or in part in all forms of media, now or hereafter known, including display on the world wide web. I understand that I may select some access restrictions as part of the online submission of this thesis or dissertation. I retain all ownership rights to the copyright of the thesis or dissertation. I also retain the right to use in future works (such as articles or books) all or part of this thesis or dissertation.

Signature:

_____ _____

Samantha M. Prezioso Date

Thermoregulation of Two *Pseudomonas aeruginosa* Virulence Factors

By

Samantha M. Prezioso
Doctor of Philosophy

Graduate Division of Biological and Biomedical Science
Microbiology and Molecular Genetics

Joanna B. Goldberg
Advisor

Graeme L. Conn
Committee Member

Charles P. Moran Jr.
Committee Member

William M. Shafer
Committee Member

David S. Weiss
Committee Member

Accepted:

Lisa A. Tedesco, Ph.D.
Dean of the James T. Laney School of Graduate Studies

Date

Thermoregulation of Two *Pseudomonas aeruginosa* Virulence Factors

By

Samantha M. Prezioso
B.S., University of Maryland, 2010

Advisor: Joanna B. Goldberg, Ph.D.

An abstract of
A dissertation submitted to the Faculty of the
James T. Laney School of Graduate Studies of Emory University
in partial fulfillment of the requirements for the degree of
Doctor of Philosophy

Graduate Division of Biological and Biomedical Science
Microbiology and Molecular Genetics

2018

Abstract

Thermoregulation of Two *Pseudomonas aeruginosa* Virulence Factors

By Samantha M. Prezioso

Pseudomonas aeruginosa is a gram-negative environmental bacteria that can, at times, act as an opportunistic pathogen. A strategy utilized by bacteria to ensure appropriate expression of genes is to sense and respond to changes in local temperature. Most research on temperature regulation focuses on the up-regulation or induction of gene expression upon a shift from 22-25°C to 37°C. However, not all virulence factors are regulated in this pattern. An important but understudied aspect of temperature regulation involves virulence factors that are expressed at higher levels at lower temperatures.

The work presented here contributes to filling this gap in knowledge by examining the thermoregulatory mechanisms of two *P. aeruginosa* virulence factors: EftM and PrpL. EftM is a methyltransferase that catalyzes a post-translational modification on elongation factor-tu, which, when it is surface exposed, enhances bacterial adhesion to human epithelial cells. Studies of EftM have revealed two independent layers of thermoregulation for this protein. These independent mechanisms are mRNA transcription initiation and post-translational protein instability, making EftM a dual thermoregulated methyltransferase. PrpL is a secreted protease that releases iron and aids in tissue invasion. This work uncovers that *prpL* mRNA is thermoregulated at the level of transcription initiation, mediated by the *hns*-like MvaT and MvaU. Further, thermoregulation is independent of two other known regulatory mechanisms of *prpL*: quorum sensing and iron dependence.

Ultimately these studies further our knowledge of the mechanisms regulating expression of these two virulence factors, which leads to a more complete understanding of *P. aeruginosa* pathogenesis. Further, this work lays the foundation for uncovering a larger network of genes thermoregulated in this unique pattern.

Thermoregulation of Two *Pseudomonas aeruginosa* Virulence Factors

By

Samantha M. Prezioso
B.S., University of Maryland, 2010

Advisor: Joanna B. Goldberg, Ph.D.

A dissertation submitted to the Faculty of the
James T. Laney School of Graduate Studies of Emory University
in partial fulfillment of the requirements for the degree of
Doctor of Philosophy

Graduate Division of Biological and Biomedical Science
Microbiology and Molecular Genetics

2018

Table of Contents

List of Tables and Figures

Chapter II

Chapter III

Chapter IV

Chapter V

Introduction

Samantha M. Prezioso

Dr. Joanna B. Goldberg, advisor

Pseudomonas aeruginosa is a gram-negative, rod-shaped bacterium that typically occupies soil-based and aquatic niches. However, *P. aeruginosa* is also an opportunistic pathogen and can cause serious and life-threatening infections in immunocompromised patients, such as those with cystic fibrosis[1] or HIV[2], those using catheters[3], and burn patients[4], to name a few. This wide range of occupiable niches[5], coupled with *P. aeruginosa*'s high intrinsic resistance to a large number of antibiotics[6], is cause for concern. In 2013 the U.S. Centers for Disease Control and Prevention (CDC) listed multi-drug resistant *P. aeruginosa* as a top priority with a serious hazard level[7]. In addition to humans, *P. aeruginosa* can cause infections in plants[8], worms and insects[9], and other mammals including livestock[10]. Overall, this opportunistic pathogen is widely adaptable and can be extremely difficult to treat.

P. aeruginosa fulfills certain requirements to be considered an opportunistic pathogen. One such requirement is the ability to group habitable niches into those in which *P. aeruginosa* cause disease, and those in which it does not[11]. As mentioned, *P. aeruginosa* can grow in a wide variety of environments, some of which result in disease (ex. a burn wound) and some of which do not (ex. soil). A second requirement is the expression of virulence factors, defined as components whose loss impairs virulence but not viability[11]. These factors conferring enhanced virulence can be grouped into three main categories: those that assist in invading the host, those causing disease, or those that help evade host defenses[12].

One type of virulence factor assisting in invading the host is proteases. Proteases are enzymes that hydrolyze the peptide bond in peptides or proteins, either within the protein (endopeptidases) or at the amino- or carboxy-terminus of the protein (aminopeptidases and carboxypeptidases)[13]. *Pseudomonas* proteases are considered to be a major virulence factor of the organism[14] and include alkaline protease (AprA), elastase (LasB), large extracellular protease (LepA), and protease IV (Piv). Protease IV was originally named as PvdS-regulated endoprotease, lysyl class[15] (PrpL), and will be referred to as *prpL*/PrpL henceforth. PrpL is a secreted protease that is initially translated as a single 48 kDa polypeptide, but undergoes two rounds of processing to reach its active 26 kDa final form[16]. Based on the amino acid sequence of this protein, it is suggested to be secreted through the type II secretion system. Following transport to the periplasm, the signal peptide at the N-terminus is cleaved to form a 45 kDa protein, with a second independent cleavage event occurring again at the N-terminus to form the mature 26 kDa protein[17] prior to final export to the extracellular space. Interestingly, the cleaved propeptide released from the N-terminus during the second round of periplasmic processing stays associated with the mature PrpL until after extracellular secretion, presumably to inhibit activity while still inside the *P. aeruginosa* cell. This cleaved, yet non-covalently associated propeptide is later degraded by the quorum-sensing regulated protease LasB, which releases PrpL to its active form[18].

Active PrpL cleaves on the carboxy side of substrate lysine residues[19], and this activity is dependent on PrpL's catalytic triad of histidine-72, aspartic

acid-122, and serine-198[17]. This catalysis is responsible for the second cleavage event mentioned above; PrpL self-cleaves after removal of the signal peptide to remove the pro-peptide, taking the enzyme to its final 26 kDa form. This catalysis is not limited to self-processing, however. PrpL activity interrupts the innate immune cascade in the activation of the Toll signaling pathway of the mealworm beetle *Tenebrio molitor*[9]. This results in disruption of Toll signaling without the activation of antimicrobial peptide production, leading to melanization and death of *T. molitor*[9]. PrpL can also degrade fibrinogen, plasminogen, and the complement component C3[19], as well as human pulmonary surfactant protein[20]. Mutants of *prpL* are less virulent in a mouse model of corneal infection[21,22], and in a chronic rat lung infection model (where bacteria are encased in agarose beads), a deletion mutant of *prpL* in PAO1 was found to be significantly less competitive than the wild-type strain[15]. PrpL has also been shown to be important in a *Galleria mellonella* (wax moth) larvae model of *P. aeruginosa* infection through its ability to degrade apolipophorin III[23]. More recently, PrpL purified from strain PA14 was shown to be a strong elicitor of immune responses in *Arabidopsis*[24]. Even more interesting is that the bacterial benefit of PrpL during infection does not appear limited to *Pseudomonas*. In a study investigating *P. aeruginosa* co-infection with *Streptococcus pneumoniae*, another respiratory pathogen, PrpL was found to augment the pathogenicity of *P. pneumoniae* through cooperation with the major *S. pneumoniae* virulence factor pneumolysin (Ply)[25]. Overall PrpL shows a wide range of enzymatic substrates and models in which this virulence factor is important.

A second type of virulence factor categorized as assisting in infection of the host is adhesion factors. Pili are a major adhesin for *P. aeruginosa*; the tail fiber protein, PilA, recognizes glycolipids through interactions with its C-terminal domain[26]. This interaction is important for the establishment of respiratory tract infections, as are interactions of the host epithelial cells with another cell-surface appendage, flagella[27]. Both pili and flagella are adhesins, but also play important roles in a second, distinct function of bacterial motility: these important adhesins are therefore dual-function with a second role in addition to adherence. Similarly, the trimethyl modification of lysine 5 of EF-Tu, a normally cytoplasmic elongation factor with an essential role in translation, can turn EF-Tu into an adhesion to human epithelial cells through molecular mimicry of the ligand to platelet activating factor receptor[28].

The protein catalyzing the lysine 5 post-translational modification of EF-Tu is the *S*-adenosyl-L-methionine (SAM)-dependent methyltransferase EftM[29]. EftM shares homology to Class I methyltransferases[29], the largest of the five (or perhaps nine[30]) known classes of methyltransferases. Class I includes all DNA and some protein methyltransferases. All class I methyltransferases contain a Rossmann-like superfold, but share as little as 10% amino acid similarity[31]. Despite limited homology, all methyltransferases utilize SAM as the methyl donor, generating *S*-adenosyl-L-homocysteine (SAH) from the methyl-depleted SAM. Lysine methyltransferases, such as EftM, transfer the methyl group to the ε-amino group of lysine through an S_N2 reaction[32]. Lysine can be mono-, di-, or tri-methylated by protein methyltransferases; EftM predominantly trimethylates

EF-Tu *in vivo*, with a minority of unmethylated, mono-, and di-methylated species also detectable[29]. When compared to wild-type *P. aeruginosa* strain PAO1, a deletion strain lacking EftM was found to be significantly less virulent in a murine model of infection[28]. Over a 96-hour infection, mice intranasally infected with PAO1 showed significantly higher morbidity than those infected with PAO1Δ*eftM*. Additionally, colony forming units (CFUs) recovered from nasal washes and lung homogenates of mice after 24 hours of infection revealed approximately one log higher recovery from those bacteria with EftM compared to those without[28], pointing to the importance of this enzyme in catalyzing an adhesin-like post-translational modification on EF-Tu.

EF-Tu is an essential, highly abundant elongation factor. This important protein binds aminoacylated transfer RNA (aa-tRNA) and delivers it to the translating ribosome. After delivery to the A site of the translating ribosome, hydrolysis of GTP is triggered. This leads to accommodation of the aa-tRNA into the A site of the ribosome and release of EF-Tu-GDP[33], the rate of which is accelerated by proper codon-anticodon matching. Translation occurs in the cellular cytoplasm. Yet, EF-Tu has been well-documented to have a second functional role on the outer membrane of bacterial cells in multiple different species, including *Lactobacillus johnsonii*[34], *Acinetobacter baumannii*[35], *Mycoplasma pneumoniae*[36], and *Pseudomonas aeruginosa*[37]. In this subcellular location EF-Tu can also be used as an adhesin, an example of a “moonlighting protein”. Moonlighting proteins are defined as those that have a second, autonomous function that is not the result of gene fusions or proteolytic

fragmentation[38]. Several bacteria utilize an abundant cytosolic protein in a second, surface-associated manner, for example, the glycolytic enzyme glyceraldehyde 3-phosphate dehydrogenase (GAPDH) in *E. coli* [39] and the chaperonin GroEL, utilized by *L. johnsonii* in the binding of epithelial cells [40]. While there have been extensive studies characterizing the effects that these proteins promote, it is not yet known how these proteins reach the outer membrane.

To summarize thus far, PrpL and EftM are both virulence factors that aid in establishment of infection. Both target lysine amino acids for their catalytic activity; EftM trimethylates lysine 5 of EF-Tu, while PrpL cleaves on the carboxy-side of lysine residues. In addition, both are in close chromosomal proximity, with the genetic locus for *prpL* at PA4175, and *eftM* three genes downstream at PA4178[41]. One further similarity not yet discussed, though, is that both are thermoregulated, and further, both show unexpected up-regulation at 25°C compared to the human body temperature of 37°C.

Temperature sensing is a strategy utilized by bacteria to gather information as to their location. There are many environmental cues available for monitoring, including pH, nutrient availability, osmotic pressure, and temperature. Sensing and responding to changes in these conditions allows for bacteria to customize or fine-tune the expression of a subset of proteins to maximize their likelihood of success in their new environment. Reasons for this may include avoidance of wasteful expenditure of cellular resources, avoidance of immune molecules, and maximization of colonization factors[42]. Many bacteria are

extremely responsive to temperature as an environmental cue: while *P. aeruginosa* can grow from 4°C to over 42°C[43], it alters transcription of 6.4% of its genome in response from a shift of just 22°C to 37°C[44]. Pathogens do not just undergo changes in temperature between the ambient environment and the core body temperature of humans; even within the human host, there are different temperatures encountered depending on the body site colonized. In a study conducted in a room at an ambient temperature of 25°C, the nasal cavity of human volunteers was measured at 25.3°C +/- 2.1°C, with increases in temperature down to the nasopharynx, measured at 33.9°C +/- 1.5°C[45]. This demonstrates that even within the human host, there is a range of temperatures to encounter. These seemingly subtle differences can impact bacterial gene expression and virulence. The proteome of *Neisseria meningitidis,* for example, changed in the expression of 375 proteins, and the bacteria showed increased aggregation, biofilm formation, and cellular adherence in a shift of 37°C to 32°C, down just five degrees[46].

Given the importance of temperature sensing, there accordingly are many mechanisms and methods by which to accomplish this goal: thermoregulation can occur during transcription, translation, or post-translationally. As a point of distinction, thermoregulation is generally considered distinct from the heat-shock or cold-shock response pathway. Heat-shock proteins (HSPs) are molecular chaperones that are induced as a stress response[47], and is generally considered a discrete reaction to a stressor instead of a general survey in environmental status and adjustment in growth conditions.

Post-translational thermoregulation can be exerted on regulatory proteins such as transcriptional regulators, kinases, and chaperones, or on individual effector proteins directly. Regardless of protein function, temperature can naturally change protein folding and therefore secondary or tertiary structure, leading to changes in function. One such example is the transcriptional regulator TlpA from *Salmonella*. TlpA has an extensive N-terminal coiled-coil dimerization domain which allows for self-dimerization at 25°C and dissociation to monomers at 37°C. This monomerization leads to a loss of DNA-binding capacity[48]. Interestingly, while TlpA was initially thought to regulate virulence, recent evidence has suggested this may not be true[49], and highlights that thermoregulation does not need to be reserved for virulence factors alone.

Translational thermoregulation is most commonly seen through the use of RNA thermometers. At low temperatures, the 5' untranslated region of the mRNA transcript adopts a hairpin structure that traps the Shine-Dalgarno sequence, and thus prevents docking by the ribosome[50]. As temperature elevates, the hairpin unfolds and the ribosome now has access to the mRNA transcript where it can translate the mRNA protein product. One of the best-studied examples of this is the *prfA* transcript in *Listeria monocytogenes*. The thermosensing region of this transcript is 127 nucleotides, forms a hairpin in lower temperatures, and unfolds by 37°C. Once translated, PrfA subsequently acts as a global activator of virulence genes[51]. Another classical example of an RNA thermometer is transcriptional activator protein ToxT from *Vibrio cholerae.* The 5'UTR of the *toxT* mRNA transcript contains a "fourU" element, which as the name suggests, is a

string of four uracils that bind the Shine-Dalgarno sequence at lower temperatures but allow accessibility to ribosomes at human body temperature. In this manner, ToxT is able to limit the downstream production of cholera toxin and toxin-coregulated pilus to human body temperature, and not ambient environmental temperature[52].

Histone-like nucleoid structuring protein (H-NS) is a transcriptional mechanism for virulence factor expression. Originally described as H1a for its similarity to the eukaryotic nuclear structuring histones[53], H-NS is a pleiotropic transcriptional repressor in gram-negative bacteria with many-yet unanswered questions. The N-terminal region of this small protein is the dimerization domain. Amino acids 1-46 are the minimum fragment required for H-NS to self-dimerize[54], an important aspect of its gene-silencing function. The N-terminal domain is separated from the C-terminal domain, the only other domain of this small protein, by a flexible linker[55]. The C-terminal domain is the portion of the protein that recognizes DNA; current work has shown that H-NS tends to bind AT-rich stretches of DNA, typically found around promoters, by utilizing the curvature (not sequence) of AT-stretches for proper docking and silencing of gene expression[56]. At lower concentrations H-NS dimerizes on the AT-rich DNA, while at higher concentrations, multimers of H-NS form[57]. This binding stiffens the DNA, leading it to be less accessible to transcription machinery; binding of H-NS can also, in some cases, cause bridges/ intrastrand loops of DNA[58].

Since DNA curvature is crucial for H-NS recognition, and temperature impacts DNA curvature, temperature can therefore impact the strength of H-NS

binding. In fact, of the 122 genes in *E. coli* transcriptionally up-regulated at 37°C compared to 23°C, 73 (60%) were recognized as being H-NS controlled[59]. In the same study H-NS was also found to contribute to the regulation of 72% of the 297 genes transcriptionally up-regulated in the opposite direction: that is, higher expression at 23°C compared to 37°C[59]. Given that genes regulated by H-NS can either be up-regulated at elevated temperature, up-regulated at lower temperature, or not effected by temperature at all, it appears that the significance of temperature to H-NS activity is multifaceted.

Initially it was believed that H-NS was restricted to *Enterobacteriaceae* and other closely related species[60] until the discovery of "*hns*-like" proteins, widespread amongst gram-negative bacteria[61]. Two such *hns*-like proteins in *P. aeruginosa* are MvaT and MvaU. MvaT was first discovered in *Pseudomonas mevalonii* for its unrelated role as a transcriptional regulator involved in mevalonate metabolism (mevalonate being an organic intermediate on the pathway from acetyl-CoA to isopentenyl pyrophosphate), hence how it received the name MvaT[62]. Despite the identification screen being planned to identify regulatory proteins in response to mevalonite, MvaT was found in this system to be constitutively expressed, bind upstream of the *mvaAB* operon, and co-purify with another peptide (most likely MvaU)[62]. MvaT was also recognized to be important for virulence gene control in *P. aeruginosa*; a transposon mutant in *mvaT* yields altered swarming motility, production of LasB/A proteases, and expression of quorum sensing molecules[63]. Despite not having the "signature" H-NS C-terminus motif, MvaT was then characterized as a *P. aeruginosa* H-NS-like

protein in 2003 though a screen for genomic fragments that complement serine sensitivity in *E. coli*[64], a classic assay to confirm *hns*-like activity of a candidate protein. Inexplicably, the authors chose to perform this screen at 25°C; while unclear, the reason for this unusual choice could be informative regarding the relationship between MvaT and temperature. A more recent study directly investigating this relationship concluded that MvaT nucleoprotein filaments are insensitive to not just salt osmolarity and pH but are also insensitive to temperature[65], in noteworthy contrast to H-NS, which is sensitive to these factors.

While most of the virulence factor thermoregulation described above is to promote protein production at 37°C and minimize expression at lower temperatures, infection physiology is not that simplistic. Thermoregulation of genes in pathogens or opportunistic pathogens can also occur in the opposite direction, with up-regulation at 25°C and down-regulation at 37°C. As a point of distinction, down-regulation at 37°C is not necessarily the same as being repressed at 37°C. There are several reasons for temperature regulation to occur in this fashion.

One such reason is frequently encountered in plant pathogens: not all pathogens infect humans, and as such, other hosts can come with a range of "optimal" temperatures for virulence factor induction. One example of a bacterial virulence factor repressed at elevated temperature is the regulatory protein VirA in *Agrobacterium tumefaciens*[66]. VirA is transmembrane sensor protein that catalyzes a phosphorelay signal to its response regulator VirG. 37°C induces a reversible conformational change in VirA such that it is no longer able to self-

phosphorylate, and therefore cannot transfer the phosphate group to the response regulator. In this way elevated temperature prevents the expression of the *vir* gene and subsequent virulence (as measured by plant tumor formation) from *A. tumefaciens.* Since EftM is also active at 25°C and comparatively inactive at 37°C, EftM may have a yet-unappreciated role in plant pathogenesis. EF-Tu is a pathogen-associated molecular pattern (PAMP) that induces PAMP-triggered immunity in the plant *Arabidopsis*[67]; since only the first 18 amino acids of EF-Tu are necessary for *Arabidopsis* recognition[68], perhaps trimethylation of EF-Tu lysine 5 masks recognition by plants. Preliminary studies utilizing whole-cell transcriptomics failed to recognize EftM as a virulence gene differentially expressed during contact with poplar trees or barley plants when compared to monoculture[69]. However, *eftM* appears to be below the limit of detection of global transcriptomic studies. Further investigation into the possibility of EftM as a plant-associated virulence factor remains yet to be explored.

A second reason for virulence factor down-regulation at 37°C is that even within humans, a variety of temperatures can be encountered depending on body site. As mentioned above, the nasal cavity, a point of entry for respiratory pathogens, is significantly lower than the core body temperature. As such, adhesin factors may be up-regulated at lower body temperatures to correspond with the initiation of infection. A classic example of this is the capsule of *Streptococcus pyogenes.* The *S. pyogenes* capsule is composed of hyaluronic acid, which is identical to the polymer found in human connective tissue. This allows *S. pyogenes* to effectively bind to CD44 on keratinocytes in the

pharyngeal mucosa and skin[70]; after dissemination to the epithelial layer or lower respiratory tract, the role of capsule is diminished and other factors take over[71], thus demonstrating that even within a human host, thermoregulation is important for responding to different sites of infection.

Third, bacterial gene products can be down-regulated upon entry to a human host in an effort to "hide" from the sophisticated immune system of these hosts. The human Toll-like receptor (TLR) family is one such immune component that recognizes conserved elements amongst microorganisms; upon activation, TLRs induce both an innate immune inflammatory response and an adaptive antigen-specific immune response[72]. Flagella are a bacterial component recognized by Toll-like receptor 5[73]. Studies of *Listeria monocytogenes* demonstrate down-regulation of flagellin at 37°C compared to 25°C. This loss of flagella does not lead to a decrease in virulence, but does avoid signaling through TLR5. While *L. monocytogenes* lacking flagella can still elicit an immune response through TLR2 and TLR9, down-regulation of flagella may represent an advantage during infection[74].

Significant effort has been made to elucidate the thermoregulatory benefit and mechanism for EftM. Recently EftM was discovered to be intrinsically thermo-sensitive, meaning it acts as a thermometer by directly sensing temperature and unfolding under the non-permissive condition. Circular dichroism revealed a melting temperature (T_m) of just 37°C for EftM from laboratory strain PAO1, meaning in the ambient environment (~25°C) EftM is folded and catalytically active[29]. However, upon transition to human body

temperature, EftM unfolds and loses catalytic capacity. While cytoplasmic proteins (such as EftM) overall tend to be less thermo-stable than inner-membrane and periplasmic proteins, which are in turn less thermo-stable than outer-membrane proteins[75], a T_m of 37°C for EftM is notably low. In fact, in a study profiling the thermal proteome of *E. coli*, the lowest observed T_m for all 1,738 proteins detected was 48.6°C for GatB[75], a protein involved in galactitol metabolism[76]. Interestingly, chronic clinical isolates of *P. aeruginosa* tend to have slightly higher levels of EftM activity at 37°C compared to acute isolates[77]. The impact of elevated EftM activity during long-term infection remains an intriguing question, and may illuminate the benefit to EftM thermoregulation.

Less is known about the thermoregulation of *prpL.* While thermoregulation was observed in several studies of global transcriptional changes between 22-25°C and 37°C[44,78,79], the mechanism mediating this transcriptional change is yet to be elucidated. Interestingly, the temperature for optimal enzymatic activity of PrpL is 45°C, with lower activity at 37°C and even lower activity still at 25°C[19]. A plausible but untested hypothesis for the biological reason behind *prpL* down-regulation upon a shift from 25°C to 37°C could therefore be to balance increased enzymatic activity at 37°C with lower protein levels.

While the production of virulence factors such as adhesins and proteases are important to establishing infection, it is not enough to simply produce these gene products. The proper timing and strength of expression is paramount to effective utilization of virulence factors, and thermoregulation is an important mechanism by which to accomplish this. While the majority of thermoregulatory

research has been with a focus on virulence factors up-regulated upon a switch from ambient temperature to 37°C, thermoregulation in the opposite fashion is equally important. PrpL and EftM are two important virulence factors in *P. aeruginosa* with many similarities; however, the precise mechanisms underlying their transcriptional thermoregulation remains unknown. Elucidation of these mechanisms may reveal novel global regulators for this important opportunistic pathogen.

The work presented here contributes to filling this gap in knowledge by examining the thermoregulation of two *P. aeruginosa* virulence factors. First, EftM is revealed to have a second distinct mechanism of thermoregulation. In addition to the previously characterized post-translational mechanism mediated through protein instability, *eftM* transcription is shown to be thermoregulated at the point of transcription initiation. Next *prpL* transcriptional thermoregulation is shown to be linked to the *hns*-like regulation of MvaT and MvaU, and is further shown to be transcribed independent from the alternative sigma factor PvdS. Additionally, phenotypic studies of EftM demonstrate no apparent secondary phenotype conferred by EftM, strengthening the importance of EftM in catalyzing a post-translational modification that acts as an adhesin during initial infection. Overall these studies contribute to understanding *Pseudomonas aeruginosa* infection by increasing our knowledge of the mechanisms underlying virulence factor up-regulation at lower temperatures.

1 Bhagirath, A. Y. *et al.* Cystic fibrosis lung environment and Pseudomonas aeruginosa infection. *BMC Pulm Med* **16**, 174, doi:10.1186/s12890-016-0339-5 (2016).

2 Manfredi, R., Nanetti, A., Ferri, M. & Chiodo, F. Pseudomonas spp. complications in patients with HIV disease: an eight-year clinical and microbiological survey. *Eur J Epidemiol* **16**, 111-118 (2000).

3 Cole, S. J., Records, A. R., Orr, M. W., Linden, S. B. & Lee, V. T. Catheter-associated urinary tract infection by Pseudomonas aeruginosa is mediated by exopolysaccharide-independent biofilms. *Infect Immun* **82**, 2048-2058, doi:10.1128/IAI.01652-14 (2014).

4 Yali, G. *et al.* Comparison of pathogens and antibiotic resistance of burn patients in the burn ICU or in the common burn ward. *Burns* **40**, 402-407, doi:10.1016/j.burns.2013.07.010 (2014).

5 Spiers, A. J., Buckling, A. & Rainey, P. B. The causes of Pseudomonas diversity. *Microbiology* **146 (Pt 10)**, 2345-2350, doi:10.1099/00221287-146-10-2345 (2000).

6 Hancock, R. E. & Speert, D. P. Antibiotic resistance in Pseudomonas aeruginosa: mechanisms and impact on treatment. *Drug Resist Updat* **3**, 247-255, doi:10.1054/drup.2000.0152 (2000).

7 Centers for Disease Control and Prevention, O. o. I. D. *Antibiotic Resistance Threats in the United States*, <http://www.cdc.gov/drugresistance/threat-report-2013> (2013).

8 Rahme, L. G. *et al.* Use of model plant hosts to identify Pseudomonas aeruginosa virulence factors. *Proc Natl Acad Sci U S A* **94**, 13245-13250 (1997).

9 Park, S. J. *et al.* Protease IV, a quorum sensing-dependent protease of Pseudomonas aeruginosa modulates insect innate immunity. *Mol Microbiol* **94**, 1298-1314, doi:10.1111/mmi.12830 (2014).

10 Al Bayssari, C., Dabboussi, F., Hamze, M. & Rolain, J. M. Emergence of carbapenemase-producing Pseudomonas aeruginosa and Acinetobacter baumannii in livestock animals in Lebanon. *J Antimicrob Chemother* **70**, 950-951, doi:10.1093/jac/dku469 (2015).

11 Brown, S. P., Cornforth, D. M. & Mideo, N. Evolution of virulence in opportunistic pathogens: generalism, plasticity, and control. *Trends Microbiol* **20**, 336-342, doi:10.1016/j.tim.2012.04.005 (2012).

12 Peterson, J. W. in *Medical Microbiology* (eds th & S. Baron) (1996).

13 Lopez-Otin, C. & Bond, J. S. Proteases: multifunctional enzymes in life and disease. *J Biol Chem* **283**, 30433-30437, doi:10.1074/jbc.R800035200 (2008).

14 Kida, Y. [Roles of Pseudomonas aeruginosa-derived proteases as a virulence factor]. *Nihon Saikingaku Zasshi* **68**, 313-323 (2013).

15 Wilderman, P. J. *et al.* Characterization of an endoprotease (PrpL) encoded by a PvdS-regulated gene in Pseudomonas aeruginosa. *Infect Immun* **69**, 5385-5394 (2001).

16 Traidej, M., Caballero, A. R., Marquart, M. E., Thibodeaux, B. A. & O'Callaghan, R. J. Molecular analysis of Pseudomonas aeruginosa protease IV expressed in Pseudomonas putida. *Invest Ophthalmol Vis Sci* **44**, 190-196 (2003).

17 Traidej, M., Marquart, M. E., Caballero, A. R., Thibodeaux, B. A. & O'Callaghan, R. J. Identification of the active site residues of Pseudomonas aeruginosa protease IV. Importance of enzyme activity in autoprocessing and activation. *J Biol Chem* **278**, 2549-2553, doi:10.1074/jbc.M208973200 (2003).

18 Oh, J., Li, X. H., Kim, S. K. & Lee, J. H. Post-secretional activation of Protease IV by quorum sensing in Pseudomonas aeruginosa. *Sci Rep* **7**, 4416, doi:10.1038/s41598-017-03733-6 (2017).

19 Engel, L. S., Hill, J. M., Caballero, A. R., Green, L. C. & O'Callaghan, R. J. Protease IV, a unique extracellular protease and virulence factor from Pseudomonas aeruginosa. *J Biol Chem* **273**, 16792-16797 (1998).

20 Malloy, J. L., Veldhuizen, R. A., Thibodeaux, B. A., O'Callaghan, R. J. & Wright, J. R. Pseudomonas aeruginosa protease IV degrades surfactant proteins and inhibits surfactant host defense and biophysical functions. *Am J Physiol Lung Cell Mol Physiol* **288**, L409-418, doi:10.1152/ajplung.00322.2004 (2005).

21 O'Callaghan, R. J. *et al.* Pseudomonas keratitis. The role of an uncharacterized exoprotein, protease IV, in corneal virulence. *Invest Ophthalmol Vis Sci* **37**, 534-543 (1996).

22 Engel, L. S. *et al.* Pseudomonas deficient in protease IV has significantly reduced corneal virulence. *Invest Ophthalmol Vis Sci* **38**, 1535-1542 (1997).

23 Andrejko, M., Cytrynska, M. & Jakubowicz, T. Apolipophorin III is a substrate for protease IV from Pseudomonas aeruginosa. *FEMS microbiology letters* **243**, 331-337, doi:10.1016/j.femsle.2004.12.024 (2005).

24 Cheng, Z. *et al.* Pathogen-secreted proteases activate a novel plant immune pathway. *Nature* **521**, 213-216, doi:10.1038/nature14243 (2015).

25 Bradshaw, J. L. *et al.* Pseudomonas aeruginosa Protease IV Exacerbates Pneumococcal Pneumonia and Systemic Disease. *mSphere* **3**, doi:10.1128/mSphere.00212-18 (2018).

26 Irvin, R. T. *et al.* Characterization of the Pseudomonas aeruginosa pilus adhesin: confirmation that the pilin structural protein subunit contains a human epithelial cell-binding domain. *Infect Immun* **57**, 3720-3726 (1989).

27 Feldman, M. *et al.* Role of flagella in pathogenesis of Pseudomonas aeruginosa pulmonary infection. *Infect Immun* **66**, 43-51 (1998).

28 Barbier, M. *et al.* Lysine trimethylation of EF-Tu mimics platelet-activating factor to initiate Pseudomonas aeruginosa pneumonia. *MBio* **4**, e00207-00213, doi:10.1128/mBio.00207-13 (2013).

29 Owings, J. P. *et al.* Pseudomonas aeruginosa EftM Is a Thermoregulated Methyltransferase. *J Biol Chem* **291**, 3280-3290, doi:10.1074/jbc.M115.706853 (2016).

30 Wlodarski, T. *et al.* Comprehensive structural and substrate specificity classification of the Saccharomyces cerevisiae methyltransferome. *PLoS One* **6**, e23168, doi:10.1371/journal.pone.0023168 (2011).

31 Struck, A. W., Thompson, M. L., Wong, L. S. & Micklefield, J. S-adenosyl-methionine-dependent methyltransferases: highly versatile enzymes in biocatalysis, biosynthesis and other biotechnological applications. *Chembiochem* **13**, 2642-2655, doi:10.1002/cbic.201200556 (2012).

32 Helin, K. & Dhanak, D. Chromatin proteins and modifications as drug targets. *Nature* **502**, 480-488, doi:10.1038/nature12751 (2013).

33 Nissen, P., Thirup, S., Kjeldgaard, M. & Nyborg, J. The crystal structure of Cys-tRNACys-EF-Tu-GDPNP reveals general and specific features in the ternary complex and in tRNA. *Structure* **7**, 143-156 (1999).

34 Granato, D. *et al.* Cell surface-associated elongation factor Tu mediates the attachment of Lactobacillus johnsonii NCC533 (La1) to human intestinal cells and mucins. *Infect Immun* **72**, 2160-2169 (2004).

35 Dallo, S. F. *et al.* Association of Acinetobacter baumannii EF-Tu with cell surface, outer membrane vesicles, and fibronectin. *ScientificWorldJournal* **2012**, 128705, doi:10.1100/2012/128705 (2012).

36 Balasubramanian, S., Kannan, T. R. & Baseman, J. B. The surface-exposed carboxyl region of Mycoplasma pneumoniae elongation factor Tu interacts with fibronectin. *Infect Immun* **76**, 3116-3123, doi:10.1128/IAI.00173-08 (2008).

37 Kunert, A. *et al.* Immune evasion of the human pathogen Pseudomonas aeruginosa: elongation factor Tuf is a factor H and plasminogen binding protein. *J Immunol* **179**, 2979-2988 (2007).

38 Wang, G. *et al.* The Roles of Moonlighting Proteins in Bacteria. *Current issues in molecular biology* **16**, 15-22 (2013).

39 Egea, L. *et al.* Role of secreted glyceraldehyde-3-phosphate dehydrogenase in the infection mechanism of enterohemorrhagic and enteropathogenic Escherichia coli: Interaction of the extracellular enzyme with human plasminogen and fibrinogen. *The International Journal of Biochemistry & Cell Biology* **39**, 1190-1203, doi:10.1016/j.biocel.2007.03.008 (2007).

40 Bergonzelli, G. E. *et al.* GroEL of Lactobacillus johnsonii La1 (NCC 533) is cell surface associated: potential role in interactions with the host and the gastric pathogen Helicobacter pylori. *Infection and immunity* **74**, 425-434, doi:10.1128/IAI.74.1.425-434.2006 (2006).

41 Winsor, G. L. *et al.* Enhanced annotations and features for comparing thousands of Pseudomonas genomes in the Pseudomonas genome database. *Nucleic Acids Res* **44**, D646-653, doi:10.1093/nar/gkv1227 (2016).

42 Lam, O., Wheeler, J. & Tang, C. M. Thermal control of virulence factors in bacteria: a hot topic. *Virulence* **5**, 852-862, doi:10.4161/21505594.2014.970949 (2014).

43 Tsuji, A., Kaneko, Y., Takahashi, K., Ogawa, M. & Goto, S. The effects of temperature and pH on the growth of eight enteric and nine glucose non-fermenting species of gram-negative rods. *Microbiol Immunol* **26**, 15-24 (1982).

44 Barbier, M. *et al.* From the environment to the host: re-wiring of the transcriptome of Pseudomonas aeruginosa from 22 degrees C to 37 degrees C. *PLoS One* **9**, e89941, doi:10.1371/journal.pone.0089941 (2014).

45 Keck, T., Leiacker, R., Riechelmann, H. & Rettinger, G. Temperature profile in the nasal cavity. *Laryngoscope* **110**, 651-654, doi:10.1097/00005537-200004000-00021 (2000).

46 Lappann, M. *et al.* Impact of Moderate Temperature Changes on Neisseria meningitidis Adhesion Phenotypes and Proteome. *Infect Immun* **84**, 3484-3495, doi:10.1128/IAI.00584-16 (2016).

47 Feder, M. E. & Hofmann, G. E. Heat-shock proteins, molecular chaperones, and the stress response: evolutionary and ecological physiology. *Annu Rev Physiol* **61**, 243-282, doi:10.1146/annurev.physiol.61.1.243 (1999).

48 Hurme, R., Berndt, K. D., Normark, S. J. & Rhen, M. A proteinaceous gene regulatory thermometer in Salmonella. *Cell* **90**, 55-64 (1997).

49 Gal-Mor, O., Valdez, Y. & Finlay, B. B. The temperature-sensing protein TlpA is repressed by PhoP and dispensable for virulence of Salmonella enterica serovar Typhimurium in mice. *Microbes Infect* **8**, 2154-2162, doi:10.1016/j.micinf.2006.04.015 (2006).

50 Klinkert, B. & Narberhaus, F. Microbial thermosensors. *Cell Mol Life Sci* **66**, 2661-2676, doi:10.1007/s00018-009-0041-3 (2009).

51 Scortti, M., Monzo, H. J., Lacharme-Lora, L., Lewis, D. A. & Vazquez-Boland, J. A. The PrfA virulence regulon. *Microbes Infect* **9**, 1196-1207, doi:10.1016/j.micinf.2007.05.007 (2007).

52 Weber, G. G., Kortmann, J., Narberhaus, F. & Klose, K. E. RNA thermometer controls temperature-dependent virulence factor expression in Vibrio cholerae.

Proc Natl Acad Sci U S A **111**, 14241-14246, doi:10.1073/pnas.1411570111 (2014).

53 Spassky, A., Rimsky, S., Garreau, H. & Buc, H. H1a, an E. coli DNA-binding protein which accumulates in stationary phase, strongly compacts DNA in vitro. *Nucleic Acids Res* **12**, 5321-5340 (1984).

54 Bloch, V. *et al.* The H-NS dimerization domain defines a new fold contributing to DNA recognition. *Nat Struct Biol* **10**, 212-218, doi:10.1038/nsb904 (2003).

55 Tendeng, C. & Bertin, P. N. H-NS in Gram-negative bacteria: a family of multifaceted proteins. *Trends Microbiol* **11**, 511-518 (2003).

56 Dame, R. T., Wyman, C. & Goosen, N. Structural basis for preferential binding of H-NS to curved DNA. *Biochimie* **83**, 231-234 (2001).

57 Badaut, C. *et al.* The degree of oligomerization of the H-NS nucleoid structuring protein is related to specific binding to DNA. *J Biol Chem* **277**, 41657-41666, doi:10.1074/jbc.M206037200 (2002).

58 Will, W. R., Whitham, P. J., Reid, P. J. & Fang, F. C. Modulation of H-NS transcriptional silencing by magnesium. *Nucleic Acids Res* **46**, 5717-5725, doi:10.1093/nar/gky387 (2018).

59 White-Ziegler, C. A. & Davis, T. R. Genome-wide identification of H-NS-controlled, temperature-regulated genes in Escherichia coli K-12. *J Bacteriol* **191**, 1106-1110, doi:10.1128/JB.00599-08 (2009).

60 Atlung, T. & Ingmer, H. H-NS: a modulator of environmentally regulated gene expression. *Mol Microbiol* **24**, 7-17 (1997).

61 Bertin, P. *et al.* H-NS and H-NS-like proteins in Gram-negative bacteria and their multiple role in the regulation of bacterial metabolism. *Biochimie* **83**, 235-241 (2001).

62 Rosenthal, R. S. & Rodwell, V. W. Purification and characterization of the heteromeric transcriptional activator MvaT of the Pseudomonas mevalonii mvaAB operon. *Protein Sci* **7**, 178-184, doi:10.1002/pro.5560070118 (1998).

63 Diggle, S. P., Winzer, K., Lazdunski, A., Williams, P. & Camara, M. Advancing the quorum in Pseudomonas aeruginosa: MvaT and the regulation of N-acylhomoserine lactone production and virulence gene expression. *J Bacteriol* **184**, 2576-2586 (2002).

64 Tendeng, C., Soutourina, O. A., Danchin, A. & Bertin, P. N. MvaT proteins in Pseudomonas spp.: a novel class of H-NS-like proteins. *Microbiology* **149**, 3047-3050, doi:10.1099/mic.0.C0125-0 (2003).

65 Winardhi, R. S. *et al.* Higher order oligomerization is required for H-NS family member MvaT to form gene-silencing nucleoprotein filament. *Nucleic Acids Res* **40**, 8942-8952, doi:10.1093/nar/gks669 (2012).

66 Jin, S., Song, Y. N., Deng, W. Y., Gordon, M. P. & Nester, E. W. The regulatory VirA protein of Agrobacterium tumefaciens does not function at elevated temperatures. *J Bacteriol* **175**, 6830-6835 (1993).

67 Schoonbeek, H. J. *et al.* Arabidopsis EF-Tu receptor enhances bacterial disease resistance in transgenic wheat. *New Phytol* **206**, 606-613, doi:10.1111/nph.13356 (2015).

68 Kunze, G. *et al.* The N terminus of bacterial elongation factor Tu elicits innate immunity in Arabidopsis plants. *Plant Cell* **16**, 3496-3507, doi:10.1105/tpc.104.026765 (2004).

69 Attila, C. *et al.* Pseudomonas aeruginosa PAO1 virulence factors and poplar tree response in the rhizosphere. *Microb Biotechnol* **1**, 17-29, doi:10.1111/j.1751-7915.2007.00002.x (2008).

70 Schrager, H. M., Alberti, S., Cywes, C., Dougherty, G. J. & Wessels, M. R. Hyaluronic acid capsule modulates M protein-mediated adherence and acts as a ligand for attachment of group A Streptococcus to CD44 on human keratinocytes. *J Clin Invest* **101**, 1708-1716, doi:10.1172/JCI2121 (1998).

71 Kang, S. O. *et al.* Thermoregulation of capsule production by Streptococcus pyogenes. *PLoS One* **7**, e37367, doi:10.1371/journal.pone.0037367 (2012).

72 Takeda, K., Kaisho, T. & Akira, S. Toll-like receptors. *Annu Rev Immunol* **21**, 335-376, doi:10.1146/annurev.immunol.21.120601.141126 (2003).

73 Gewirtz, A. T., Navas, T. A., Lyons, S., Godowski, P. J. & Madara, J. L. Cutting edge: bacterial flagellin activates basolaterally expressed TLR5 to induce epithelial proinflammatory gene expression. *J Immunol* **167**, 1882-1885 (2001).

74 Way, S. S. *et al.* Characterization of flagellin expression and its role in Listeria monocytogenes infection and immunity. *Cell Microbiol* **6**, 235-242 (2004).

75 Mateus, A. *et al.* Thermal proteome profiling in bacteria: probing protein state in vivo. *Mol Syst Biol* **14**, e8242, doi:10.15252/msb.20188242 (2018).

76 Nobelmann, B. & Lengeler, J. W. Molecular analysis of the gat genes from Escherichia coli and of their roles in galactitol transport and metabolism. *J Bacteriol* **178**, 6790-6795 (1996).

77 Barbier, M. *et al.* Novel phosphorylcholine-containing protein of Pseudomonas aeruginosa chronic infection isolates interacts with airway epithelial cells. *J Infect Dis* **197**, 465-473, doi:10.1086/525048 (2008).

78 Wurtzel, O. *et al.* The single-nucleotide resolution transcriptome of Pseudomonas aeruginosa grown in body temperature. *PLoS Pathog* **8**, e1002945, doi:10.1371/journal.ppat.1002945 (2012).

79 Termine, E. & Michel, G. P. Transcriptome and secretome analyses of the adaptive response of Pseudomonas aeruginosa to suboptimal growth temperature. *Int Microbiol* **12**, 7-12 (2009).

Elfamycins: Inhibitors of Elongation Factor-Tu

Samantha M. Prezioso[1, 2], Nicole E. Brown[3], Joanna B. Goldberg*[2, 4]

Published in Molecular Microbiology 2017 Oct , doi:10/1111/mmi.13750

[1] Microbiology and Molecular Genetics Program, Graduate Division of Biological and Biomedical Sciences, Emory University School of Medicine, Atlanta, Georgia 30322 USA

[2] Division of Pulmonology, Allergy/Immunology, Cystic Fibrosis and Sleep, Department of Pediatrics, Emory University School of Medicine, Atlanta, Georgia 30322 USA

[3] Department of Pharmacology, Emory University School of Medicine, Atlanta, Georgia 30322, USA

[4] Emory+Children's Center for Cystic Fibrosis and Airway Disease Research, Atlanta, GA 30322, USA

Abstract

Elfamycins are a relatively understudied group of antibiotics that target the essential process of translation through impairment of EF-Tu function. For the most part, the utility of these compounds has been as laboratory tools for the study of EF-Tu and the ribosome, as their poor pharmacokinetic profile and solubility has prevented implementation as therapeutic agents. However, due to the slowing of the antibiotic pipeline and the rapid emergence of resistance to approved antibiotics, this group is being reconsidered. Some researchers are using screens for novel naturally produced variants, while others are making directed, systematic chemical improvements on publically disclosed compounds. As an example of the latter approach, a GE2270 A derivative, LFF571, has completed phase 2 clinical trials, thus demonstrating the potential for elfamycins to become more prominent antibiotics in the future.

Introduction

Translation of mRNA transcripts into proteins is the vital cellular function provided by the ribosome. After initiation, the ribosome relies on the elongation factor-thermo unstable (EF-Tu) to deliver subsequent amino acyl-tRNAs (aa-tRNA) to the A-site of the programmed ribosome in order to elongate the newly synthesized protein. EF-Tu is a G protein, possessing an intrinsic ability to hydrolyze GTP to GDP (GTPase activity) and contributes to the overall fidelity of translation. This hydrolysis occurs during a process termed ‘decoding,’ and provides a level of proofreading between the codon-anticodon pairing of the tRNA and the mRNA transcript.

EF-Tu forms a complex with GTP and an aa-tRNA (Figure 1A). Upon binding the A-site of the ribosome and achieving the appropriate conformation, EF-Tu hydrolyzes

GTP to GDP, loses affinity for the aa-tRNA/ribosome, and dissociates. Antibiotics can disrupt EF-Tu function by either preventing its association with the aa-tRNA or impairing dissociation away from the ribosome after hydrolysis of GTP to GDP – the signal which normally allows EF-Tu to leave and the next round of decoding to proceed.

There are four main families of EF-Tu inhibitors (Figure 1B); the prototypes of these families are kirromycin, enacylocin IIa, pulvomycin, and GE2270 A. These four share little structural similarity, but can be grouped into two main mechanisms of action. Kirromycin and enacyloxin IIa prevent EF-Tu:GDP from dissociating from the ribosome after it's enzymatic activity has been realized, thus trapping EF-Tu on the ribosome and preventing the next round of elongation. Conversely, pulvomycin and GE2270 A inhibit the formation of the EF-Tu:GTP and aa-tRNA ternary complex, thus preventing EF-Tu from associating with the ribosome and performing it's enzymatic activity. These compounds collectively have been given the designation 'elfamycins,' for their ability to target prokaryotic elongation factor Tu (EF-Tu), and are defined by their target, rather than a conserved structure. With development of resistance to other classic antibiotics, interest has renewed in inhibitors of EF-Tu.

EF-Tu GTPase activity

EF-Tu belongs to the G protein family, a collection of GTPase enzymes that bind guanosine nucleotides (GTP and GDP) and possess the intrinsic ability to hydrolyze GTP to GDP. The overall structure of EF-Tu consists of three domains (Figure 1A). Domain 1, or the G domain, is largely responsible for the GTPase activity of EF-Tu [1]. This domain is often called the Ras-like domain due to its similarity to the eukaryotic G protein, Ras [2]. Domains 2 and 3 form anti-parallel beta-barrels that allosterically

regulate the activity of domain 1, including an enhanced affinity for GDP over GTP [1]. Moreover, domain 2 has been shown to enhance the GTPase activity of EF-Tu [3]. Domain 3 can be phosphorylated at Thr-382 by the toxin Doc of bacteriophage P1 toxin-antitoxin system *phd-doc* [4]. This phosphorylation blocks translation elongation, which ultimately leads to cell death. Interestingly, kirromycin has been found to block phosphorylation by Doc, potentially through steric hindrance; this suggests that the P1 toxin/antitoxin system for maintenance of phage in the bacterial chromosome may mimic the effects of bacterial antibiotic kirromycin [5].

GTPases are often described as molecular switches. Binding of GTP renders EF-Tu in an 'on' conformation, while GTP hydrolysis turns EF-Tu 'off.' EF-Tu, like other G proteins, contains a GTPase fold in domain 1 which allows for binding of the guanosine nucleotide [6]. This fold consists of 5 loops, designated G-1 through G-5, that are similar to folds observed in other nucleotide binding proteins [6]. The G-1 loop, also called the P-loop (Figure 1A; orange), is responsible for making contact with the β-phosphate of the guanosine nucleotide [7,8]. Upon GTP hydrolysis, mobile elements called switch regions undergo a conformational change. The G-2 loop corresponds to switch I (Figure 1A; yellow) which participates in binding a magnesium ion important for stabilizing the guanosine nucleotide in the G protein fold [9]. The G-3 loop and following α-helix corresponds to switch II (Figure 1A; blue) which binds the magnesium ion and γ-phosphate of GTP [10].

GTP binding alters the conformation of EF-Tu to increase its affinity for aa-tRNAs [11]. GTP binding induces EF-Tu to become more compact as switch II engages the γ-phosphate of GTP and domain 2 shifts closer to domain 1, as seen in Figure 1A with the

non-hydrolyzable GTP analog GppNHp [12]. As seen in Figure 1A, the movement of switch II causes domain 3 to pack against switch II and opens a cleft between domains 1 and 2 for both the 5'- and 3'-ends of the aa-tRNA to bind [13]. The tRNA acceptor stem contacts the switch regions in domain 1 while the tRNA T stem binds domain 3 [13]. The resulting EF-Tu:GTP:aa-tRNA ternary complex is then able to bind the mRNA programmed ribosome.

Upon forming a complex with the ribosome, the EF-Tu:GTP:aa-tRNA undergoes a conformational change that increases the rate of GTP hydrolysis [14,15]. This conformational change and subsequent increase in GTPase activity is dependent on and preceded by codon-anticodon pairing [16,17]. Upon establishing a codon-anticodon interaction, a domain closure occurs in the 30S ribosomal subunit which alters the tRNA conformation at the acceptor end, disorders switch I, and breaks a hydrophobic gate between Val20 (P-loop) and Ile60 (switch I) to allow GTPase hydrolysis catalyzed by His84 (switch II) (*Escherichia coli* numbering) [18]. His84 is believed to serve as a base to activate the water molecule responsible for nucleophilic attack on the γ-phosphate in the GTP hydrolysis reaction [19]. While free EF-Tu:GTP:aa-tRNA has a slow GTPase rate in the absence of the ribosome [20], upon binding the ribosome and achieving the appropriate conformation, the GTPase rate of EF-Tu is greatly accelerated and contributes to the fidelity of decoding.

Antibiotics targeting EF-Tu

Given the important role of EF-Tu in decoding and translational fidelity, microbial viability can be disrupted by inhibiting EF-Tu activity. In contrast to ribosome-targeting antibiotics such as gentamicin, which induce aberrant protein translation by disrupting

the fidelity of codon-anticodon pairing while still allowing synthesis of the growing peptide chain to progress, elfamycins halt protein synthesis elongation altogether by stalling the progression of the ribosome in the elongation cycle [21,22]. Over 30 antibiotics have been found to bind EF-Tu, the majority of which were discovered in actinomycetes. While these compounds effectively inhibit the activity of bacterial EF-Tu, they show relatively little toxicity against the mitochondrial elongation factor as assessed in a mitochondrial translation system [23]. Kirromycin was shown to be less inhibitory to mitochondrial translation than several representative macrolides [23] and have a 200-fold difference in inhibition when challenged against mitochondrial vs *E. coli* ribosomes [23]. Below the four main classes of EF-Tu antibiotics are discussed; MICs against representative strains are presented in Table 1.

Kirromycin

Kirromycin was discovered to target EF-Tu in 1972 [24]. The soil-dwelling *Streptomyces* family of bacteria are natural producers kirromycin, which was discovered in *Streptomyces collinus* Tü 365 [24] but is also produced in *Streptomyces ramocissimus* [25] (antibiotic originally described as mocimycin; later found to be identical to kirromycin [26]). Additional antibiotics with similar structures to the linear polyketide antibiotic kirromycin (Figure 1B) include aurodox [27] (referred to as X-5108 in early publications), discovered in *Streptomyces goldiniensis* [28]; efrotomycin [27]; phenelfamycin A-C, E, F, discovered in 1988 [29]; and phenelfamycin G and H, discovered in 2011 [30].

Kirromycin has a narrow spectrum against a few Gram-positive bacteria as well as a few Gram-negatives (Table 1) [31]. Kirromycin can interact with EF-Tu in both its GDP and GTP bound form [32], though kirromycin shows higher affinity for EF-Tu:GTP.

As shown in Figure 1C, kirromycin binds the EF-Tu:GDP complex between domain 1 and domain 3, thereby inducing EF-Tu to maintain the conformation it would adopt when GTP is bound [33]. This leaves EF-Tu in a constitutive 'on'-like state, even when bound to GDP, resulting in the ternary complex remaining bound to the ribosome after GTP hydrolysis. Since EF-Tu dissociation does not occur after hydrolysis of GTP, the kirromycin-bound EF-Tu prevents the incoming of subsequent EF-Tu:GTP:aa-tRNA complexes [33], which results in a ribosome 'traffic jam' and cessation of protein synthesis.

Enacyloxin IIa

Enacyloxin IIa is the only EF-Tu antibiotic to be discovered in non-actinomycetes. It is a linear polyenic antibiotic (Figure 1B) produced by *Frateuria* sp. W-315 (previously belonging to the *Gluconobacter* genus). Both this bacterial strain and its antibiotic product were identified and characterized through an antifungal screen in 1982 [34]. While the newly isolated compound was found to be only slightly active against fungi and not active at all against yeast, fortuitously the screen was extended to gram-positive and gram-negative bacteria. There it was found to be active against a wide range of gram-positive and gram-negative bacteria [34] (Table 1). Like kirromycin, enacyloxin IIa inhibits EF-Tu function by preventing dissociation from the ribosome. Structural studies have indicated enacyloxin IIa binds EF-Tu between the domain 1 and domain 3 (Figure 1C) and its binding site overlaps with kirromycin [35]. As seen with kirromycin, enacyloxin IIa binding to the EF-Tu:GDP complex induces a conformation similar to the GTP bound EF-Tu [35] and therefore this conformation prevents EF-Tu:GDP from dissociating from the ribosome [35] resulting in disruption of protein synthesis, yielding a bacteriostatic

mechanism of inhibition [36].

Pulvomycin

Pulvomycin was first discovered in 1957 and is produced by *Streptoverticillium netropsis* and *Streptomyces albosporeus* var. *labilomyceticus* [37]. Pulvomycin is active against some gram-positive and gram-negative bacteria (Table 1), and of particular note, the intrinsically highly antibiotic-resistant opportunistic pathogen *Burkholderia cepacia* [38]. Upon binding EF-Tu, pulvomycin makes contact with all three domains (Figure 1C), binding at the interface of domain 1 and domain 3 and extending to contact domain 2 [39]. Pulvomycin binding locks EF-Tu into its GTP-bound state and prevents association with aa-tRNAs by masking the sites necessary for contact with both the 3' and 5' ends of the aa-tRNA [39], thereby inhibiting protein synthesis.

GE2270 A

GE2270 A, a thiopeptide, was discovered in 1991 as a product from the rare actinomycete genus *Planobispora rosea* ATCC53773 [40]. GE2270 is naturally produced by *P. rosea* in 10 different forms with various methylation states and activities, but GE2270 A is the form with the highest antibacterial activity [41]. GE2270 A is active against a wide range of gram-positive bacteria [40] (Table 1) and demonstrates a similar effect on EF-Tu as pulvomycin, though its binding site and structure differs. As seen in Figure 1C, GE2270 A binds to domain 2 and makes some contact with domain 1 of EF-Tu, disrupting the binding of the aa-tRNA 3' end [39]. Unlike pulvomycin, GE2270 A does not interfere with the interaction of the aa-tRNA 5' end [39]. But like pulvomycin, GE2270 A widens the interface between domain 1 and 2, preventing GTP hydrolysis [39]. Despite having similar mechanistic outcomes, pulvomycin-resistant forms of EF-Tu retain

sensitivity to GE2270 [42].

Production of elfamycins in bacteria

Several peptide antibiotics, such as vancomycin [43] and daptomycin [44], are synthesized nonribosomally, meaning that their synthesis is not dependent on mRNA but rather a series of template-free nonribosomal peptide synthetases (NRPSs) that assemble peptides not directly inscribed in the bacterial genome [45]. Kirromycin, a large linear polyketide, is also non-ribosomally synthesized from a precursor molecule of acetyl-CoA [46]. The biosynthesis gene clusters involved in creating kirromycin from this precursor were first identified in *Streptomyces* as modular polyketide synthases (PKS) and nonribosomal peptide synthetases [47]. Modular polyketide synthases involved in kirromycin production are large, multifunctional enzymes that can catalyze all the steps necessary for production of polyketides, characterizing them as Type I PKSs, while nonribosomal peptide synthetases catalyze regiospecific and stereospecific reactions to assemble peptides. A more detailed study on kirromycin biosynthesis confirmed the genes involved in synthesis by gene disruption and monitoring for loss of antibiotic production by HPLC/MS, as well as radiolabeling precursors for confirmation of biosynthesis enzyme function through monitoring position of the radiolabel in the completed compound [46]. Enacyloxin IIa synthesis is interesting in that *Frateuria* W-315 actually secretes a different form of the compound outside the bacterial cell; enacyloxin IVa is released into the culture fluid, which is then dehydrogenated at C-15 by the enzyme enacyloxin oxidase (ENX oxidase), therefore becoming enacyloxin IIa [48]. GE2270, a thiopeptide, was hypothesized to also be generated in a similar nonribosomal manner but is actually ribosomally originated [49]. A genetic mining strategy

was devised to identify genes involved in the production of the thiopeptide backbone: this was accomplished by designing primers against the predicted nucleotide coding sequence when using the amino acid sequence of the antibiotic as a template. This identified cluster of chromosomally-encoded genes was designated *tpdA-tpdG,* for **t**hio**p**epti**d**e. Ancilliary *tpd* genes encode enzymes required for maturing the precursor peptide, as well as introducing modifications specific to the particular thiopeptide [49]. Most elfamycins, however, are not ribosomally originated as discussed above.

Production of EF-Tu, the target, in bacteria

EF-Tu is the most abundant protein produced in the bacterial cell [12]. Most proteobacteria, such as *E. coli,* encode two copies of the gene for EF-Tu [50]; *tufA* and *tufB* [51,52]. In *Salmonella* and related species, these are widely separated on the chromosome (700 kb on opposite sides of the origin of replication). Both are at the end of operons, are 99% identical at the coding level, and produce near-identical proteins [53] differing only in their carboxy-terminal amino acid. In *E. coli* and *Salmonella,* approximately two-thirds of cellular EF-Tu was shown to be expressed from the *tufA* copy of the gene, while only one-third of total cellular EF-Tu came from *tufB* [54]*.* However, when *tufA* was inactivated, *tufB* expression increased to produce expression equaling two-thirds of the typical amount seen in the cell; this implies that *tufB* could sense and compensate for cellular levels by doubling its normal production [53]. The autoregulatory mechanism of *tufB* was shown to be due to the *tufB* 5'UTR mediating Rho-dependent transcriptional termination in response to rate of translation elongation (as dictated by EF-Tu levels in the cell) [55].

A natural question to ask when bacteria produce antibiotics is how they avoid

self-intoxication. Interestingly, it was discovered in the early 1990s that *S. ramocissimus* (a producer strain for kirromycin) encodes three copies of the *tuf* gene (*tuf1-3;* producing EF-Tu1-EF-Tu3), but only one (*tuf1*) yields the standard EF-Tu protein sequence in appreciable quantities [56]. This standard version is constitutively expressed and is sensitive to kirromycin. In 2007 it was shown that *S. ramocissimus* produces a minor quantity of EF-Tu from *tuf3* in exponential phase, and this version of EF-Tu (65% amino acid homology to *tuf1*) is resistant to kirromycin (as well as pulvomycin and GE2270 A) [57]. While this seemed like a plausible resistance mechanism for circumventing the toxicity associated with producing kirromycin, antibiotic synthesis actually occurs in stationary phase. Therefore, the induction of *tuf3* does not correlate with kirromycin production and further did not respond to kirromycin induction [57], eliminating the possibility of this third EF-Tu copy allowing for compound production without self-intoxication. In addition, antibiotic-sensitive EF-Tu displays dominance in a mixed population of sensitive and resistant EF-Tu, rendering an additional resistant copy ineffective. Thus, while the presence of *tuf3* is an attractive explanation for resistance in the producer strain, the real mechanism has yet to be determined.

In a survey of *P. rosea,* the producer strain for GE2270 A also possessing three copies of EF-Tu, EF-Tu1 was discovered to have accumulated a number of mutations, any combination of which could have lead to the observed resistance of the resulting EF-Tu against GE2270 A [58]. Individual assessment of each mutation in an *E. coli* wild-type EF-Tu background lead to the conclusion that G257S and G275A (*E. coli* numbering) were the only natural mutations in *P. rosea* EF-Tu1 that conferred resistance to GE2270 A by allowing productive interactions of the EF-Tu:GTP:GE2270

A complex with the ribosome [59]. However, the other copies of EF-Tu in the producer strain remain sensitive to the produced antibiotic.

Recent work with enacyloxin in *Frateuria* showed that like kirromycin, the producer strain of this antibiotic does not encode a resistant copy of EF-Tu to avoid self-intoxication. This was demonstrated when EF-Tu purified from *Frateuria* sp. W-315 was inhibited by enacyloxin IIa in a poly(U)-dependent poly(Phe) synthesis assay at similar levels as susceptible EF-Tu, showing that intrinsic resistance in the coding sequence for EF-Tu is not the mechanism utilized by *Frateuria* sp. W-315 to avoid self-intoxication [60]. The mechanism by which *Frateuria* is therefore resistant to the enacyloxin it produces remains an intriguing question. As mentioned above, enacyloxin IVa is secreted from the cell and is processed extracellularly to its final form of enacyloxin IIa. This precursor secretion may therefore be the mechanism by which *Frateuria* sp. W-315 avoids inhibiting its own EF-Tu. Similarly, the actinomyces WAC5292 was reported to possess an ABC transporter, FacT, which protects the producer from self-intoxication from the kirromycin-like antibiotic factumycin rather than a mechanism of EF-Tu alteration [61].

Elfamycin resistance

Of major concern to any clinically implemented antibiotic is bacterial resistance. Studies examining the generation of elfamycin-resistant forms of EF-Tu in bacterial populations are complicated by the fact that *E. coli,* and most other proteobacteria [50], contain two virtually identical copies encoding for EF-Tu as stated above. It was recognized that in some species, such as *Salmonella,* either copy (but not both) is dispensable for cell viability [53]. However, it took another ten years of research before it was accepted that either copy is dispensable in *E. coli* as well [62].

Inactivating one copy of the gene encoding EF-Tu enabled researchers to more easily identify EF-Tu mutants that conferred elfamycin resistance, as inactivating one copy of the *tuf* genes allows for a homogenous pool of mutant EF-Tu proteins in the cell, all coded by the one remaining copy of *tuf*. If the population were to be mixed, the wild-type copy of the protein (that which is sensitive to the effect of the antibiotic) would be dominant when challenged with kirromycin or enacyloxin IIa (i.e. trapped on the ribosome, and physically blocking the resistant copy from performing it's enzymatic role). Earlier techniques, such as that developed by Zeef and Bosch in 1993 [63], circumvented this problem by inactivating *tufB* in *E. coli* using Mu phage insertion, then mutagenizing *tufA* before using a recombinant phage M13mp to deliver the mutagenized *tufA* to the chromosome. Resistant mutants were subsequently isolated and identified. Together these efforts identified several mutational 'hot spots' in the single copy of EF-Tu that are responsible for kirromycin resistance. The strategy of inactivating one copy of *tuf* allowed a rush of studies identifying EF-Tu amino acid substitutions that conferred resistance to this understudied group of compounds. These studies, done in the late 1990s, are cited in modern reviews as tables of resistance mutations in EF-Tu; an example being Olsthoorn-Tieleman's [57] reporting of Abdulkarim's [64] findings of mutations causing resistance to kirromycin. However, this citation and others fail to mention the caveat that the original studies identifying these mutations were done in strains that contained one inactivated copy of EF-Tu [14,64]. Overall, resistance is easy to generate in a laboratory with a sensitized background strain (single *tuf* gene) and reveals valuable information as to binding mechanisms of elfamycins, but the emergence of resistance in a natural environment against a bacterial

strain with two (or three) copies of the *tuf* genes has not sufficiently been addressed.

In contrast to the sensitive-dominant nature of mixed EF-Tu populations against kirromycin: when a bacterial culture is challenged with GE2270 A, a mixed population of susceptible and resistant EF-Tu is resistant-dominant. This antibiotic prevents ternary complex formation, instead of trapping an existing complex, meaning that the resistant form of EF-Tu is still able to access free ribosomes [58]. Although pulvomycin also prevents ternary complex formation, resistance to pulvomycin and GE2270 A do not appear to be interchangeable [42,58].

In addition to the complication of multiple gene copies of EF-Tu, compound permeability issues further obfuscate the question of bacterial resistance to the elfamycins. Several groups posit that the narrow spectrum of action of elfamycins is based on permeability barriers to some cells [42], whereas others counter that EF-Tu itself is resistant [65,66] and that there are no permeability barriers. Either way, the poor pharmacokinetics of compounds such as GE2270 have been stated to ultimately render these drugs unsuitable for clinical use [67,68], but have not prevented them from being useful as laboratory tools in crystallography and EF-Tu function studies (see below).

Interestingly, the mechanism of streptomycin resistance gave a hint as to a second mechanism by which a cell could naturally acquire kirromycin resistance. Mutations in *rpsL* (ribosome small subunit, protein S12) confer high-level resistance to the aminoglycoside streptomycin. Similarly, the same *rpsL*500 allele (R53L; *E. coli* numbering) conferring resistance to streptomycin was shown to bypass the dominant effect of sensitive EF-Tu in a bacterium where one *tuf* copy is resistant and the other is sensitive [69]. This is accomplished by the mutant S12 protein preferentially interacting

with the resistant copy of EF-Tu, thus saturating ribosomal complexes with a resistant form of EF-Tu through exclusion of the sensitive version of the protein. While this mechanism of resistance only requires one copy of *tuf* to be mutated, not both, there is still a second mutation necessary in a separate gene (*rpsL)*, and thus it is still necessary for the cell to acquire mutations in two separate gene loci. As shown for other antibiotics, such as the quinolones [70], it is achievable for a cell to acquire several mutations to enable resistance. While it is therefore feasible for natural elfamycin resistance to develop, multiple protein mutations need to occur in combination to acquire resistance, potentially making elfamycins clinically preferential to a class of antibiotics that only requires a single mutation to achieve resistance.

Utility of elfamycins in the study of ribosomal function

Elfamycins have proved to be useful laboratory reagents, allowing for significant advances in several areas of ribosomal biology. Cryo-electron microscopy is a powerful tool for solving ribosome structure, and kirromycin has been used to trap EF-Tu [71] and aa-tRNA [72] in action, allowing for uniform particles that can be analyzed by single-particle reconstruction for determination of structure. These have provided insights into EF-Tu GTPase activity and subsequent EF-Tu dissociation from the ternary complex, two events critical for tRNA accommodation into the peptidyl transferase center of the ribosome [73-75]. Recently kirromycin was used to help achieve an improved high-resolution cryo-electron microscopy structure of the 70S ribosome complex [76]. The antibiotic stalled the ternary complex EF-Tu:GDP:Phe-tRNA^{Phe} on the 70S ribosome which, when analyzed by aberration-corrected and computational sorting analysis, then yielded a model of high enough resolution for the visualization of all 35 rRNA

modifications (i.e. base methylation, ribose methylation, pseudouridylation) for the first time [76]. This accurate visualization of modifications as small as a single methyl group provides valuable information. For example, single modifications can impact antibiotic sensitivity: loss of methylation of ribosomal rRNA base A2503 (*E. coli* numbering) contributes to resistance against the broad-spectrum gram-positive pathogen antibiotic linezolid. A high-resolution structure allows for mechanistic determination of the effect of this loss, and revealed that an absence of methylation at this rRNA base destabilized the stacking interaction with A2059, subsequently disrupting the binding site for the antibiotic.

Kirromycin's ability to trap aa-tRNAs on the ribosome also contributed to a surprising discovery about transfer-messenger RNAs (tmRNAs; dual-function RNA that helps stalled ribosomes) [77]. When kirromycin was added to Phe-tRNA^{Phe} on the translating ribosome, peptidyl transfer rate was inhibited 1000-fold, as to be expected. However, when tmRNA and its accessory protein SmpB replaced the charged tRNA, rate of peptidyl transfer was only inhibited 40-fold, meaning peptide transfer to tmRNA is relatively resistant to kirromycin when compared to canonical tRNAs. This suggests that the tmRNA-SmpB complex is released from EF-Tu more easily than canonical tRNAs, presumably when in its GTP-bound confirmation, not the GDP confirmation typically seen when tRNA is released from EF-Tu. Since kirromycin blocks the conformational change accompanying GTP hydrolysis, using kirromycin to show that peptidyl transfer is relatively unaffected in the presence of the compound was a useful laboratory tool that helped show that the conformational change in EF-Tu accompanying GTP hydrolysis may not be important in tmRNA's mechanism of action [77].

As stated previously, pulvomycin can stabilize the EF-Tu:EF-Ts complex; it naturally follows that this elfamycin has played a role in studying the mechanism of the guanine exchange catalyzed during their interaction. A series of five x-ray crystallographic structures were determined for intermediate complexes in this exchange, which allowed for a schematic representation to be built, detailing the guanine nucleotide exchange reaction [78]. Crystals of EF-Tu:EF-Ts complexed with a GppNHp, a nonhydrolyzable analog of GTP (EF-Tu:GppNHp:EF-Ts), were of significantly higher resolution when formed in the presence of pulvomycin than those formed without. In addition, pulvomycin allowed for the intermediate complex just prior to the release of EF-Ts to be solved. Pulvomycin prevents the movement of EF-Tu domain 1, thus trapping EF-Tu:Mg^{2+}:GTP with EF-Ts for formation of crystals [78]. These examples illustrate some of the multiple uses of pulvomycin during crystallographic studies of the EF-Tu cycle. Elfamycins are useful tools for the study of cell physiology beyond just translation, as well. Kirromycin, for example, was used in a study of the interaction between EF-Tu and MreB, a protein that impacts cell shape [79]; this study determined that EF-Tu also impacts cell shape, with kirromycin being used to determine that EF-Tu activity in translation is independent from colocalization activity with MreB. Thus, elfamycins are not only useful in the context of new antibiotics for clinical treatment, but also as laboratory tools allowing for advancement in studies of the ribosome, translation, and cell physiology.

Modern resurgence and future outlook

The efficacy of many antibiotics in clinical use are challenged by the rapid spread of antibiotic resistance alleles between strains and prevalence of multi-drug resistant

strains in the community; elfamycins do not currently have resistance determinants in widespread circulation between bacterial populations, making them an attractive option for a revival in research and development towards clinical implementation. Interest seems to be largely abandoned since the peak in studies in the late 1990s; perhaps the spectrum of activity was deemed too narrow to be of widespread use in combating infection, or perhaps due to problems with poor compound solubility [80] and pharmacokinetics [67]. However, the antibiotic pipeline has steadily slowed down in recent years [81]. Second-generation derivatives offer an opportunity to improve on the natural compounds, such as was done with second and third generation β-lactams, second through fifth generation cephalosporins, and second through fourth generation quinolones. In addition, no current clinically used drugs target EF-Tu, which reduces the risk of pre-existing cross-resistance to any newly deployed elfamycin.

Several groups have fortunately taken the initiative on improving elfamycins. One method for improvement over current options is to screen nature for effective compounds already in existence in the microbial world. In 2011, two novel, naturally produced derivatives of previously-known elfamycins [30] were identified from microbes in Malaysia. These new compounds were designated phenelfamycin G and H, and differ from those previously described by the presence of a hydroxyl group at C-30. However, these compounds were demonstrated to have a very narrow range of activity; namely, only against *Propionibacterium acnes*. While this limits the potential for treatment of clinically significant pathogens, it does represent an opportunity to treat cosmetic or chronic acne without disruption of the gut microflora. Another group, in 2012, rediscovered factumycin from serpentine soil in Santa Clara hills, Cuba [61]. This

previously known elfamycin, similar to kirromycin, was newly found to be produced by the actinomycete strain WAC5292 and was demonstrated to have activity against the human pathogen *Acinetobacter baumannii*. Most interesting about this compound is the finding that multidrug resistant strains of *A. baumannii* were actually more susceptible to factumycin than non-multidrug resistant strains, and that factumycin could be used in combination with certain other antibiotics (ex. penicillin G, daptomycin) to further increase activity against multi-drug resistant strains [61] when tested *in vitro*.

Work is also being undertaken on improving the quality of these antibiotics through rational design. One group has exacted synthetic modifications on GE2270 A in 2015 which resulted in an improved derivative named NAI003 [82]. This compound has also been demonstrated to have strong activity against *P. acnes*, again without targeting other commensal bacteria; targeted antibiotics which leave the microbiome unaltered appear to be a bigger health benefit than previously thought [83], making these modifications attractive from a clinical standpoint. Another group has combined the head moiety from enacyloxin IIa with the tail of kirromycin, and thus increased the binding affinity for EF-Tu of the resulting enacyloxin IIa derivative [35]. The pharmaceutical company Novartis has designed and synthesized 4-aminothiazolyl analogs of GE2270 A [84]. They have added functional groups that increase compound solubility while simultaneously facilitating passage through the bacterial membrane; the resulting antibiotic was named LFF571. These efforts increased solubility from barely measurable, to >10 mg/mL. These modifications were further demonstrated to increase clinical relevance by being tested in a hamster model of *Clostridium difficile* infection. The successful protection of hamsters from *C. difficile* for 21 days represents a

promising route of treatment of infection in humans. Currently, LFF571 has completed Phase 2 clinical trials [85]. This multi-center trial (ClinicalTrials.gov identifier: NCT01232595) examined LFF571 against primary episodes or first reoccurrences of moderate *C. difficile* infections by randomly assigning patients to 125 mg vancomycin or 200 mg LFF571 four times daily for a total of 10 days. 90.6% of the LFF571-treated patients achieved a clinical cure to infection, whereas 78.3% of the vancomycin-treated patients reached clinical cure. Tolerances to the antibiotics were generally similar, as was rate of relapse in infection [85]; this represents a large step forward in bringing an elfamycin to the clinic.

An interesting follow-up study with LFF571 examined *C. difficile* toxin production at sub-inhibitory concentrations of antibiotic. Sub-inhibitory concentrations are known to change transcription activity, with some responses being: increased virulence factor production, decreased carbon catabolism, and an increase in prophage gene expression [86]. Of concern is reports that subinhibitory concentrations of vancomycin and metronidazole can actually increase *C. difficile* toxin production when grown in culture [87]. In contrast, LFF571 was shown to decrease toxin expression; it was hypothesized that this was due to LFF571's effects on inhibiting protein translation, which would be consistent with the effects of several other translation-inhibiting compounds [88]. Overall, LFF571 and NAI003, and the approach taken to arrive at these compounds, are promising for the implementation of the elfamycin family as a new group of antibiotics in an era where options are rapidly being depleted.

Concluding statement

Elfamycins are an interesting and underappreciated group of antibiotics that target a clinically unprecedented protein, the essential translation factor EF-Tu. Most bacteria have multiple copies of the gene encoding EF-Tu, and sensitive forms of the protein are typically dominant over resistant forms, making elfamycins attractive antibiotics in an era when the numbers of clinical options available are rapidly declining. With a renewed effort in increasing compound solubility and permeability, several clinical trials are already underway to begin to utilize these antibiotics in a manner beyond just the laboratory and into the clinic for the treatment of patients.

Acknowledgements

SMP was supported in part by a training grant from the National Institute of Allergy And Infectious Diseases of the NIH to Emory University (T32AI106699, Antimicrobial Resistance and Therapeutic Discovery Training Program). Molecular graphics and analyses were performed with the UCSF Chimera package. Chimera is developed by the Resource for Biocomputing, Visualization, and Informatics at the University of California, San Francisco (supported by NIGMS P41-GM103311).

We would like to thank Dr. William Shafer and Dr. Eryn Bernardy for review and critical comments of the manuscript.

References

1 Parmeggiani, A. *et al.* Properties of a genetically engineered G domain of elongation factor Tu. *Proc Natl Acad Sci U S A* **84**, 3141-3145 (1987).

2 Jurnak, F. Structure of the GDP domain of EF-Tu and location of the amino acids homologous to ras oncogene proteins. *Science* **230**, 32-36 (1985).

3 Nock, S. *et al.* Properties of isolated domains of the elongation factor Tu from Thermus thermophilus HB8. *Eur J Biochem* **234**, 132-139 (1995).

4 Castro-Roa, D. *et al.* The Fic protein Doc uses an inverted substrate to phosphorylate and inactivate EF-Tu. *Nat Chem Biol* **9**, 811-817, doi:10.1038/nchembio.1364 (2013).

5 Cruz, J. W. *et al.* Doc toxin is a kinase that inactivates elongation factor Tu. *J Biol Chem* **289**, 7788-7798, doi:10.1074/jbc.M113.544429 (2014).

6 Sprang, S. R. G protein mechanisms: insights from structural analysis. *Annual review of biochemistry* **66**, 639-678, doi:10.1146/annurev.biochem.66.1.639 (1997).

7 Kjeldgaard, M., Nyborg, J. & Clark, B. F. The GTP binding motif: variations on a theme. *FASEB journal : official publication of the Federation of American Societies for Experimental Biology* **10**, 1347-1368 (1996).

8 Dahl, L. D., Wieden, H. J., Rodnina, M. V. & Knudsen, C. R. The importance of P-loop and domain movements in EF-Tu for guanine nucleotide exchange. *J Biol Chem* **281**, 21139-21146, doi:10.1074/jbc.M602068200 (2006).

9 Abel, K., Yoder, M. D., Hilgenfeld, R. & Jurnak, F. An alpha to beta conformational switch in EF-Tu. *Structure* **4**, 1153-1159 (1996).

10 Knudsen, C., Wieden, H. J. & Rodnina, M. V. The importance of structural transitions of the switch II region for the functions of elongation factor Tu on the ribosome. *J Biol Chem* **276**, 22183-22190, doi:10.1074/jbc.M102186200 (2001).

11 Louie, A. & Jurnak, F. Kinetic studies of Escherichia coli elongation factor Tu-guanosine 5'-triphosphate-aminoacyl-tRNA complexes. *Biochemistry* **24**, 6433-6439 (1985).

12 Kavaliauskas, D., Nissen, P. & Knudsen, C. R. The busiest of all ribosomal assistants: elongation factor Tu. *Biochemistry* **51**, 2642-2651, doi:10.1021/bi300077s (2012).

13 Nissen, P. *et al.* Crystal structure of the ternary complex of Phe-tRNAPhe, EF-Tu, and a GTP analog. *Science* **270**, 1464-1472 (1995).

14 Mesters, J. R., Potapov, A. P., de Graaf, J. M. & Kraal, B. Synergism between the GTPase activities of EF-Tu.GTP and EF-G.GTP on empty ribosomes. Elongation factors as stimulators of the ribosomal oscillation between two conformations. *Journal of molecular biology* **242**, 644-654, doi:10.1006/jmbi.1994.1614 (1994).

15 Pape, T., Wintermeyer, W. & Rodnina, M. V. Complete kinetic mechanism of elongation factor Tu-dependent binding of aminoacyl-tRNA to the A site of the E. coli ribosome. *The EMBO journal* **17**, 7490-7497, doi:10.1093/emboj/17.24.7490 (1998).

16 Rodnina, M. V., Fricke, R., Kuhn, L. & Wintermeyer, W. Codon-dependent conformational change of elongation factor Tu preceding GTP hydrolysis on the ribosome. *The EMBO journal* **14**, 2613-2619 (1995).

17 Blanchard, S. C., Gonzalez, R. L., Kim, H. D., Chu, S. & Puglisi, J. D. tRNA selection and kinetic proofreading in translation. *Nature structural & molecular biology* **11**, 1008-1014, doi:10.1038/nsmb831 (2004).

18 Schmeing, T. M. *et al.* The crystal structure of the ribosome bound to EF-Tu and aminoacyl-tRNA. *Science* **326**, 688-694, doi:10.1126/science.1179700 (2009).

19 Daviter, T., Wieden, H. J. & Rodnina, M. V. Essential role of histidine 84 in elongation factor Tu for the chemical step of GTP hydrolysis on the ribosome. *Journal of molecular biology* **332**, 689-699 (2003).

20 Gromadski, K. B. & Rodnina, M. V. Kinetic determinants of high-fidelity tRNA discrimination on the ribosome. *Molecular cell* **13**, 191-200 (2004).

21 Wolf, H., Zahner, H. & Nierhaus, K. Kirromycin, an inhibitor of the 30 S ribosomal subunits function. *FEBS letters* **21**, 347-350 (1972).

22 Cetin, R. *et al.* Enacyloxin IIa, an inhibitor of protein biosynthesis that acts on elongation factor Tu and the ribosome. *The EMBO journal* **15**, 2604-2611 (1996).

23 Zhang, L. *et al.* Antibiotic susceptibility of mammalian mitochondrial translation. *FEBS letters* **579**, 6423-6427, doi:10.1016/j.febslet.2005.09.103 (2005).

24 Wolf, H. & Zahner, H. [Metabolic products of microorganisms. 99. Kirromycin]. *Archiv fur Mikrobiologie* **83**, 147-154 (1972).

25 Tieleman, L. N., van Wezel, G. P., Bibb, M. J. & Kraal, B. Growth phase-dependent transcription of the *Streptomyces ramocissimus* tuf1 gene occurs from two promoters. *Journal of bacteriology* **179**, 3619-3624 (1997).

26 Maehr, H., Leach, M., Yarmchuk, L. & Stempel, A. Antibiotic X-5108. V. Structures of antibiotic X-5108 and mocimycin. *J Am Chem Soc* **95**, 8449-8450 (1973).

27 Dolle, R. E. & Nicolaou, K. C. Total Synthesis of Elfamycins - Aurodox and Efrotomycin .1. Strategy and Construction of Key Intermediates. *Journal of the American Chemical Society* **107**, 1691-1694, doi:DOI 10.1021/ja00292a038 (1985).

28 Berger, J., Lehr, H., Teitel, S., Maehr, H. & Grunberg, E. A new antibiotic X-5108 of *Streptomyces* origin. I. Production, isolation and properties. *The Journal of antibiotics* **26**, 15-22 (1973).

29 Jackson, M., Karwowski, J. P., Theriault, R. J., Maus, M. L. & Kohl, W. L. Phenelfamycins, a novel complex of elfamycin-type antibiotics. I. Discovery, taxonomy and fermentation. *The Journal of antibiotics* **41**, 1293-1299 (1988).

30 Brotz, E. *et al.* Phenelfamycins G and H, new elfamycin-type antibiotics produced by Streptomyces albospinus Acta 3619. *The Journal of antibiotics* **64**, 257-266, doi:10.1038/ja.2010.170 (2011).

31 Tavecchia, P. *et al.* Synthesis and biological evaluation of new fragments from kirromycin antibiotic. *The Journal of antibiotics* **49**, 1249-1257 (1996).

32 Pingoud, A., Urbanke, C., Wolf, H. & Maass, G. The binding of kirromycin to elongation factor Tu. Structural alterations are responsible for the inhibitory action. *Eur J Biochem* **86**, 153-157 (1978).

33 Vogeley, L., Palm, G. J., Mesters, J. R. & Hilgenfeld, R. Conformational change of elongation factor Tu (EF-Tu) induced by antibiotic binding. Crystal structure of the complex between EF-Tu.GDP and aurodox. *J Biol Chem* **276**, 17149-17155, doi:10.1074/jbc.M100017200 (2001).

34 Watanabe, T., Izaki, K. & Takahashi, H. New polyenic antibiotics active against gram-positive and -negative bacteria. I. Isolation and purification of antibiotics produced by Gluconobacter sp. W-315. *The Journal of antibiotics* **35**, 1141-1147 (1982).

35 Parmeggiani, A. *et al.* Enacyloxin IIa pinpoints a binding pocket of elongation factor Tu for development of novel antibiotics. *J Biol Chem* **281**, 2893-2900, doi:10.1074/jbc.M505951200 (2006).

36 Watanabe, T., Suzuki, T. & Izaki, K. New polyenic antibiotics active against gram-positive and gram-negative bacteria. V. Mode of action of enacyloxin IIa. *The Journal of antibiotics* **44**, 1457-1459 (1991).

37 Zief, M., Woodside, R. & Schmitz, H. Pulvomycin. *Antibiotics & chemotherapy* **7**, 384-386 (1957).

38 McKenzie, N. L. *et al.* Induction of antimicrobial activities in heterologous streptomycetes using alleles of the Streptomyces coelicolor gene absA1. *The Journal of antibiotics* **63**, 177-182, doi:10.1038/ja.2010.13 (2010).

39 Parmeggiani, A. *et al.* Structural basis of the action of pulvomycin and GE2270 A on elongation factor Tu. *Biochemistry* **45**, 6846-6857, doi:10.1021/bi0525122 (2006).

40 Selva, E. *et al.* Antibiotic GE2270 a: a novel inhibitor of bacterial protein synthesis. I. Isolation and characterization. *The Journal of antibiotics* **44**, 693-701 (1991).

41 Selva, E. *et al.* Components of the GE2270 complex produced by *Planobispora rosea* ATCC 53773. *The Journal of antibiotics* **48**, 1039-1042 (1995).

42 Zeef, L. A. *et al.* Pulvomycin-resistant mutants of *E. coli* elongation factor Tu. *The EMBO journal* **13**, 5113-5120 (1994).

43 Recktenwald, J. *et al.* Nonribosomal biosynthesis of vancomycin-type antibiotics: a heptapeptide backbone and eight peptide synthetase modules. *Microbiol-Sgm* **148**, 1105-1118 (2002).

44 Robbel, L. & Marahiel, M. A. Daptomycin, a bacterial lipopeptide synthesized by a nonribosomal machinery. *The Journal of biological chemistry* **285**, 27501-27508, doi:10.1074/jbc.R110.128181 (2010).

45 Sieber, S. A. & Marahiel, M. A. Molecular mechanisms underlying nonribosomal peptide synthesis: approaches to new antibiotics. *Chem Rev* **105**, 715-738, doi:10.1021/cr0301191 (2005).

46 Weber, T. *et al.* Molecular analysis of the kirromycin biosynthetic gene cluster revealed beta-alanine as precursor of the pyridone moiety. *Chemistry & biology* **15**, 175-188, doi:10.1016/j.chembiol.2007.12.009 (2008).

47 Weber, T., Welzel, K., Pelzer, S., Vente, A. & Wohlleben, W. Exploiting the genetic potential of polyketide producing *Streptomycetes*. *J Biotechnol* **106**, 221-232 (2003).

48 Oyama, R. *et al.* An extracellular quinoprotein oxidase that catalyzes conversion of enacyloxin IVa to enacyloxin IIa. *Biosci Biotechnol Biochem* **58**, 1914-1917 (1994).

49 Morris, R. P. *et al.* Ribosomally synthesized thiopeptide antibiotics targeting elongation factor Tu. *J Am Chem Soc* **131**, 5946-5955, doi:10.1021/ja900488a (2009).

50 Lathe, W. C., 3rd & Bork, P. Evolution of *tuf* genes: ancient duplication, differential loss and gene conversion. *FEBS letters* **502**, 113-116 (2001).

51 van der Meide, P. H., Vijgenboom, E., Talens, A. & Bosch, L. The role of EF-Tu in the expression of *tufA* and *tufB* genes. *European journal of biochemistry / FEBS* **130**, 397-407 (1983).

52 Bosch, L., Kraal, B., Van der Meide, P. H., Duisterwinkel, F. J. & Van Noort, J. M. The elongation factor EF-Tu and its two encoding genes. *Prog Nucleic Acid Res Mol Biol* **30**, 91-126 (1983).

53 Hughes, D. Both genes for EF-Tu in Salmonella typhimurium are individually dispensable for growth. *Journal of molecular biology* **215**, 41-51, doi:10.1016/S0022-2836(05)80093-2 (1990).

54 van der Meide, P. H., Vijgenboom, E., Dicke, M. & Bosch, L. Regulation of the expression of *tufA* and *tufB*, the two genes coding for the elongation factor EF-Tu in *Escherichia coli*. *FEBS letters* **139**, 325-330 (1982).

55 Brandis, G., Bergman, J. M. & Hughes, D. Autoregulation of the *tufB* operon in *Salmonella*. *Mol Microbiol* **100**, 1004-1016, doi:10.1111/mmi.13364 (2016).

56 Vijgenboom, E. *et al.* Three tuf-like genes in the kirromycin producer *Streptomyces ramocissimus*. *Microbiology* **140 (Pt 4)**, 983-998, doi:10.1099/00221287-140-4-983 (1994).

57 Olsthoorn-Tieleman, L. N., Palstra, R. J., van Wezel, G. P., Bibb, M. J. & Pleij, C. W. Elongation factor Tu3 (EF-Tu3) from the kirromycin producer Streptomyces ramocissimus Is resistant to three classes of EF-Tu-specific inhibitors. *J Bacteriol* **189**, 3581-3590, doi:10.1128/JB.01810-06 (2007).

58 Mohrle, V. G., Tieleman, L. N. & Kraal, B. Elongation factor Tu1 of the antibiotic GE2270A producer *Planobispora rosea* has an unexpected resistance profile against EF-Tu targeted antibiotics. *Biochemical and biophysical research communications* **230**, 320-326, doi:10.1006/bbrc.1996.5947 (1997).

59 Zuurmond, A. M. *et al.* GE2270A-resistant mutations in elongation factor Tu allow productive aminoacyl-tRNA binding to EF-Tu.GTP.GE2270A complexes. *Journal of molecular biology* **304**, 995-1005, doi:10.1006/jmbi.2000.4260 (2000).

60 Crechet, J. B., Malosse, C. & Hountondji, C. EF-Tu from the enacyloxin producing Frateuria W-315 strain: Structure/activity relationship and antibiotic resistance. *Biochimie* **127**, 59-69, doi:10.1016/j.biochi.2016.04.019 (2016).

61 Thaker, M. N. *et al.* Biosynthetic gene cluster and antimicrobial activity of the elfamycin antibiotic factumycin. *Medchemcomm* **3**, 1020-1026, doi:10.1039/c2md20038d (2012).

62 Zuurmond, A. M., Rundlof, A. K. & Kraal, B. Either of the chromosomal tuf genes of E. coli K-12 can be deleted without loss of cell viability. *Molecular & general genetics : MGG* **260**, 603-607 (1999).

63 Zeef, L. A. & Bosch, L. A technique for targeted mutagenesis of the EF-Tu chromosomal gene by M13-mediated gene replacement. *Molecular & general genetics : MGG* **238**, 252-260 (1993).

64 Abdulkarim, F., Liljas, L. & Hughes, D. Mutations to kirromycin resistance occur in the interface of domains I and III of EF-Tu.GTP. *FEBS letters* **352**, 118-122 (1994).

65 Kraal, B. *et al.* Antibiotic resistance mechanisms of mutant EF-Tu species in Escherichia coli. *Biochemistry and cell biology = Biochimie et biologie cellulaire* **73**, 1167-1177 (1995).

66 Miele, A. *et al.* Differential susceptibilities of enterococcal species to elfamycin antibiotics. *Journal of clinical microbiology* **32**, 2016-2018 (1994).

67 Flinspach, K., Kapitzke, C., Tocchetti, A., Sosio, M. & Apel, A. K. Heterologous expression of the thiopeptide antibiotic GE2270 from Planobispora rosea ATCC 53733 in Streptomyces coelicolor requires deletion of ribosomal genes from the expression construct. *PLoS One* **9**, e90499, doi:10.1371/journal.pone.0090499 (2014).

68 Just-Baringo, X., Albericio, F. & Alvarez, M. Thiopeptide antibiotics: retrospective and recent advances. *Mar Drugs* **12**, 317-351, doi:10.3390/md12010317 (2014).

69 Tubulekas, I., Buckingham, R. H. & Hughes, D. Mutant ribosomes can generate dominant kirromycin resistance. *J Bacteriol* **173**, 3635-3643 (1991).

70 Huseby, D. L. *et al.* Mutation Supply and Relative Fitness Shape the Genotypes of Ciprofloxacin-Resistant Escherichia coli. *Mol Biol Evol* **34**, 1029-1039, doi:10.1093/molbev/msx052 (2017).

71 Stark, H. *et al.* Ribosome interactions of aminoacyl-tRNA and elongation factor Tu in the codon-recognition complex. *Nat Struct Biol* **9**, 849-854, doi:10.1038/nsb859 (2002).

72 Valle, M. *et al.* Incorporation of aminoacyl-tRNA into the ribosome as seen by cryo-electron microscopy. *Nat Struct Biol* **10**, 899-906, doi:10.1038/nsb1003 (2003).

73 Schuette, J. C. *et al.* GTPase activation of elongation factor EF-Tu by the ribosome during decoding. *The EMBO journal* **28**, 755-765, doi:10.1038/emboj.2009.26 (2009).

74 Villa, E. *et al.* Ribosome-induced changes in elongation factor Tu conformation control GTP hydrolysis. *Proceedings of the National Academy of Sciences of the United States of America* **106**, 1063-1068, doi:10.1073/pnas.0811370106 (2009).

75 Valle, M. *et al.* Cryo-EM reveals an active role for aminoacyl-tRNA in the accommodation process. *The EMBO journal* **21**, 3557-3567, doi:10.1093/emboj/cdf326 (2002).

76 Fischer, N. *et al.* Structure of the *E. coli* ribosome-EF-Tu complex at <3 A resolution by Cs-corrected cryo-EM. *Nature* **520**, 567-570, doi:10.1038/nature14275 (2015).

77 Miller, M. R. & Buskirk, A. R. An unusual mechanism for EF-Tu activation during tmRNA-mediated ribosome rescue. *RNA* **20**, 228-235, doi:10.1261/rna.042226.113 (2014).

78 Thirup, S. S., Van, L. B., Nielsen, T. K. & Knudsen, C. R. Structural outline of the detailed mechanism for elongation factor Ts-mediated guanine nucleotide exchange on elongation factor Tu. *J Struct Biol* **191**, 10-21, doi:10.1016/j.jsb.2015.06.011 (2015).

79 Defeu Soufo, H. J. *et al.* Bacterial translation elongation factor EF-Tu interacts and colocalizes with actin-like MreB protein. *Proceedings of the National Academy of Sciences of the United States of America* **107**, 3163-3168, doi:10.1073/pnas.0911979107 (2010).

80 Tocchetti, A. *et al.* Capturing linear intermediates and C-terminal variants during maturation of the thiopeptide GE2270. *Chemistry & biology* **20**, 1067-1077, doi:10.1016/j.chembiol.2013.07.005 (2013).

81 Cooper, M. A. & Shlaes, D. Fix the antibiotics pipeline. *Nature* **472**, 32, doi:10.1038/472032a (2011).

82 Fabbretti, A. *et al.* A derivative of the thiopeptide GE2270A highly selective against Propionibacterium acnes. *Antimicrobial agents and chemotherapy*, doi:10.1128/AAC.05155-14 (2015).

83 Hajela, N. *et al.* Gut microbiome, gut function, and probiotics: Implications for health. *Indian J Gastroenterol* **34**, 93-107, doi:10.1007/s12664-015-0547-6 (2015).

84 LaMarche, M. J. *et al.* Discovery of LFF571: an investigational agent for Clostridium difficile infection. *Journal of medicinal chemistry* **55**, 2376-2387, doi:10.1021/jm201685h (2012).

85 Mullane, K. *et al.* Multicenter, randomized clinical trial to compare the safety and efficacy of LFF571 and vancomycin for *Clostridium difficile* infections. *Antimicrobial agents and chemotherapy* **59**, 1435-1440, doi:10.1128/AAC.04251-14 (2015).

86 Davies, J., Spiegelman, G. B. & Yim, G. The world of subinhibitory antibiotic concentrations. *Curr Opin Microbiol* **9**, 445-453, doi:10.1016/j.mib.2006.08.006 (2006).

87 Gerber, M. *et al.* Effect of sub-MIC concentrations of metronidazole, vancomycin, clindamycin and linezolid on toxin gene transcription and production in *Clostridium difficile*. *J Med Microbiol* **57**, 776-783, doi:10.1099/jmm.0.47739-0 (2008).

88 Sachdeva, M. & Leeds, J. A. Subinhibitory concentrations of LFF571 reduce toxin production by *Clostridium difficile*. *Antimicrobial agents and chemotherapy* **59**, 1252-1257, doi:10.1128/AAC.04436-14 (2015).

89 Pettersen, E.F., Goddard, T.D., Huang, C.C., Couch, G.S., Greenblatt, D.M., Meng, E.C., and Ferrin, T.E. UCSF Chimera-a visualization system for exploratory research and analysis. *J Comput Chem* **25**: 1605-1612 (2004).

90 ACD/Chemsketch, version 12.01, Advanced Chemistry Development, Inc., Toronto, ON, Canada, http://www.acdlabs.com (2010).

91 Leeds, J. A. *et al.* In vitro and in vivo activities of novel, semisynthetic thiopeptide inhibitors of bacterial elongation factor Tu. *Antimicrobial agents and chemotherapy* **55**, 5277-5283, doi:10.1128/AAC.00582-11 (2011).

92 Mahenthiralingam, E. *et al.* Enacyloxins are products of an unusual hybrid modular polyketide synthase encoded by a cryptic Burkholderia ambifaria Genomic Island. *Chemistry & biology* **18**, 665-677, doi:10.1016/j.chembiol.2011.01.020 (2011).

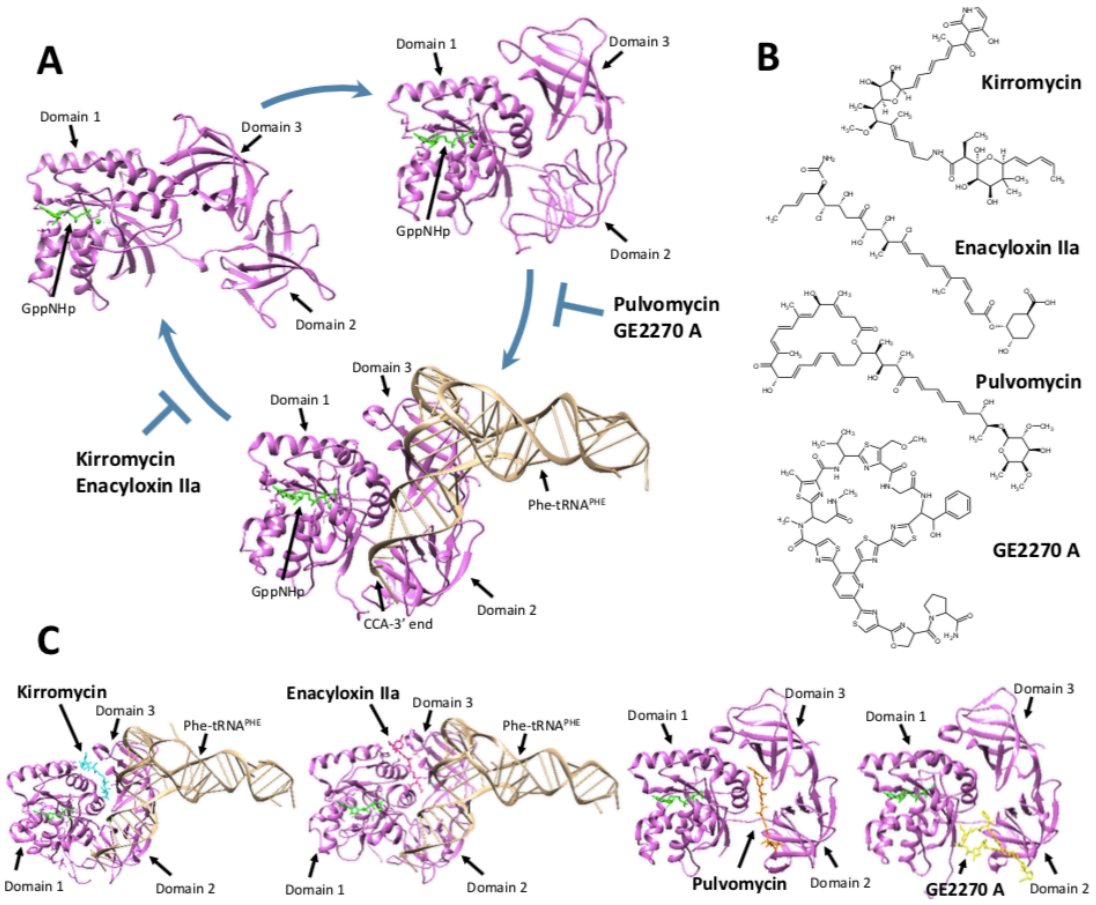

Figure 1 – Crystal Structures and Chemical Structures of EF-Tu and its inhibitors. **(A) Crystal structures of the EF-Tu cycle.** EF-Tu from *Thermus aquaticus* is indicated in purple, while bound GDP, GTP analogue, and/or magnesium ion are indicated in green. Top right: Crystal structure of active EF-Tu bound to GppNHp, a non-hydrolyzable GTP analogue (PDB ID: 1EXM). Bottom: Crystal structure of active EF-Tu bound to GppNHp and Phe-tRNA^{Phe}. Bound Phe-tRNAPhe is indicated in tan (PDB ID: 1TTT). Top left: After accommodation of the tRNA into the ribosomal A site, GTP is hydrolyzed to GDP. Structure of inactive EF-Tu bound to GDP (PDB ID: 1TUI). P-loop indicated in orange, Switch I in yellow, and Switch II in blue. Images drawn using Chimera [89]. **(B) Chemical Structures of EF-Tu Inhibitors, drawn using ChemSketch [90]. (C) Crystal structures of inhibitors bound to EF-Tu**. **First:** Kirromycin binds

between domain 1 and 3 in the crystal structure of the EF-Tu:GppNHp:Phe-tRNA^{Phe} complex. *Escherichia coli* EF-Tu activated with a non-hydrolyzable GTP analogue, GppHNp, bound to Phe-tRNA^{Phe} and kirromycin. In the model, EF-Tu is indicated in purple, GppNHp in green, Phe-tRNA^{Phe} in tan, and kirromycin in cyan (PDB ID: 1OB2). **Second:** Enacyloxin IIa binds between domain 1 and 3 in the crystal structure of the EF-Tu:GppNHp:Phe-tRNA^{Phe} complex. *T. aquaticus* EF-Tu activated with a non-hydrolyzable GTP analogue, GppHNp, bound to Phe-tRNA^{Phe} and enacyloxin IIa. In the model, EF-Tu is indicated in purple, GppNHp in green, Phe-tRNA^{Phe} in tan, and enacyloxin IIa in magenta (PDB ID: 1OB5). **Third:** Pulvomycin binds at the interface of EF-Tu's three domains in the crystal structure of EF-Tu:GppNHp complex. *Thermus thermophilus* EF-Tu activated with a non-hydrolyzable GTP analogue, GppHNp, bound to pulvomycin. In the model, EF-Tu is indicated in purple, GppNHp in green, and pulvomycin in orange (PDB ID: 2C78). **Fourth:** GE2270 A binds between domains 1 and 2 in the crystal structure of EF-Tu:GppNHp complex. *T. thermophilus* EF-Tu activated with a non-hydrolyzable GTP analogue, GppHNp, bound to GE2270 A. In the model, EF-Tu is indicated in purple, GppNHp in green, and GE2270 A in yellow (PDB ID: 2C77). Images drawn using Chimera [89].

Kirromycin	**MIC (µg/mL)**	**Reference**
Gram-Positive		
Enterococcus faecium NB05001	2	91
Enterococcus faecium NB05019	2	91
Staphylococcus aureus NB01001	>32	91
Enterococcus faecalis NB04004	>32	91
Enterococcus faecalis NB04006	>32	91
Gram-Negative		
Moraxella catarrhalis ATCC 8176	0.06	31
Haemophilus influenzae type B ATCC 19418	4	31
Neisseria gonorhoeae ISM68/126	0.06	31
Escherichia coli SKF 12140	>128	31
Enacyloxin IIa		
Gram-Positive		
Enterococcus hirae ATCC 8043	1	34
Staphylococcus aureus 209 P	50	34
Gram-Negative		
Acinetobacter baumannii OXA23 clone 2	3	92
Burkholderia dolosa LMG 18943	7.5	92
Pseudomonas aeruginosa NCTC 12903	>100	92
Pulvomycin		
Gram-Positive		
Staphylococcus aureus ATCC 29213	2	38
Enterococcus faecalis ATCC 29212	4	38
Staphylococcus aureus CMRSA - 1	32	38
Enterococcus faecalis ATCC 51299	32	38
Gram-Negative		
Burkholderia cepacia C3865	8	38
Pseudomonas aeruginosa PAO1	32	38
Acinetobacter baumannii ATCC 17978	32	38
Escherichia coli NU14	32	38
Klebsiella pneumoniae HQ142423	>128	38
GE2270 A		
Gram-Positive		
Clostridium difficile L1363 ATCC9689	0.03	40
Enterococcus faecium NB05001	0.03	91
Enterococcus faecium NB05019	0.06	91
Enterococcus faecalis L149 ATCC7080	0.13	40
Staphylococcus aureus L165 Tour	0.25	40
Staphylococcus aureus NB01001	0.25	91
Enterococcus faecalis NB04004	0.25	91
Gram-Negative		
Pseudomonas aeruginosa L4 ATCC 10145	>128	40
Klebsiella pneumoniae L142 ISM	>128	40
Neisseria gonorhoeae L997 ISM68/126	32	40
Chlamydia trachomatis	>128	40
Escherichia coli L47 SKF12140	>128	40

Table 1 – Minimum Inhibitory Concentrations (MICs) for Elfamycin Antibiotics

Trimethylation of Elongation Factor-Tu by the Dual Thermoregulated Methyltransferase EftM Does Not Impact Its Canonical Function in Translation

Samantha M. Prezioso[1,2], Duc M. Duong[3], Emily G. Kuiper[4,5,#], Qiudong Deng[3], Sebastián Albertí[6], Graeme L. Conn[5,7], Joanna B. Goldberg[2,7,8*]

Submitted for publication in September 2018.

Affiliations

[1]Microbiology and Molecular Genetics (MMG) Program, Graduate Division of Biological and Biomedical Sciences, Emory University, Atlanta, GA 30322, USA.

[2]Division of Pulmonology, Allergy/Immunology, Cystic Fibrosis and Sleep, Department of Pediatrics, Emory University School of Medicine, Atlanta, GA 30322, USA.

[3]Emory Integrated Proteomics Core, Emory University, Atlanta GA 30322

[4]Biochemistry, Cell and Developmental Biology (BCDB) Program, Graduate Division of Biological and Biomedical Sciences, Emory University, Atlanta, GA 30322, USA.

[5]Department of Biochemistry, Emory University School of Medicine, Atlanta, GA 30322, USA.

[6]Instituto Universitario de Investigación en Ciencias de la Salud, Universidad de las Islas Baleares, Palma de Mallorca, Spain.

[7]Emory Antibiotic Resistance Center, Atlanta, GA 30322, USA.

[8]Emory+Children's Center for Cystic Fibrosis and Airway Disease Research, Atlanta, GA 30322, USA.

[#]Current Address: Department of Cancer Immunology and Virology, Dana-Farber Cancer Institute, Boston, MA 02215, USA.

Abstract

The *Pseudomonas aeruginosa* methyltransferase EftM trimethylates elongation factor-Tu (EF-Tu) on lysine 5 to form a post-translational modification important for initial bacterial adherence to host epithelial cells. EftM methyltransferase activity is directly temperature regulated. The protein stability of EftM is tuned with a melting temperature (T_m) around 37°C such that the enzyme is stable and active at 25°C, but is completely inactivated by protein unfolding at higher temperatures. This leads to higher observable levels of EF-Tu trimethylation at the lower temperature. Here we report an additional layer of thermoregulation resulting in lower *eftM* mRNA transcript level at 37°C compared to 25°C and show that this regulation occurs at the level of transcription initiation. To begin to define the impact of this system on *P. aeruginosa* physiology, we demonstrate that EF-Tu is the only substrate for EftM. Further, we interrogated the proteome of three different wild-type *P. aeruginosa* strains, their *eftM* mutants, and these mutants complemented with *eftM* and conclude that trimethylation of EF-Tu by EftM does not impact EF-Tu's canonical function in translation. In addition to furthering our knowledge of this *Pseudomonas* virulence factor, this study provides an intriguing example of a protein with multiple layers of thermoregulation.

Introduction

Pseudomonas aeruginosa is an important opportunistic pathogen that can thrive in a wide variety of environments and hosts[1]. Temperature change is one of the potential signals that cue the transition from the environment to the human host. In response to this change, *P. aeruginosa* strain PAO1 has been shown to modulate 6.4% of its transcriptome in the shift from 23°C (ambient environmental temperature), to 37°C (human body temperature)[2]. Most virulence factor thermoregulation occurs such that the output of the virulence factor is triggered or increased at 37°C in response to a mammalian host[3]. However, not all bacterial hosts are warm-blooded, and further, increased production of a virulence factor may actually be counterproductive to the long-term success of a bacterium. Therefore, to fine-tune expression to the new environment, some bacterial virulence factors are decreased in expression at 37°C. One example of this regulatory trend in *P. aeruginosa* is Piv (protease IV; PA4175). This protein shows lower expression at 37°C than 25°C, despite being well accepted as an important virulence factor during infection[4,5]. Thermoregulation resulting in reduced virulence factor expression and/or activity is important but understudied compared to the more typically observed up-regulation at 37°C and down-regulation at 25°C.

Another example of a *P. aeruginosa* virulence factor that is down-regulated upon transition to 37°C is EftM, a *S*-adenosyl-L-methionine (SAM)-dependent methyltransferase that trimethylates elongation factor-Tu (EF-Tu) on lysine 5 ($K5me^3$). In addition to its essential canonical role in delivering charged

tRNAs to the ribosome during translation[6], EF-Tu is found on the bacterial cell surface[7]. While this post-translational modification does not appear to alter the ability of EF-Tu to be surface-localized[8], once in this subcellular location, K5me^3-modified EF-Tu performs a moonlighting role that increases bacterial adherence to human epithelial cells[8]. Interestingly, EftM activity is post-translationally controlled through inherent protein instability; EftM is stably folded at lower temperature (25°C) but unfolds and loses methyltransferase activity at elevated temperatures (37°C). However, whether there are additional thermoregulatory mechanisms impacting EftM regulation is less clearly defined. Several studies have investigated global RNA changes in *P. aeruginosa* in response to temperature by a variety of techniques, including microarray[2,5] and RNA-seq[9]. These studies reported no information on *eftM* in response to temperature, most likely because the *eftM* transcript level is below the limit of detection using these approaches. This limitation thus necessitated a directed approach for investigating the impact of temperature on *eftM.* Here we demonstrate *eftM* thermoregulation directly though RT-qPCR and show that the steady state levels of *eftM* are higher at 25°C than 37°C. Further, using reporter fusions, we reveal that this additional layer of thermoregulation is controlled at the level of transcriptional initiation.

EftM's only currently recognized cellular target for methylation is EF-Tu. EF-Tu is an extremely abundant protein in the cell during exponential phase growth, accounting for 6-13.5% of total cellular protein and outnumbering ribosomes 8-14 to one, depending on growth rate[10]. As mentioned, EF-Tu is an

elongation factor that delivers charged tRNA to the ribosome during translation and contributes to proofreading of the growing peptide chain[11]. This canonical function is essential for bacterial cells[12]; however, post-translational modifications can alter this function. For example, in *Escherichia coli,* EF-Tu lysine 56 is methylated in response to bacterial energy state with monomethylation being observed during exponential phase growth and dimethylation being observed during nutrient limitation, such as in stationary phase. Lysine 56 methylation affects EF-Tu canonical function by slowing the rate of EF-Tu GTP hydrolysis and therefore reducing translation capacity[13]. In addition to methylation, EF-Tu can be phosphorylated, such as by the toxin Doc that phosphorylates EF-Tu threonine 382 in *E. coli*. This single post-translational modification is sufficient to completely halt translation through inactivation of *E. coli* EF-Tu[14]. EftM trimethylates EF-Tu on K5me^3, found on the disordered loop at the protein amino-terminus. Given the essential nature of EF-Tu during translation and the impact post-translational modification of EF-Tu can have on its canonical role in protein synthesis, we aimed to uncover the impact of EF-Tu K5me^3 on EF-Tu's canonical function in translation. To do so, we utilized whole-cell proteomics to assess the proteome of three different *P. aeruginosa* strains in a label-free, unbiased manner to expose any effect K5me^3 has on the global *Pseudomonas* proteomic landscape. These analyses reveal that methylation of EF-Tu by EftM has limited impact on the proteome under the conditions examined.

Results

P. aeruginosa has higher mRNA steady-state levels of *eftM* at 25°C compared to 37°C

We have previously noted that in PAO1 the K5me^3 modification of EF-Tu is more prominent at 25°C compared to 37°C[15] and we showed that this thermoregulation was due, at least in part, to the unfolding of EftM at the higher temperature[16]. To determine whether another layer(s) of thermoregulation exists in addition to EftM protein stability, we first measured *eftM* mRNA levels by RT-qPCR. From this we observed an average of 48 copies of 25°C *eftM* transcript per 1000 copies of our standard internal reference gene *omlA,* and only 11 copies of 37°C *eftM* transcript per 1000 *omlA*. By comparing these steady state levels we conclude an average of 4X upregulation of PAO1 *eftM* mRNA transcripts at 25°C compared to 37°C (**Figure 1**). In contrast for *rpoD*, used as a control transcript unaffected by temperature, similar levels were observed at both temperatures as expected[17].

Chronic infection isolate PAHM4, originally isolated from non-CF bronchiectasis, encodes a mutated *mutS* and is therefore a hypermutator strain[18]. This defect in DNA mismatch-repair results in an ~1,000-fold increase in mutation rate and allowed for adaptation of the strain to the human lung. Interestingly, this strain shows a less extreme disparity between the levels of EF-Tu trimethylation at 25°C vs 37°C[8]. The amino acid sequence of $EftM_{PAHM4}$ has 28 differences compared to the PAO1 protein. Ongoing studies have shown that these amino acid changes confer elevated thermostability such that the mid-point

melting temperature (T_m) of EftM from PAHM4 is 42°C (unpublished observations) compared to ~36°C PAO1 EftM[16]. To determine whether the *eftM* transcript is also impacted by temperature in PAHM4, we performed RT-qPCR analysis and found that steady state levels of PAHM4 *eftM* are about 3X higher at 25°C compared to 37°C. Again, no significant differences in relative expression of *rpoD* were observed (**Figure 1**). These results indicate that, in addition to EftM being post-translationally thermoregulated through protein instability[16], *eftM* is transcriptionally thermoregulated resulting in elevated mRNA levels at 25°C. Importantly this result holds true for both PAO1 and PAHM4, indicating that the two layers of thermoregulation are not interlinked.

Complementation of *eftM* mutants and maintenance of thermoregulation

We previously described the construction of a mutant, PAO1Δ*eftM*, which is unable to modify EF-Tu. Interestingly, when this deletion strain was complemented with a multi-copy plasmid expressing *eftM* from a constitutive promoter, ablation of EF-Tu K5me[3] temperature regulation was observed[15]. This was presumed to be due to overproduction of EftM and accumulation of EF-Tu methylation. To determine whether we could complement the *eftM* mutation while maintaining thermoregulation as observed in the wild-type strain, we transferred a single copy of *eftM* driven from its native promoter to an innocuous site of the *P. aeruginosa* chromosome of PAO1Δ*eftM*. Wild-type PAO1 (WT), mutant PAO1Δ*eftM* (Δ), and the single-copy complemented PAO1Δ*eftM* strain (Comp) were grown at 25°C or 37°C and assessed for trimethylation of EF-Tu by

Western blotting with an αTrimethyl Lysine antibody. Antibody to EF-Tu served as an internal loading control. As seen in **Figure 2A** (lower panel), the levels of EF-Tu are similar between all strains. As previously noted, WT shows greater trimethylation of EF-Tu at 25°C compared to 37°C, while Δ shows no trimethylation at either temperature. Importantly, the level of trimethylation observed in the single-copy complement (Comp) was similarly temperature regulated compared to WT, indicating this construct reverses the original defect in the deletion mutant and resembles WT with respect to temperature regulation of EftM activity.

To confirm that the effect was not PAO1-specific, we performed similar single-copy native-promoter complementation and subsequent Western blot analysis with a PA14 transposon mutant, PA14 *eftM*::tn, and showed that both the WT and Comp of these strains showed similar thermoregulation of trimethylation of EF-Tu (**Figure 2B**), while PA14 *eftM*::tn did not methylate EF-Tu at either temperature. We also constructed an *eftM* mutant in PAHM4 in the same manner as described for PAO1Δ*eftM*. As seen in **Figure 2C**, consistent with previous observations[8], PAHM4 wild-type shows slightly more trimethylation of EF-Tu at 25°C compared to 37°C, while the newly constructed deletion mutant shows no trimethylation at either temperature. Complementing PAHM4Δ*eftM* with $eftM_{PAHM4}$ in single-copy with the native PAHM4 promoter restored expression to that seen in the parental strain (**Figure 2C**).

We additionally transferred eftM_{PAHM4} to PAO1Δ*eftM*. This set of PAO1 wild-type, deletion, PAO1-complemented *eftM,* and PAHM4-complemented *eftM*

strains in one isogenic background allowed us to directly compare EftM with lower and higher T_ms. When assessed by Western blotting, we noticed increased but not equal levels of methylation on EF-Tu at 37°C compared to 25°C for PAO1Δ*eftM*+*eftM*$_{PAHM4}$. The difference between EF-Tu trimethylation in the *eftM*$_{PAO1}$-complemented strain and the *eftM*$_{PAHM4}$-complemented PAO1 strain (**Figure 2A**) tells us that all information necessary for thermoregulation can be transferred with the upstream intergenic region and coding sequence for *eftM* and is not dependent on genomic context of *eftM* in the chromosome.

Transcription of *eftM* is initiated from the same promoter at 25°C and 37°C

A potential mechanism for *eftM* transcriptional thermoregulation could be the utilization of different promoters at different temperatures; we therefore next studied the transcriptional thermoregulation of *eftM* by mapping the promoter. To accomplish this we defined the transcription start site (TSS) for both PAO1 and PAHM4 grown at both 25°C and 37°C and used this information for promoter prediction analysis. Using 5' rapid amplification of cDNA ends (5'RACE) with mRNA harvested from cells grown at either 25°C or 37°C, we found the same TSS 26-27 nucleotides upstream of the translation start codon (ATG) in both strains (**Figure 3A**).

Using the transcription start site as a guide we predicted *eftM*'s promoter to be (-35) TTCGCC and (-10) TACCAT (**Figure 3B**). Despite differences between PAO1 and PAHM4 in the *eftM* upstream region, this prediction is conserved with one G→C polymorphism in the -35. To confirm this promoter

prediction, we mutated the native promoter of *eftM* so that the -10 region was scrambled from TACCAT to ATTACC. This construct was then transferred to PAO1Δ*eftM*. Unlike the construct with the wild-type sequence (Comp), this strain (-10Scr) showed no trimethylation of EF-Tu at either temperature (**Figure 2A**). This result indicates that there is no transcription of *eftM* and thus proper identification of the promoter (**Figure 3B**).

Thermoregulation is at the level of transcription initiation

RT-qPCR revealed *eftM* mRNA steady state levels are higher at 25°C than 37°C (**Figure 1**). Steady-state mRNA levels are modulated by a variety of factors, including transcription initiation and mRNA stability/decay. While 5'RACE implied the same promoter was driving transcription at both temperatures (**Figure 3**), this does not eliminate the possibility that transcription factors are altering transcription initiation in response to temperature. To investigate transcription initiation as the point of transcriptional thermoregulation, the entire 99-nucleotide *eftM* intergenic region, including the native *eftM* promoter and ribosome binding site, were fused seamlessly to a promoterless *lacZ* cassette and inserted in single copy to the PAO1 CTX attachment site[19]. An *rpoD* reporter was constructed and again utilized as a control for no change in response to temperature. Both reporter strains were probed by standard β-galactosidase assay for levels of transcription initiation, as proxied by LacZ activity, at 25°C compared to 37°C (**Figure 4**). Our *eftM* reporter strain showed an average of a 207% increase in transcription initiation at 25°C compared to 37°C, while the

rpoD control showed no significant difference, implying that transcription initiation is a mechanism mediating *eftM* thermoregulation.

EF-Tu is the only cellular substrate for EftM

Our previous analysis of EftM protein stability[16], and the current work here, reveal EftM to be a dual thermoregulated methyltransferase that trimethylates EF-Tu robustly at 25°C. Post-translational modifications are known to be able to impact EF-Tu's canonical role in translation. However, to study the impact of EF-Tu lysine 5 trimethylation on *Pseudomonas* physiology, we first needed to confirm that EF-Tu is the only substrate of EftM, allowing us to more firmly attribute any phenotype observed to EftM-mediated methylation of EF-Tu.

Whole cell lysates of PAO1Δ*eftM* grown at 25°C were obtained and EF-Tu was removed using five rounds of immune-depletion. We first confirmed successful depletion of EF-Tu from the cellular lysate by probing for EF-Tu (**Figure 5A**). We also probed for RpoA as a control to ensure that protein was not non-specifically being depleted. Next we performed an *in vitro* methylation assay using radiolabeled SAM (adenosyl-L-methionine, S-[methyl-^{3}H]) to detect other proteins receiving methyl-^{3}H. Undepleted lysates (U) revealed methylation of a single protein, EF-Tu, at ~40 kDa as previously described[16]. In comparison, we observed no tritiated proteins between 15 kDa-170 kDa for the *in vitro* methylation reaction of the EF-Tu depleted lysate (U5) (**Figure 5B**). This result implies that EF-Tu is the sole substrate for EftM. Re-addition of recombinant EF-Tu to the depleted lysate resulted in the reemergence of a single ~40 kDa band

(**Figure 5B**). Together, these results suggest that any physiological impact the presence of EftM has on the cell can be attributed exclusively to trimethylation of EF-Tu, and not modification of other proteins.

Trimethylation of EF-Tu by EftM has little impact on the cellular steady-state proteome

While other post-translational modifications can impact EF-Tu's canonical role in translation[13] the K5me[3] modification does not appear to alter global translation, as evidenced by similar total cellular protein and overall bacterial growth rate for PAO1 and PAO1Δ*eftM*[15]. Therefore we hypothesized that if this particular post-translational modification impacted EF-Tu canonical function, the result would be altered abundance of specific proteins and not altered translation rate in general. Such an influence on translation would be similar, for example, to how EF-P increases translation of proteins with polyproline stretches[20]. To test this idea we compared the entire proteome in an unbiased, label-free method between the wild-type strain, a strain in which *eftM* was inactivated, and a complemented mutant that restores *eftM* activity to native levels.

For our standard laboratory strain PAO1 and its derivatives, we grew strains at 25°C until mid-exponential phase. This is the temperature at which EftM is stable and active, and also the temperature at which we observed additional up-regulation at the level of transcription. Mid-exponential phase was assessed because that is the condition under which EF-Tu is most abundant and active, thus maximizing any potential differences in translation due to methylation

status. To ensure reliable and reproducible insights, we performed a full comparison in PAO1 two independent times, named Data Set #1 and Data Set #2 (**Raw data not shown**). In each data set, the wild-type PAO1 (WT), Δ*eftM* deletion (Δ), and PAO1-complemented (Comp) strains were grown and analyzed in independent biological triplicates.

Data were first examined by plotting detection intensity (label-free quantitation; LFQ) for each individual protein as comparisons between strains. WT and Comp showed a 1:1 trend line, indicating that these two strains were well matched (**Figure 6A, left**). We plotted the same for WT vs. Δ and Comp vs. Δ to identify outliers in protein abundance (**Figure 6A, center and right**). EftM was immediately apparent as different between the strains with and without EftM (red arrows), but other obvious significant differences were not immediately apparent.

To examine the data in more depth, data sets were analyzed for proteins significantly changing between WT and Δ using a *p*-value of 0.05 as the cut-off for significance, while no minimum for fold-change was imposed. These values were chosen in line with our goal of identifying any potential differences for further exploration, even those that are weak. The same analysis was then performed comparing Comp to Δ, and the two lists cross-referenced for those proteins that showed overlap with fold-changes in the same direction (i.e. both higher in the strain with EftM or both higher in the strain without EftM). This final list of significantly changing proteins consisted of 12 proteins for Data Set #1, and 18 proteins for Data Set #2 (**Figure 6B**). Ultimately no proteins overlapped

and were deemed significant from both Data Sets, as evaluated by changes in protein abundance with $p<0.05$. Combining the lists yielded from Data Set #1 and Data Set #2 resulted in 30 candidate proteins. Twenty-three proteins were detected in both analyses, but only showed significance in one set. Six proteins showed significance in one set but were not detected (below the limit of detection) in the alternate set, meaning they cannot be strictly eliminated as proteins potentially impacted by EF-Tu lysine 5 trimethylation (**Figure 6B, 6C, bold**). The remaining protein was EftM, which despite being very lowly expressed, was detected in Data Set #2 as being present in the wild-type and complement and absent in the deletion strain, with a *p*-value of 1.33×10^{-7}. This result gave us additional confidence in the quality and accuracy of our analysis.

In addition to PAO1, strain PA14 was also analyzed for global proteome changes to eliminate potential strain bias in our conclusions. Again, the analysis of the PA14 strains (WT, Δ, Comp) was performed in biological triplicate at 25°C at mid-exponential phase. We observed just two proteins that were statistically significant. One was due to an absence of detection of the protein in all three biological replicates of Δ (**Supplemental Table 1**). This protein, PA14_24370, is a homolog of PA3076 and was detected in all three strains of the PAO1 Data Set #2 series with no significant changes between strains. The other is PA14_64050, which was detected in both PAO1 Data Set #1 and Data Set #2 with no significant changes.

Lastly we took advantage of our clinical isolate PAHM4, which contains a version of EftM with structural stability at elevated temperature, and performed

the same comparisons between the proteomes of these strains (WT, Δ, and Comp). For this analysis the strains were grown at 37°C instead of 25°C. Elevated growth temperature allowed us to capture data on any proteins that would have not been expressed in our 25°C analysis. In addition to temperature elevation, the PAHM4 data set is different in that the PAHM4 genome has 377,121 bp of DNA not found in our other two analyzed strains[18]. PAHM4 also expresses several gene clusters not normally translated in our standard laboratory reference strains, including those conferring a mucoid phenotype. Overall this allowed us to examine a widely different pool of expressed proteins to detect anything that would have been missed with our initial experimental conditions. Of the 10 candidate proteins derived from this strain comparison, the analysis of PAHM4 ultimately yielded the same conclusion (**Supplemental Table 2**) as for PAO1 and PA14. One protein (PAHM4_RS15825) was detected as being more abundant in the deletion strain but is encoded in a region of the genome that has no PAO1 or PA14 equivalent, meaning there is no way to compare this finding with other data sets. One (PAHM4_RS17805) is a homolog of PA2912, but this protein was not detected in PAO1 or PA14. The other eight proteins identified as significantly changing in PAHM4 were detected in at least one data set of PAO1 and PA14, where they were confidently determined to be not significant.

Discussion

P. aeruginosa is an opportunistic pathogen that can survive and thrive in a wide variety of environments and temperatures, including those which are terrestrial, freshwater, or marine ranging from 4°C to 42°C, as well as diverse hosts such as plants, worms, and mammals[21,22]. This wide range of inhabitable environments requires a flexible repertoire of gene expression to customize the proteomic output of the bacterium to the appropriate environment. Temperature sensing is one way in which to accomplish this goal. With over 6.26 million base pairs and 5,570 open reading frames in PAO1[23], timing of gene expression in the appropriate context is an important aspect of bacterial pathogenesis.

Temperature-mediated regulation of protein expression can be achieved by the cell in a variety of manners. One point of regulation can be transcriptional, through the use of temperature-sensitive transcription factors. Post-transcriptional control can be attained through RNA secondary structure, most commonly termed RNA thermometers. Post-translational control is accomplished through selective degradation of proteins with temperature-responsive proteases or inherent temperature sensitivity of the protein.

While not common, some proteins are thermoregulated at two levels of production, or “dual-thermoregulated”. One example is LcrF, a global regulator in *Yersinia pseudotuberculosis* that is thermoregulated at both the translational and transcriptional level. The 5’UTR of *lcrF* mRNA has an RNA thermometer, while transcription is repressed by nucleoid-like protein YmoA, a protein which is selectively degraded at 37°C[24].

We previously reported that EftM is intrinsically thermo-unstable, meaning at the down-regulated temperature (37°C), the enzyme itself was unfolded and inactive. Therefore EftM can be considered a “protein thermometer” that directly senses and responds to elevated temperature. Here we have uncovered a second layer of regulation for this protein, making it a dual thermoregulated methyltransferase. Not only does EftM itself unfold at 37°C, but transcription of the mRNA encoding this methyltransferase is also down-regulated, demonstrating an intriguing second level of thermoregulation. This is curious, as levels of *eftM* transcript in the cell are intrinsically relatively low. In fact, in three different studies of temperature regulation, *eftM* was undetectable at either temperature by whole-cell transcriptome profiling[2,5,9]. Down-regulation at 37°C further lowers these transcript levels in a seemingly redundant attenuation mechanism. It is interesting to note that in our hypermutator clinical isolate PAHM4, protein stability is enhanced, while transcriptional thermoregulation is relatively unaltered, leaving only one layer of thermoregulation in this particular strain for the shift from ambient to physiological temperature.

Since EftM trimethylates EF-Tu, the elongation factor that delivers charged tRNAs to the translating ribosome, we were interested in how this modulation would affect protein synthesis. However, we first needed to confirm that EF-Tu was the only substrate for EftM methylation. If there were other substrates or interactions, we would not be able to attribute any phenotype observed exclusively to EF-Tu trimethylation.

Our typical read-out for EftM activity is Western blot with a trimethyl lysine antibody. This works extremely well for detecting trimethylation of EF-Tu, as we observe no bands in whole cell lysates of an *eftM*-deleted strain, and one distinct band at the size of EF-Tu for strains containing active EftM. This method of detection presents problems for identifying substrates outside of EF-Tu, however. Therefore to test whether EftM modified other substrates we utilized an *in vitro* methylation assay that included EftM, radiolabeled SAM, and EF-Tu depleted *P. aeruginosa* lysates. Using a radiolabeled SAM on an EF-Tu depleted lysate was important for two reasons. First, observation of tritiated methyl transfer is non-specific in its readout, whereas an antibody is specific to trimethylation with reactivity that can be influenced by structural context. Secondly, EF-Tu can be over 10% of the total cellular protein in exponential phase of growth. Given that EF-Tu is a known substrate for EftM, the signal from EF-Tu has the potential to overshadow the signal from any other substrates. By eliminating EF-Tu in our whole-cell lysates through immunoprecipitation we were able to more sensitively see any other potential methyl-transfer event. After successfully depleting both 25°C and 37°C lysates for EF-Tu, we performed an *in vitro* methylation reaction with radio-labeled SAM and recombinant purified EftM. We observed no substrates for EftM. We then re-added EF-Tu to our reaction conditions and observed methyl transfer, showing that our reaction conditions were appropriate and our purified EftM was active. Overall we can conclude that EftM's only substrate for cellular methylation is EF-Tu.

This information allowed us to undertake a large-scale proteomic analysis of three distinct *P. aeruginosa* isolates to assess the impact that EftM-mediated EF-Tu trimethylation has on EF-Tu's canonical role in protein translation. With the proteomes of three strains and derivatives analyzed in biological triplicate, in an unbiased, label-free method, we observed no significant and reproducible differences in protein levels dependent on EF-Tu K5me^3 status. We chose to use mid-exponential phase of growth as our standard for our study given that EF-Tu is most prominent and active in translation during these conditions. A growth temperature of 25°C was chosen for PAO1 and PA14 because that is the temperature under which we see multiple layers of up-regulation in EftM expression, as reported previously[16] and in this current study. We also chose to analyze the PAHM4 proteome at 37°C to take advantage of our strain with increased EftM stability. Including this strain in our study widened our pan-proteome analysis to proteins beyond just those expressed in our laboratory strains, giving us confidence that the effect of EF-Tu trimethylation on canonical function was assessed with a wide variety of protein templates.

Out of the over 5,000 open-reading frames in *P. aeruginosa* PAO1 genome, we detected 2,327 unique proteins in Data Set #1 and 2,648 unique proteins in Data Set #2, with a total of 2,733 proteins observed between the two. We anticipated that, were EF-Tu K5me^3 impacting translation, we would see a change in abundance in a set of these expressed proteins. Yet from these candidates we have found a very small number, only eight, which we could not strictly eliminate as potentially changing in response to EftM presence. These

eight proteins (PA2115, PA1489, PA3984, PA2647, PA2897, PA4588; **Figure 6**. PAHM4_RS15825, PAHM4_RS17805, **Supplemental Table 2**) were determined to be significantly changing with a *p*-value <0.05, and were not detected in any additional data sets for comparison. Therefore these eight proteins are potentially differentially translated in response to EF-Tu lysine 5 methylation status. However, due to the modest fold-changes observed (1.085 → 2.197 fold), and the small number of final candidates with no apparent connections or similarities, we ultimately conclude that we there is little alteration of EF-Tu's canonical function in *P. aeruginosa* in response to K5 methylation status. It is possible that EF-Tu K5me^3 has impact under other conditions not tested, such as during stationary phase or nutrient limitation, or only alters lowly expressed proteins which are thus under the limit of detection of our instrumentation. Additionally, cellular pellets were washed to remove traces of growth media that would interfere with mass-spectrometry analysis. This processing removes secreted proteins from our samples. Despite these caveats, our investigation has provided the first analysis of EF-Tu K5me^3's impact on translation and has demonstrated no widespread effect of EftM on protein production.

Given that EftM does not broadly impact the proteome of *P. aeruginosa* through post-translational modification of EF-Tu, the previously-defined role of K5me^3 EF-Tu as an adhesin to platelet-activating factor receptor-containing epithelial cells[15] may be more important than previously appreciated, especially given the wide degree of conservation of EftM throughout the *Pseudomonads* and *Vibrio* genus. Dual thermoregulation also hints to the importance of

maintaining an appropriate level of EftM in the cell. EftM may be beneficial in the ambient environment or during the initial stages of infection, such as for adherence to epithelial cells. However, upon sensing a shift to 37°C, *P. aeruginosa* not only stops transcribing and therefore translating new EftM, but also rapidly inactivates the current pool of EftM through unfolding of the existing protein. There is no known demethylase associated with EftM, suggesting that the pool of methylated EF-Tu is all that remains of EftM's impact on the cell. This most likely takes several generations to dilute out, giving *P. aeruginosa* a gradual transition to unmethylated EF-Tu – in stark contrast to the immediate and redundant shut-off of EftM. PAHM4 has a form of EftM with increased thermostability. It will be interesting to elucidate the benefit to this particular strain gaining a thermostable form of EftM. It may be a benefit during chronic non-cystic fibrosis bronchiectasis, the infection from which this isolate was gathered, or there may be compensatory mutations elsewhere in the genome that eliminate the detriment to thermostable EftM. Further investigation into this strain may reveal a widened scope to EftM function in the cell.

Methods

Strains

PAO1, PA14, and PAHM4 with derivatives are described in **Supplemental Table 3**. PAO1Δ*eftM*, previously described, was created by deletion of 100 bp within the coding sequence of *eftM*[15]. PA14_08970::MAR2xT7 (PA14 *eftM*::tn) is a transposon mutant from the PA14 library[25]. PAHM4Δ*eftM* was made using the same general strategy as PAO1Δ*eftM* with two major differences: first, selection for double recombinants was performed with gentamicin 400 μg/ml instead of 30 μg/ml, and second, the gentamicin cassette was not subsequently removed.

Complementation strains were constructed using the Tn*7* system for site-specific integration into the *P. aeruginosa* chromosome[26]. Briefly, 500 bp upstream of the coding sequence for *eftM*, as well as the entire *eftM* coding sequence, were cloned from PAO1 (oligos SMP10+SMP45; **Supplemental Table 4**) or PAHM4 genomic DNA (oligos SMP17+SMP47; **Supplemental Table 4**) with the addition of a FLAG-tag at the C-terminal end of the protein. After PCR fragments were ligated into pUC18T-miniTn*7*T-Tp, the resulting construct was inserted in single copy at the Tn*7* attachment site by electroporation along with the helper plasmid pTNS3 into PAO1Δ*eftM* or PAHM4Δ*eftM*. Reporter strains for β-galactosidase assays were constructed using the CTX system for single-copy delivery to the *Pseudomonas* genome[19] with subsequent FRT-mediated excision of the plasmid backbone using pFLP2. The *rpoD* reporter plasmid was created by amplifying P_{rpoD} with primers SMP176+SMP177 and *lacZ* with SMP178+SMP179; the *eftM* reporter plasmid was created by amplifying P_{eftM}

with SMP189+SMP196 and *lacZ* with SMP179+SMP184. Fragments were seamlessly fused with the CTX plasmid using isothermal assembly to create translational fusions. All reporters were inserted into PAO1 through electroporation. A promoterless *lacZ* was inserted as a negative control. All plasmid constructs described were confirmed by Sanger sequencing and integrations confirmed through PCR.

Western immunoblots

P. aeruginosa was grown at indicated temperature in LB with rotation until mid-exponential phase (OD_{600}=0.8). Cultures were standardized such that an amount of cells equivalent to 1 mL of an OD_{600}=1 culture were harvested by centrifugation, then the cell pellet was resuspended in 100 µl Laemmli buffer. Suspensions were boiled for 5 minutes, 10 µl loaded into a 10% polyacrylamide gel, and samples were separated by SDS-PAGE. After transfer to PVDF, membranes were blocked and incubated in αTrimethyl Lysine (ImmuneChem ICP0601, blocked with 5% BSA), αEF-Tu (Hycult mAb 900, blocked with 5% skim milk), or αRpoA (Neoclone, blocked with 5% milk) at 4°C overnight with rocking. Next membranes were incubated with appropriate secondary antibody for one hour at room temperature, exposed with Pierce ECL Western Blotting Substrate (ThermoFisher), and imaged on a ChemiDoc MP Imaging System.

Depletion of EF-Tu from *P. aeruginosa* lysates and *in vitro* methylation

PAO1Δ*eftM* was grown to mid-exponential at 25°C or 37°C. Cells were lysed by sonication and depleted 5 times by incubating lysate with an α-EF-Tu antibody (Hycult Biotech). The complex was then immobilized by magnetic Protein G

Dynabeads (ThermoFisher) and a magnet while the rest of the lysate was transferred to a fresh tube. Lysate was collected after each round and analyzed by immunoblot using α-EF-Tu or α-RpoA (Neoclone; loading control). For the *in vitro* methylation reaction, 20 μg of the undepleted or final depleted lysate was incubated with 3.6 μg purified EftM (8 μM final concentration) and [^{3}H]-SAM at 25°C for 20 minutes, then separated by SDS-PAGE. The gel was dried, exposed to a tritium screen overnight, and scanned using a Typhoon imager. Recombinant *P. aeruginosa* EF-Tu (rEF-Tu) purified from *E. coli*[16] was added to final depleted lysate as a control and to determine the limit of detection.

RNA isolation and RT-qPCR

Strains were grown at the indicated temperature in LB with rotation until exponential phase was achieved (OD_{600}=0.8). After harvesting, cells were lysed and nucleic acid isolated with a MasterPure RNA Purification Kit (Epicentre) according to manufacturer's instructions. Residual contaminating DNA was removed with TURBO DNase (ThermoFisher) and isolated RNA was converted to cDNA with TaqMan Reverse Transription reagents (Invitrogen) prior to analysis with FastStart Universal SYBR Green Master (Rox; Roche) on a Roche LightCycler 96. Primers SMP155+SMP156 were utilized for *eftM;* oJV1040+oJV1041 for *omlA*; and *rpoD* F+*rpoD* R for *rpoD*[17] (**Supplemental Table 4**). Significance was determined by two-way ANOVA with Sidak multiple comparisons analysis (GraphPad Prism version 6.0).

5' Rapid amplification of cDNA ends (5' RACE)

mRNA was isolated as described above from strain PAO1 and PAHM4 grown at both 25°C and 37°C. 5'RACE was performed as per manufacturer's instructions using the 5'RACE System for Rapid Amplification of cDNA Ends, version 2.0 (Thermo Fisher). Briefly mRNA was converted to cDNA with Gene Specific Primer 1 (GSP1), 3'end of the cDNA tailed with a poly-C tail, and the resulting cDNA amplified with primer GSP2 before Sanger sequencing for the junction between the 5'untranslated region (UTR) and the poly-C tail. GSPs utilized for reverse transcription and nested amplification are SMP22 and SMP49 (**Supplemental Table 4**). Transcription start site determination allowed for promoter prediction using Virtual Footprint Version 3.0[27].

β-galactosidase assays

Reporter strains were grown in LB at 25°C or 37°C to mid-exponential phase prior to collection for the assay. After centrifugation, pellets were resuspended in 1 mL Z buffer (60 mM sodium phosphate dibasic, 40 mM sodium phosphate monobasic, 10 mM potassium chloride, 1 mM magnesium sulfate, 50 mM β-mercaptoethanol, pH 7.0). Sample aliquots were added to Z buffer to a total volume of 1 mL (200 µl of P_{rpoD} was added to 800 µl Z buffer; 900 µl P_{eftM} to 100 µl Z buffer). Then 100 µl chloroform 50 µl 0.1% SDS were added to each sample, vortexed, and samples incubated at 30°C. After addition of 200 µl of 4 mg/mL ortho-nitrophenyl-β-galactoside, reactions were timed until the development of a yellow color, at which point 400 µl of 1 M sodium carbonate was added to terminate the reaction. Cell debris was removed by centrifugation and the sample supernatant was read at 420 nm. Miller units were calculated as follows: (1,000 x

A_{420}) / (reaction time in minutes x cell suspension volume in mL x OD_{600}). Significance was determined by two-way ANOVA with Sidak multiple comparisons analysis (GraphPad Prism version 6.0).

Proteomic sample preparation

P. aeruginosa was grown overnight at 25°C in liquid culture with aeration. After back-dilution to OD_{600}=0.05, cells were allowed to grow until exponential phase was achieved (OD_{600}=0.8). Cells were harvested by centrifugation and washed with sterile PBS before re-pelleting and storage at -80°C until analysis. After thawing, the cell pellet was lysed in 200 µL of urea lysis buffer (8M urea, 100 mM $NaHPO_4$, pH 8.5), including 2 µL (100x stock) HALT protease and phosphatase inhibitor cocktail (Pierce). Protein supernatants were transferred to new 1.5 mL Eppendorf tubes and sonicated (Sonic Dismembrator, Fisher Scientific) 3 times for 5 seconds with 15 second intervals of rest at 30% amplitude to disrupt nucleic acids and subsequently vortexed. Protein concentration was determined by the bicinchoninic acid (BCA) method, and samples were frozen in aliquots at −80°C. Protein homogenates equivalent to 100 µg of total protein were then treated with 1 mM dithiothreitol (DTT) at 25°C for 30 minutes, followed by 5 mM iodoacetimide (IAA) at 25°C for 30 minutes in the dark. The lysate was next digested with 1:100 (w/w) lysyl endopeptidase (Wako) at 25°C overnight. The samples were then diluted with 50 mM NH_4HCO_3 to a final concentration of ~1M urea and further digested overnight with 1:50 (w/w) trypsin (Promega) at 25°C. Resulting peptides were desalted with a Sep-Pak C18 column (Waters) and dried under vacuum.

LC-MS/MS analysis

Dried peptides were resuspended in 100 µL of peptide loading buffer (0.1% formic acid, 0.03% trifluoroacetic acid, 1% acetonitrile). Peptide mixtures (2 µL) were separated on a self-packed C18 (1.9 µm Dr. Maisch, Germany) fused silica column (25 cm x 75 µM internal diameter (ID); New Objective, Woburn, MA) by a Dionex Ultimate 3000 RSLCNano and monitored on a Fusion mass spectrometer (ThermoFisher Scientific, San Jose, CA). Elution was performed over a 120-minute gradient at a rate of 300 nl/minute with buffer B ranging from 3% to 80% (buffer A: 0.1% formic acid in water, buffer B: 0.1 % formic in acetonitrile). The mass spectrometer cycle was programmed to collect at the top speed for 3-second cycles. The MS scans (400-1600 m/z range, 200,000 AGC, 50 ms maximum ion time) were collected at a resolution of 120,000 at m/z 200 in profile mode and the HCD MS/MS spectra (0.7 m/z isolation width, 30% collision energy, 10,000 AGC target, 35 ms maximum ion time) were detected in the ion trap. Dynamic exclusion was set to exclude previous sequenced precursor ions for 20 seconds within a 10 ppm window. Precursor ions with +1, and +8 or higher charge states were excluded from sequencing.

Proteomic data analysis

RAW data for the samples was analyzed using MaxQuant v1.5.2.8 with Thermo Foundation 2.0 for RAW file reading capability. The search engine Andromeda, integrated into MaxQuant, was used to search strain-appropriate *Pseudomonas* protein databases (Downloaded from pseudomonas.com[28]), plus 245 contaminant proteins from the common repository of adventitious proteins

(cRAP) built into MaxQuant. Methionine oxidation (+15.9949 Da), asparagine and glutamine deamidation (+0.9840 Da), and protein N-terminal acetylation (+42.0106 Da) were variable modifications (up to 5 allowed per peptide); cysteine was assigned a fixed carbamidomethyl modification (+57.0215 Da). Only fully tryptic peptides were considered with up to 2 miscleavages in the database search. A precursor mass tolerance of ±20 ppm was applied prior to mass accuracy calibration and ±4.5 ppm after internal MaxQuant calibration. The match between runs option was used and quantification was based on final normalized LFQ outputs.

For both PAO1 Data Set 1 and Data Set 2, wild-type (WT), deletion (Δ), and complement (Comp) strains were grown and analyzed in biological triplicate. Signal was $\log_2$-transformed and averaged across the biological triplicates, with p-values determined within the biological triplicates by ANOVA with Tukey post-hoc pairwise comparison or two tailed *t*-test when ANOVA was not possible. Results were filtered for proteins in which $p<0.05$ for both WT vs. Δ and Comp vs. Δ with fold changes occurring in the same direction. The same was repeated with PA14 strains and PAHM4 strains.

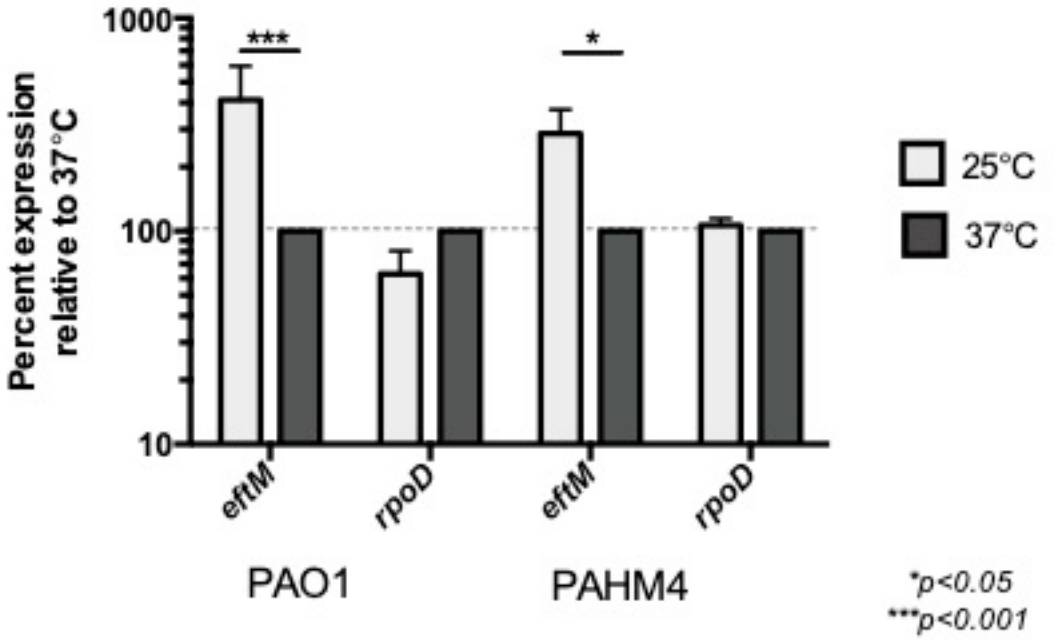

Figure 1: *P. aeruginosa* has higher mRNA steady-state levels of *eftM* at 25°C compared to 37°C. RT-qPCR was utilized to assess steady-state mRNA levels from mid-exponential cells grown at 25°C compared to those grown at 37°C. CT values for *eftM* were normalized to *omlA* as an internal control, then each temperature pair was compared by setting 37°C as 100%. *rpoD* was evaluated in the same manner as a control for no change in response to temperature. Error bars represent standard deviation of the mean. Significance was determined by two-way ANOVA with Sidak multiple comparisons analysis. N=3.

A

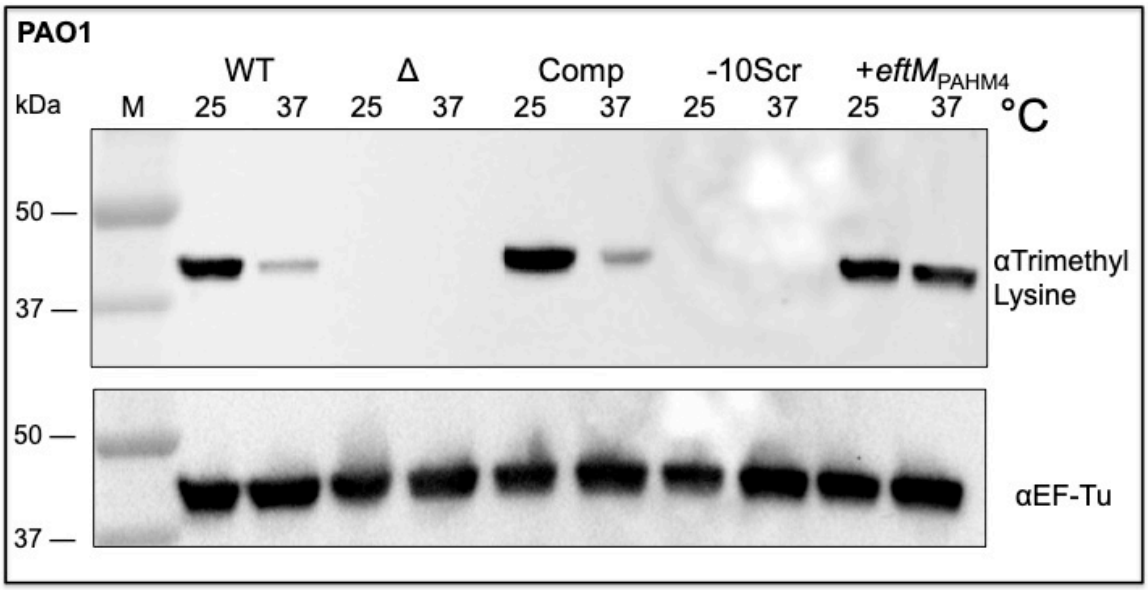
PAO1
WT
Δ
Comp
-10Scr
+eftM PAHM4
kDa
M
25
37
25
37
25
37
25
37
25
37
°C
50
37
αTrimethyl Lysine
50
37
αEF-Tu

B

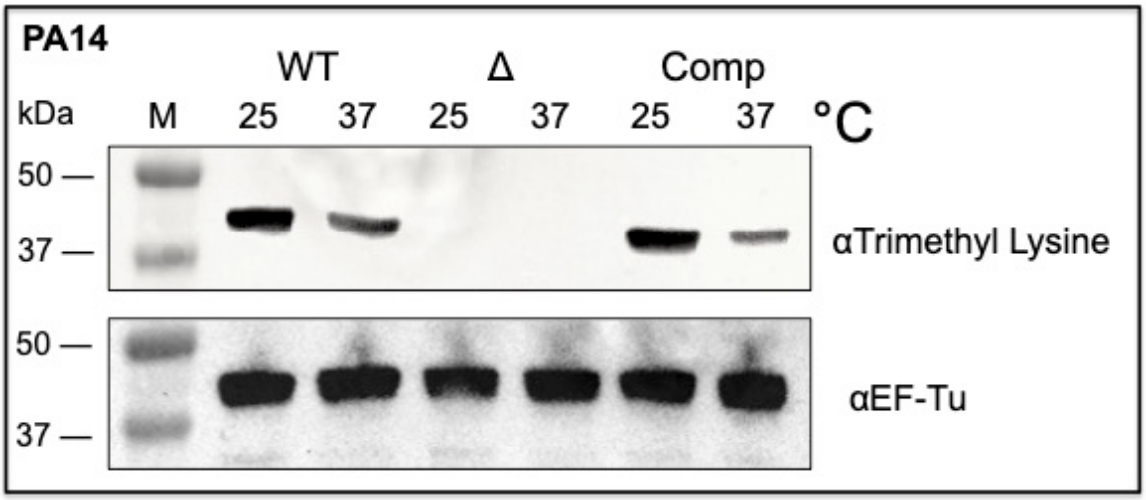
PA14
WT
Δ
Comp
kDa
M
25
37
25
37
25
37
°C
50
37
αTrimethyl Lysine
50
37
αEF-Tu

C

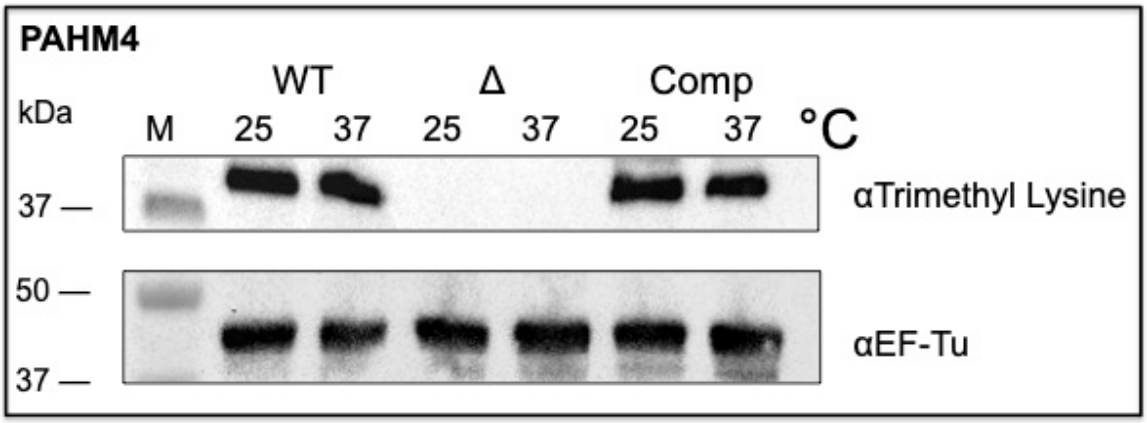
PAHM4
WT
Δ
Comp
kDa
M
25
37
25
37
25
37
°C
37
αTrimethyl Lysine
50
37
αEF-Tu

Figure 2: Survey of EftM activity in various strains. Western immunoblot with αTrimethyl Lysine (top) and αEF-Tu (bottom; loading control) for the following samples grown to mid-log at 25°C and 37°C:

A. PAO1 strain set. WT=PAO1, Δ=PAO1Δ*eftM*, Comp=PAO1Δ*eftM* *att*Tn7::$P_{PAO1\text{-}500}$-$eftM_{PAO1}$, -10Scr=PAO1Δ*eftM* *att*Tn7::$P_{PAO1\text{-}10SCR}$-$eftM_{PAO1}$, +$eftM_{PAHM4}$=PAO1ΔeftM *att*Tn7::$P_{HM4\text{-}500}$-$eftM_{HM4}$.

B. PA14 strain set. WT=PA14, Δ=PA14 *eftM*::tn, Comp=PA14 *eftM*::tn *att*Tn7:: $P_{PAO1\text{-}10SCR}$-$eftM_{PAO1}$.

C. PAHM4 strain set. WT=PAHM4, Δ=PAHM4Δ*eftM*, Comp=PAHM4Δ*eftM* *att*Tn7::$P_{PAHM4\text{-}500}$-$eftM_{PAHM4}$.

A

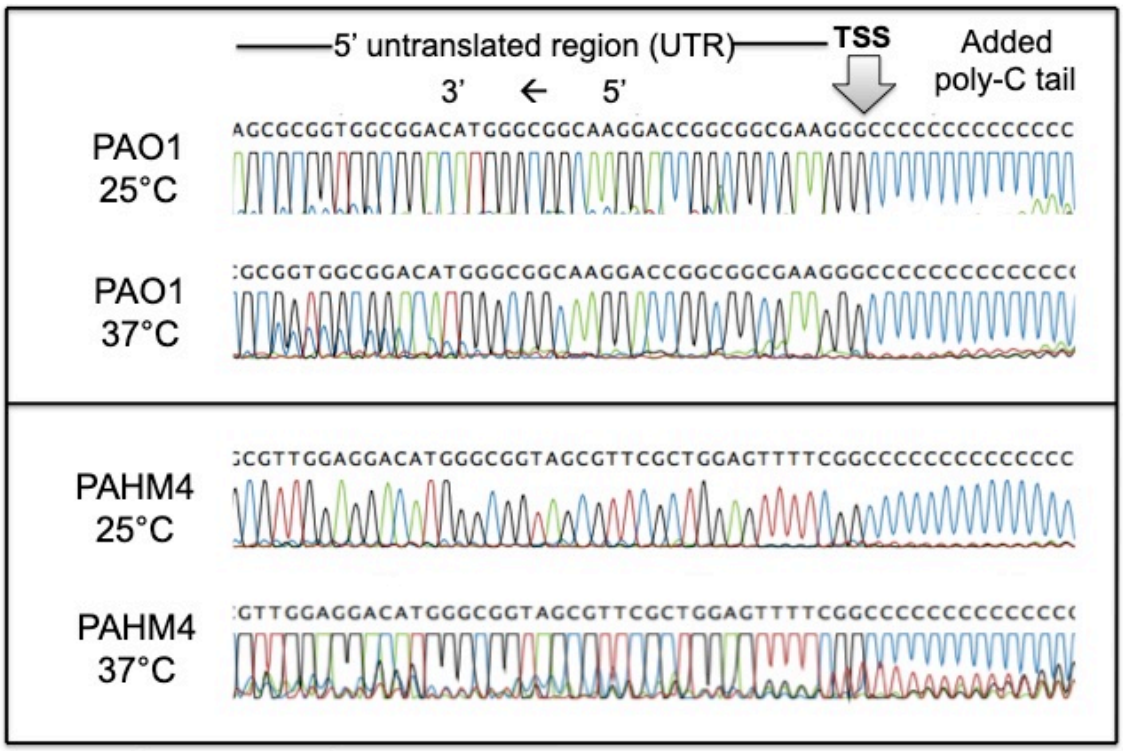

Reverse Complement Sequencing Traces

B

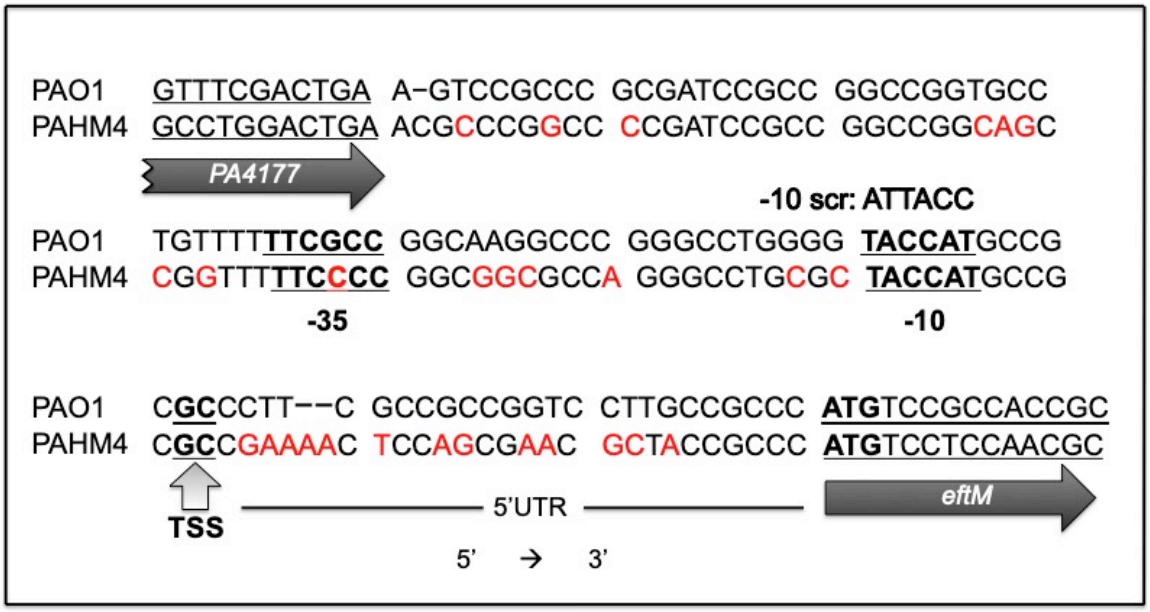

Figure 3: Mapping of *eftM* transcription start site and prediction of the promoter.

A: Sequencing trace files. 5'RACE was utilized to define the transcription start site for *eftM* in PAO1 and PAHM4 at 25°C and 37°C, with the same transcription start site (grey arrow) observed under both temperatures. Traces are the reverse complement of the 5' untranslated region (UTR), with the transcription start site defined as the point of junction with the assay-added poly-nucleotide tail.

B: Sequences of the *eftM* intergenic region for PAO1 and PAHM4 are aligned with differences in red. Transcription Start Site (TSS) revealed in (A) is annotated, and the predicted -10 and -35 underlined. The sequence for the scrambled promoter strain (-10 Scr; PAO1Δ*eftM att*Tn7::$P_{eftM\text{-}10SCR}$-*eftM* FLAG) is detailed above the predicted -10 region.

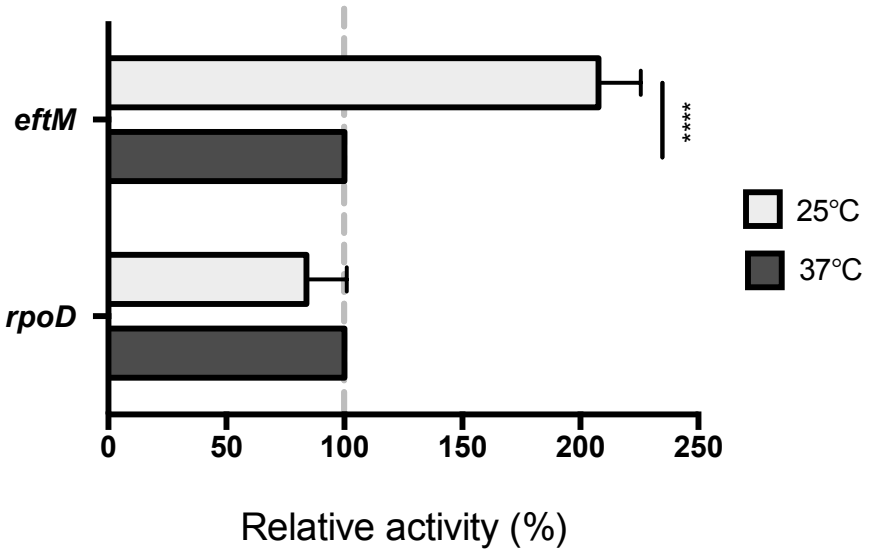

Figure 4: Thermoregulation is at the level of transcription initiation.

β-galactosidase assay of the P_{eftM} reporter strain (PAO1 *att*CTX::P_{eftM}-*lacZ*) grown to mid-exponential phase at either 25°C or 37°C. Miller units of each 25°C sample were normalized as a percent reactivity of the corresponding sample grown at 37°C. P_{rpoD} reporter strain (PAO1 *att*CTX::P_{rpoD}-*lacZ*) was used as a control. Error bars represent standard deviation of the mean; significance was determined by two-way ANOVA with Sidak multiple comparisons analysis. N=3. *****p<0.0001.*

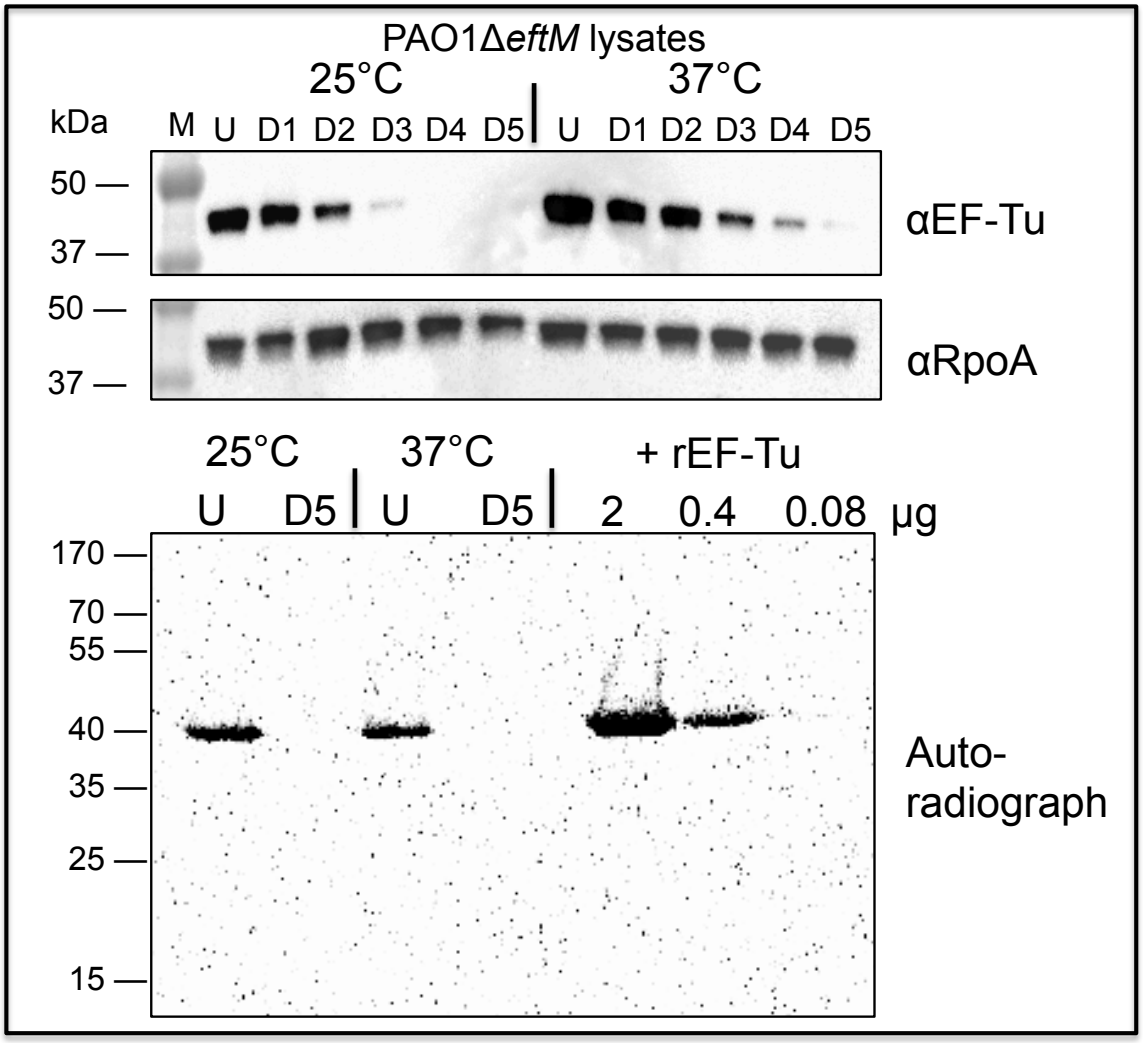

Figure 5: EF-Tu is the only substrate for EftM.

A: PAO1Δ*eftM* was grown to mid-exponential phase at 25°C or 37°C. The soluble lysate (U) from each sample was depleted for EF-Tu five subsequent times (D1-D5) by immunoprecipitation and analyzed by Western immunoblot using α-EF-Tu or α-RpoA (loading control).

B: 20 μg of undepleted (U) or fully depleted (D5) lysate was incubated with 3.6 μg purified EftM (8 μM final concentration) and [^{3}H]-SAM at 25°C for 20 minutes

and separated by SDS-PAGE. The gel was dried and exposed to a tritium screen overnight for the presence of proteins methylated by EftM. Recombinant EF-Tu (rEF-Tu) was added to D5 as a control for EftM enzyme activity and to indicate limit of detection.

A

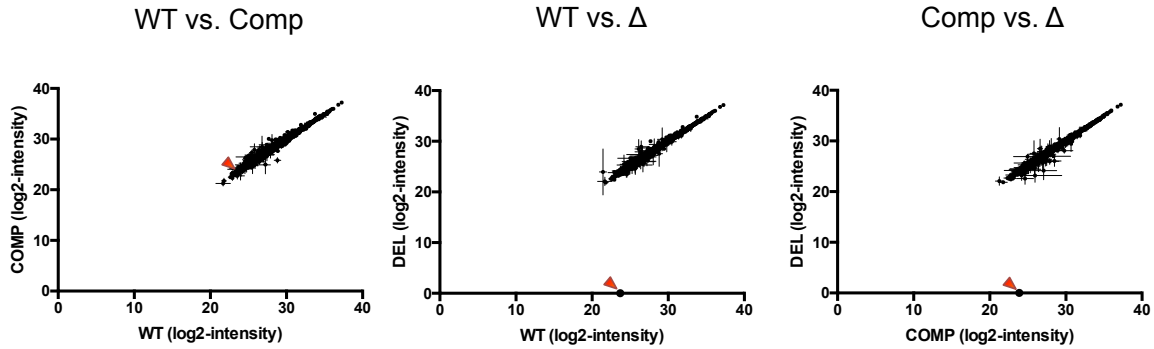

B

	Data Set 1				Corresponding Values from Data Set 2			
	Fold change WT vs Δ	p-value WT vs Δ	Fold change Comp vs Δ	p-value Comp vs Δ	Fold change WT vs Δ	p-value WT vs Δ	Fold change Comp vs Δ	p-value Comp vs Δ
PA5412 ★	2.94E+07	2.72E-08	3.55E+07	3.72E-10	1.441	0.242	-1.303	0.436
PA2115	2.197	0.004	1.601	0.040	N.D.	N/A	N.D.	N/A
PA1193	1.584	0.024	1.772	0.010	-1.100	0.550	-1.171	0.311
PA2812	1.500	0.032	1.606	0.017	1.139	0.610	1.083	0.824
PA3555 (*arnD*)	1.368	0.001	1.185	0.019	-1.120	0.556	-1.018	0.984
PA4729 (*panB*)	-1.336	0.004	-1.200	0.035	-1.021	0.824	-1.065	0.242
PA3849	1.308	0.015	1.249	0.033	-1.044	0.677	-1.031	0.811
PA0608	1.249	0.018	1.395	0.003	-1.006	0.967	-1.041	0.340
PA4258 (*rplV*)	1.247	0.040	1.237	0.046	1.168	0.041	1.101	0.193
PA4263 (*rplC*)	1.209	0.010	1.158	0.030	1.084	0.206	1.035	0.699
PA0484	1.191	0.043	1.182	0.037	-1.087	0.942	-1.066	0.957
PA5133	1.156	0.021	1.167	0.016	1.108	0.353	1.035	0.872

C

	Data Set 2					Corresponding Values from Data Set 1			
	Fold change WT vs Δ	p-value WT vs Δ	Fold change Comp vs Δ	p-value Comp vs Δ		Fold change WT vs Δ	p-value WT vs Δ	Fold change Comp vs Δ	p-value Comp vs Δ
PA4178 (*eftM*) ★	1.35E+07	1.34E-07	1.54E+07	1.34E-09		N.D.	N/A	N.D.	N/A
PA1489	-1.994	0.004	-1.994	0.029		N.D.	N/A	N.D.	N/A
PA5545	-1.553	0.006	-1.553	0.036	♯	-191.5	0.374	1.505	0.960
PA3984 (*cutE*)	-1.472	3.915E-04	-1.190	0.022		N.D.	N/A	N.D.	N/A
PA3642 (*rnhB*)	1.413	0.019	1.633	0.004		1.452	0.027	1.239	0.178
PA2647 (*nuoL*)	1.375	1.078E-04	1.099	0.047		N.D.	N/A	N.D.	N/A
PA1822 (*fimL*)	-1.360	1.250E-05	-1.069	0.038		1.170	0.159	-1.041	0.848
PA3658 (*glnD*)	-1.355	0.002	-1.355	0.033	♯	-46010	0.116	1.117	0.989
PA2897	-1.293	0.013	-1.293	0.044		N.D.	N/A	N.D.	N/A
PA3796	-1.278	0.018	-1.278	0.020		1.419	0.438	-1.104	0.927
PA5073	-1.272	0.001	-1.272	0.001		1.692	0.388	1.455	0.554
PA1455 (*fliA*)	-1.247	0.027	-1.247	0.030		1.698	0.147	1.454	0.320
PA4588 (*gdhA*)	1.240	0.042	1.263	0.030		N.D.	N/A	N.D.	N/A
PA5553 (*atpC*)	1.214	0.021	1.175	0.045		1.143	0.271	-1.012	0.986
PA4453	1.206	0.013	1.205	0.014		1.149	0.275	1.130	0.350
PA1049 (*pdxH*)	-1.139	0.002	-1.139	0.012		1.044	0.942	-1.111	0.714
PA0156	-1.128	0.023	-1.128	0.005		1.036	0.970	-1.080	0.868
PA3047	-1.099	0.038	-1.099	0.005		1.395	0.067	1.232	0.255

Figure 6: Whole-cell proteomic analysis reveals that trimethylation of EF-Tu by EftM has little impact on the proteome.

A: Plot of the log_2-transformed label-free quantification (LFQ) intensities for all proteins detected in PAO1 Data Set 2. EftM is denoted by the red arrows.

B: Proteins from PAO1 Data Set 1 significantly changing in Δ (PAO1Δ*eftM*) compared to WT (PAO1) and Comp (PAO1Δ*eftM att*Tn7::P_{eftM}-*eftM*-FLAG). The corresponding values from Data Set 2 are listed to the right for comparison.

C: Proteins from Data Set 2 significantly changing in Δ (PAO1Δ*eftM*) compared to WT (PAO1) and Comp (PAO1Δ*eftM att*Tn7::P_{eftM}-*eftM*-FLAG). The corresponding values from Data Set 1 are listed to the right for comparison.

Bold; proteins detected in one data set only. Positive fold change; abundance is higher in strain with EftM. Negative fold change; abundance is higher in strain without EftM. ⋆ denotes that the protein was not detected in all three biological triplicates of Δ; ♯ denotes not detected in biological triplicates of WT. N.D; not detected in all three biological triplicates of all three strains (WT, Δ, Comp) for that data set. N/A; not applicable.

Supplemental Table 1

		Significant Proteins from PA14				Corresponding Values from PAO1 Data Set 1				Corresponding Values from PAO1 Data Set 2				Corresponding Values from PAHM4			
		Fold change WT vs Δ	p-value WT vs Δ	Fold change Comp vs Δ	p-value Comp vs Δ	Fold change WT vs Δ	p-value WT vs Δ	Fold change Comp vs Δ	p-value Comp vs Δ	Fold change WT vs Δ	p-value WT vs Δ	Fold change Comp vs Δ	p-value Comp vs Δ	Fold change WT vs Δ	p-value WT vs Δ	Fold change Comp vs Δ	p-value Comp vs Δ
PA14_24370	⋆	**1.3E+07**	**4.2E-10**	**1.1E+07**	**3.1E-11**	N.D.	N/A	N.D.	N/A	-1.298	0.367	-1.094	0.870	-1.212	0.345	-1.288	0.190
PA14_64050	♯	**-1.3E+05**	**0.003**	**-1.283**	**0.019**	1.066	0.985	1.037	0.991	-1.680	0.056	-1.467	0.151	N.D.	N/A	N.D.	N/A

Supplemental Table 2

		Significant Proteins from PAHM4				Corresponding Values from PAO1 Data Set 1				Corresponding Values from PAO1 Data Set 2					Corresponding Values from PA14			
		Fold change WT vs Δ	p-value WT vs Δ	Fold change Comp vs Δ	p-value Comp vs Δ	Fold change WT vs Δ	p-value WT vs Δ	Fold change Comp vs Δ	p-value Comp vs Δ	Fold change WT vs Δ	p-value WT vs Δ	Fold change Comp vs Δ	p-value Comp vs Δ		Fold change WT vs Δ	p-value WT vs Δ	Fold change Comp vs Δ	p-value Comp vs Δ
PAHM4_RS15825	N/A	**-1.647**	**0.015**	**-1.668**	**0.014**	N/A	N/A	N/A	N/A	N/A	N/A	N/A	N/A		N/A	N/A	N/A	N/A
PAHM4_RS08095	(PA5074)	**-1.480**	**2.914E-04**	**-1.153**	**0.044**	1.967	0.083	1.588	0.241	-1.164	0.343	-1.083	0.713		1.088	0.919	-1.072	0.949
PAHM4_RS12930	(PA3712)	**1.457**	**0.012**	**1.476**	**0.010**	1.179	0.642	1.066	0.932	-1.255	0.091	-1.085	0.645		1.242	0.497	-1.139	0.758
PAHM4_RS25435	(PA3106)	**-1.394**	**0.030**	**-1.363**	**0.039**	-1.191	0.705	-1.025	0.993	-1.106	0.430	1.077	0.609		-1.057	0.928	1.129	0.716
PAHM4_RS17805	(PA2912)	**-1.348**	**4.795E-06**	**-1.085**	**0.007**	N.D.	N/A	N.D.	N/A	N.D.	N/A	N.D.	N/A		N.D.	N/A	N.D.	N/A
PAHM4_RS18780	(PA1117)	**-1.330**	**0.020**	**-1.336**	**0.018**	1.344	0.640	1.651	0.395	-1.031	0.980	1.094	0.841	♯	-319.367	0.837	1.013	0.999
PAHM4_RS16925	(PA0354)	**-1.242**	**0.001**	**-1.133**	**0.015**	1.053	0.872	-1.250	0.152	1.000	1.000	1.010	0.979		-1.076	0.832	1.014	0.993
PAHM4_RS10405	(PA1880)	**-1.235**	**0.021**	**-1.287**	**0.009**	N.D.	N/A	N.D.	N/A	-1.070	0.926	-1.189	0.770		1.091	0.868	-1.097	0.851
PAHM4_RS00050	(PA0225)	**-1.138**	**0.042**	**-1.137**	**0.044**	N.D.	N/A	N.D.	N/A	-1.347	0.480	1.139	0.856		N.D.	N/A	N.D.	N/A
PAHM4_RS05090	(PA4329)	**1.098**	**0.001**	**1.052**	**0.024**	1.045	0.781	1.089	0.437	1.046	0.658	-1.058	0.535		1.142	0.461	-1.046	0.902

Supplemental Table 1: Whole-cell proteomic analysis of PA14 reveals that trimethylation of EF-Tu by EftM has little impact on the proteome.

Proteins from PA14 significantly changing in Δ (PA14 *eftM*::tn) compared to WT (PA14) and Comp (PA14 *eftM::*tn *att*Tn7::P_{eftM}-*eftM*-FLAG). The corresponding values from PAO1 and PAHM4 are listed to the right for comparison.

Bold; proteins detected in one data set only. Positive fold change; abundance is higher in strain with EftM. Negative fold change; abundance is higher in strain without EftM. ⋆ denotes that the protein was not detected in all three biological triplicates of Δ; ♯ denotes not detected in biological triplicates of WT. N.D; not detected in all three biological triplicates of all three strains (WT, Δ, Comp) for that data set. N/A; not applicable.

Supplemental Table 2: Whole-cell proteomic analysis of PAHM4 reveals that trimethylation of EF-Tu by EftM has little impact on the proteome.

Proteins from PAHM4 significantly changing in Δ (PAHM4Δ*eftM*) compared to WT (PAHM4) and Comp (PAHM4Δ*eftM att*Tn7::$P_{eftM\text{-}HM4}$-$eftM_{HM4}$-FLAG). The corresponding values from PAO1 and PA14 are listed to the right for comparison.

Bold; proteins detected in one data set only. Positive fold change; abundance is higher in strain with EftM. Negative fold change; abundance is higher in strain without EftM. ⋆ denotes that the protein was not detected in all three biological triplicates of Δ; ♯ denotes not detected in biological triplicates of WT. N.D; not detected in all three biological triplicates of all three strains (WT, Δ, Comp) for that data set. N/A; not applicable.

Supplemental Table 3. Strain List

ID	Genotype	Reference
PAO1	*P. aeruginosa* PAO1	Barbier, Owings *et al* 2013
PAO1Δ*eftM*	PAO1 *eftM* Δ255-487	Barbier, Owings *et al* 2013
PASP09	PAO1ΔeftM *att*Tn7::P_{eftM}-$eftM_{PAO1}$-FLAG	This Study
PASP106	PAO1ΔeftM *att*Tn7::$P_{eftM\text{-}10SCR}$-$eftM_{PAO1}$-FLAG	This Study
PASP20	PAO1ΔeftM *att*Tn7::P_{eftM}-$eftM_{HM4}$-FLAG	This Study
PASP76	PAO1 *att*CTX::P_{eftM}-*lacZ FRT*	This Study
PASP65	PAO1 *att*CTX::P_{rpoD}-*lacZ FRT*	This Study
PA14	*P. aeruginosa* PA14	Rahme, Stevens *et al.* 1995
PA14 *eftM*::tn	PA14_08970::MAR2xT7	Liberati *et al.* 2006
PASP12	PA14 *eftM::*tn *att*Tn7::P_{eftM}-$eftM_{PAO1}$-FLAG	This Study
PAHM4	*P. aeruginosa* PAHM4	Varga *et al.* 2015
PAHM4Δ*eftM*	PAHM4 *eftM*Δ255-487	This Study
PASP51	PAHM4Δ*eftM att*Tn7::P_{eftM}-$eftM_{HM4}$-FLAG	This Study

Supplemental Table 4. Oligonucleotides

ID	Target	Sequence
SMP10	complementation of *eftM* (PAO1)	TGG ATC CCC AGA CCT TCC ACG GCA GTT G
SMP45	complementation of *eftM* (PAO1) with FLAG tag	TGA ATT CCT ACT TGT CAT CGT CAT CCT TGT AGT CGC GCT TCA CGC AGA C
SMP216	creation of scrambled -10 promoter	AAG GCC CGG GCC TGG GGA TTA CCG CCG CGC CCT TCG CCG CCG GTC C
SMP217	creation of scrambled -10 promoter	CAG GTG CTG CAG CTC GGC GAA
SMP17	complementation of eftM (PAHM4)	TGG ATC CAA CCA GAT CCT CCA CGG CAG TTG
SMP47	complementation of eftM (PAHM4) with FLAG tag	TGA ATT CCT ACT TGT CAT CGT CAT CCT TGT AGT CGC GCT TGA TGC AGG C
SMP189	P_{eftM}-*lacZ* reporter	TGG ATC CCC CGG GCT GCA GGA GTC CGC CCG CGA TCC GCC GGC CGG T
SMP196	P_{eftM}-*lacZ* reporter	TCA TGG TCA TGG GCG GCA AGG ACC GGC GGC GAA GGG CGC
SMP184	P_{eftM}-*lacZ* reporter	TCC TTG CCG CCC ATG ACC ATG ATT ACG GAT TC
SMP179	P_{eftM}-*lacZ* and P_{rpoD}-*lacZ* reporter	CGA GGT CGA CGG TAT CGA TAA GCT TTA TTT TTG ACA CCA GAC C
SMP176	P_{rpoD}-*lacZ* reporter	TGG ATC CCC CGG GCT GCA GGC CTT GAA AAG CAG TTC TTC GAC
SMP177	P_{rpoD}-*lacZ* reporter	TCA TGG TCA TAA CAC CCT ATC CAC TGA AGG T
SMP178	P_{rpoD}-*lacZ* reporter	GGA TAG GGT GTT ATG ACC ATG ATT ACG GAT TC
SMP155	*eftM* qPCR	GAC ATC AAC CAG CCG ATG CTC
SMP156	*eftM* qPCR	CAG CCC TGC GTT GTA GTG GA
rpoD F	*rpoD* qPCR	GGG CGA AGA AGG AAA TGG TC
rpoD R	*rpoD* qPCR	CAG GTG GCG TAG GTG GAG AA
oJV1040	*omlA* qPCR	AAA ATC GAC ATC CAG CAA GG
oJV1041	*omlA* qPCR	GGT CGC TGT CGT TGA AGA AC
SMP22	*eftM* 5' RACE GSP1	TGC GTT GTA GTG GAT CGA ATA G
SMP49	*eftM* 5' RACE GSP2	GAG CAT CGG CTG GTT GAT GTC

References

1 Mathee, K. *et al.* Dynamics of Pseudomonas aeruginosa genome evolution. *Proc Natl Acad Sci U S A* **105**, 3100-3105, doi:10.1073/pnas.0711982105 (2008).

2 Barbier, M. *et al.* From the environment to the host: re-wiring of the transcriptome of Pseudomonas aeruginosa from 22 degrees C to 37 degrees C. *PLoS One* **9**, e89941, doi:10.1371/journal.pone.0089941 (2014).

3 Lam, O., Wheeler, J. & Tang, C. M. Thermal control of virulence factors in bacteria: a hot topic. *Virulence* **5**, 852-862, doi:10.4161/21505594.2014.970949 (2014).

4 Wilderman, P. J. *et al.* Characterization of an endoprotease (PrpL) encoded by a PvdS-regulated gene in Pseudomonas aeruginosa. *Infect Immun* **69**, 5385-5394 (2001).

5 Termine, E. & Michel, G. P. Transcriptome and secretome analyses of the adaptive response of Pseudomonas aeruginosa to suboptimal growth temperature. *Int Microbiol* **12**, 7-12 (2009).

6 Thompson, R. C. EFTu provides an internal kinetic standard for translational accuracy. *Trends Biochem Sci* **13**, 91-93 (1988).

7 Widjaja, M. *et al.* Elongation factor Tu is a multifunctional and processed moonlighting protein. *Sci Rep* **7**, 11227, doi:10.1038/s41598-017-10644-z (2017).

8 Barbier, M. *et al.* Novel phosphorylcholine-containing protein of Pseudomonas aeruginosa chronic infection isolates interacts with airway epithelial cells. *J Infect Dis* **197**, 465-473, doi:10.1086/525048 (2008).

9 Wurtzel, O. *et al.* The single-nucleotide resolution transcriptome of Pseudomonas aeruginosa grown in body temperature. *PLoS Pathog* **8**, e1002945, doi:10.1371/journal.ppat.1002945 (2012).

10 Furano, A. V. Content of elongation factor Tu in Escherichia coli. *Proc Natl Acad Sci U S A* **72**, 4780-4784 (1975).

11 Noel, J. K. & Whitford, P. C. How EF-Tu can contribute to efficient proofreading of aa-tRNA by the ribosome. *Nat Commun* **7**, 13314, doi:10.1038/ncomms13314 (2016).

12 Abdulkarim, F., Tuohy, T. M., Buckingham, R. H. & Hughes, D. Missense substitutions lethal to essential functions of EF-Tu. *Biochimie* **73**, 1457-1464 (1991).

13 Van Noort, J. M. *et al.* Methylation in vivo of elongation factor EF-Tu at lysine-56 decreases the rate of tRNA-dependent GTP hydrolysis. *Eur J Biochem* **160**, 557-561 (1986).

14 Cruz, J. W. *et al.* Doc toxin is a kinase that inactivates elongation factor Tu. *J Biol Chem* **289**, 7788-7798, doi:10.1074/jbc.M113.544429 (2014).

15 Barbier, M. *et al.* Lysine trimethylation of EF-Tu mimics platelet-activating factor to initiate Pseudomonas aeruginosa pneumonia. *MBio* **4**, e00207-00213, doi:10.1128/mBio.00207-13 (2013).

16 Owings, J. P. *et al.* Pseudomonas aeruginosa EftM Is a Thermoregulated Methyltransferase. *J Biol Chem* **291**, 3280-3290, doi:10.1074/jbc.M115.706853 (2016).

17 Savli, H. *et al.* Expression stability of six housekeeping genes: A proposal for resistance gene quantification studies of Pseudomonas aeruginosa by real-time quantitative RT-PCR. *J Med Microbiol* **52**, 403-408, doi:10.1099/jmm.0.05132-0 (2003).

18 Varga, J. J. *et al.* Genotypic and phenotypic analyses of a Pseudomonas aeruginosa chronic bronchiectasis isolate reveal differences from cystic fibrosis

and laboratory strains. *BMC Genomics* **16**, 883, doi:10.1186/s12864-015-2069-0 (2015).

19 Hoang, T. T., Kutchma, A. J., Becher, A. & Schweizer, H. P. Integration-proficient plasmids for Pseudomonas aeruginosa: site-specific integration and use for engineering of reporter and expression strains. *Plasmid* **43**, 59-72, doi:10.1006/plas.1999.1441 (2000).

20 Ude, S. *et al.* Translation elongation factor EF-P alleviates ribosome stalling at polyproline stretches. *Science* **339**, 82-85, doi:10.1126/science.1228985 (2013).

21 LaBauve, A. E. & Wargo, M. J. Growth and laboratory maintenance of Pseudomonas aeruginosa. *Curr Protoc Microbiol* **Chapter 6**, Unit 6E 1, doi:10.1002/9780471729259.mc06e01s25 (2012).

22 Spiers, A. J., Buckling, A. & Rainey, P. B. The causes of Pseudomonas diversity. *Microbiology* **146 (Pt 10)**, 2345-2350, doi:10.1099/00221287-146-10-2345 (2000).

23 Stover, C. K. *et al.* Complete genome sequence of Pseudomonas aeruginosa PAO1, an opportunistic pathogen. *Nature* **406**, 959-964, doi:10.1038/35023079 (2000).

24 Bohme, K. *et al.* Concerted actions of a thermo-labile regulator and a unique intergenic RNA thermosensor control Yersinia virulence. *PLoS Pathog* **8**, e1002518, doi:10.1371/journal.ppat.1002518 (2012).

25 Liberati, N. T. *et al.* An ordered, nonredundant library of Pseudomonas aeruginosa strain PA14 transposon insertion mutants. *Proc Natl Acad Sci U S A* **103**, 2833-2838, doi:10.1073/pnas.0511100103 (2006).

26 Choi, K. H. & Schweizer, H. P. mini-Tn7 insertion in bacteria with single attTn7 sites: example Pseudomonas aeruginosa. *Nat Protoc* **1**, 153-161, doi:10.1038/nprot.2006.24 (2006).

27 Munch, R. *et al.* Virtual Footprint and PRODORIC: an integrative framework for regulon prediction in prokaryotes. *Bioinformatics* **21**, 4187-4189, doi:10.1093/bioinformatics/bti635 (2005).

28 Winsor, G. L. *et al.* Enhanced annotations and features for comparing thousands of Pseudomonas genomes in the Pseudomonas genome database. *Nucleic Acids Res* **44**, D646-653, doi:10.1093/nar/gkv1227 (2016).

Acknowledgments

This work was supported in part by grants from the National Institutes of Health (R21AI103651) and the Cystic Fibrosis Foundation (GOLDBE14P0 and GOLDBE17P0) to JBG and in part by the Emory Integrated Proteomics Core (EIPC), which is subsidized by the Emory University School of Medicine and is one of the Emory Integrated Core Facilities. Additional support was provided by the Georgia Clinical & Translational Science Alliance of the National Institutes of Health under Award Number UL1TR002378. SMP was supported in part by a training grant from the National Institute of Allergy and Infectious Diseases of the NIH to Emory University (T32AI106699, Antimicrobial Resistance and Therapeutic Discovery Training Program.

We would like to thank Dr. Keith Wilkinson for helpful discussions during the proteomic data analysis. We would also like to thank Dr. William Shafer, Dr. Charles Moran, and members of the Goldberg Laboratory for their comments during the preparation of this manuscript, as well as Dr. Nicholas Seyfried and Dr. Eric Dammer for their contribution through the EIPC.

Contributions

SMP, EGK, SA, GLC, JBG conceived and planned experiments. SMP, DMD, EGK, QD, SA carried out experiments. SMP, DMD, EGK, QD analyzed data. SMP and JBG wrote the manuscript. All authors contributed to and approved the final version of the manuscript.

Phenotypic Studies of EftM

Samantha M. Prezioso[1,2], Dina A. Moustafa[2,4], Joanna B. Goldberg[2,3,4]

[1]Microbiology and Molecular Genetics (MMG) Program, Graduate Division of Biological and Biomedical Sciences, Emory University, Atlanta, GA 30322, USA.

[2]Division of Pulmonology, Allergy/Immunology, Cystic Fibrosis and Sleep, Department of Pediatrics, Emory University School of Medicine, Atlanta, GA 30322, USA.

[3]Emory Antibiotic Resistance Center, Atlanta, GA 30322, USA.

[4]Emory+Children's Center for Cystic Fibrosis and Airway Disease Research, Atlanta, GA 30322, USA.

Introduction

Pseudomonas aeruginosa is metabolically diverse and ecologically significant gram-negative bacteria[1]. Members of the *Pseudomonas* family are found in an astonishingly wide range of environments, including terrestrial, freshwater, and marine habitats. *P. aeruginosa* can infect plants, worms, mammals, and humans. It can degrade aromatic compounds, halogenated substrates, recalcitrant organic residues, and triclosan[1]. There is a wide range of temperatures at which *P. aeruginosa* can grow[2]. Overall, this organism is extremely flexible. For this reason, in a laboratory setting, it can be challenging to identify the optimal conditions under which a novel gene of interest is physiologically relevant. The metabolic flexibility and relatively large genome of *P. aeruginosa* leads to a wide variety of relevant conditions for consideration when performing studies.

One such relatively newly discovered gene being studied is *eftM*, which encodes an *S*-adenosyl-L-methionine-dependent methyltransferase[3] that trimethylates elongation factor-Tu (EF-Tu) on Lysine 5 (K5me[3]). EftM is not an essential protein, and deletion of this gene appears to have little to no impact on growth rate or total cellular protein content[4]. The current major phenotype associated with EftM activity is in creating a post-translational modification on EF-Tu that can, when EF-Tu is surface-associated, act as an adhesin to human epithelial cells. This adhesin-like K5me[3] modification of EF-Tu binds the platelet-activating factor receptor through molecular mimicry of platelet activating factor. Utilizing K5me[3] in this fashion is unique amongst respiratory pathogens; others

use phosphorylcholine to engage platelet activating factor receptor[5]. EftM accomplishing this interaction through trimethyl lysine, instead, is the only known example of modification performing the same role.

The impact of trimethylated EF-Tu as an adhesin during murine intranasal infection challenge has been investigated[4]. However, the impact on adherence and survival in this murine model is modest. Yet, EftM appears to be widely conserved amongst *P. aeruginosa.* In addition, EftM homologues are found in *Pseudomonas* species such as *P. mendocina, P. stutzeri, P. fulva,* and *P. syringae.* EftM homologues can be identified in other gamma-proteobacteria as well, such as *Shewanella* and *Vibrio* sp[4]. Therefore, given: the wide-spread conservation of EftM amongst *Pseudomonads*; the modest phenotype conferred by EftM; and the ability of *P. aeruginosa* to grow and respond to a wide variety of environments, we hypothesized that there may be additional phenotypic roles of EftM on the cell yet to be revealed. While a large phenotypic impact of EftM is still yet to be elucidated, the diverse phenotypic studies presented here are an important foundation for future work in uncovering the full significance to this intriguing methyltransferase.

Results and Discussion

Part I: Impact of EftM on phenotypic attributes of *P. aeruginosa*

Biofilm formation

Biofilms are organized communities of bacteria enclosed in a matrix of extracellular polymeric substances, consisting mainly of biomolecules, exopolysaccharides, extracellular DNA (eDNA), and polypeptides[6]. Biofilm formation goes through cycles where environmental cues are received, leading to a reversible adhesion of planktonic bacteria onto a surface permissive to biofilm formation. The biofilm matures in a process involving complex regulatory cascades[6], until a period of dispersal where free-swimming bacteria are free to seed new biofilm colonies[7]. The initial adherence step of biofilm formation is of particular interest to our studies with EftM, given EftM's known phenotype in catalyzing a post-translational modification on EF-Tu that acts as an adhesin to human bronchoepithelial cells. We therefore were curious as to whether or not EftM would impact biofilm formation; we hypothesized that since bacteria in biofilms are phenotypically different than free-swimming bacteria, with an increased selection for bacteria that are highly adherent but with reduced motility[8], that EftM-mediated EF-Tu modification could increase biofilm mass in PAO1 by increasing the adhesion during initial biofilm formation.

To assess this hypothesis, I tested both PAO1 and PA14 sets of strains for biofilm formation after 24 hours at 25°C. The wild-type strains, *eftM* deletion mutants, complements, and several control strains including PA14 defective for

biofilm formation[9] were grown in the same 96-well plate in octuplicate, with a 25°C growth temperature being chosen because of the thermo-sensitive nature of EftM. My results indicate no statistically significant difference in biofilm formation in strains with, versus those without, EftM (**Figure 1**). One exception, however, was a statistically significant and reproducible difference between the PAO1 wild-type strain and its corresponding deletion and complement strain. Further investigation with additional wild-type strains of PAO1 (data not shown) revealed this difference to be an artifact of strain construction, with differences most likely being due to the alteration of pili (known contributors to biofilm adhesion) during the creation of PAO1Δ*eftM* (see **Figure 11, 13**).

These data imply that methylated EF-Tu does not aid biofilm formation. We hypothesized that since EF-Tu K5me^3 acts as an adhesin to human epithelial cells, biofilm formation may also be enhanced for strains carrying EftM. However, these data do not support this theory. Instead, it can be inferred that EF-Tu K5me^3 has specificity for human epithelial cells, and does not act as an adhesin in general. Alternatively, laboratory culture dishes may not be the right surface for studying this system, and biofilm formation on biotic surfaces such as cell cultures would reveal EftM-mediated differences. Lastly, biofilm formation was only measured after 24 hours. It is possible that maximum biofilm mass is not altered for strains with EftM, but rather that biofilms form at a faster rate for strains with EftM. Time-courses of biofilm formation would investigate this possibility.

Long-term survival and regrowth

Persister cells are stochastic phenotypic variants of bacteria that are genetically identical to their parental population. These variants are dormant, making them highly tolerant to antibiotics and therefore difficult to treat[10]. Persister cell formation is a medically important aspect of *P. aeruginosa* physiology; in a study looking at longitudinal *P. aeruginosa* isolates from cystic fibrosis patients with chronic airway infections, a 100-fold increase in persister cell formation was observed over those from early isolates[11]. There are several known mechanisms for persister cell formation. Additionally, bacteria can have multiple mechanisms in place ranging up to at least 79 separate toxin-antitoxin systems in *Mycobacterium tuberculosis*[12]. *P. aeruginosa* has a HigB-HigA toxin-antitoxin system[13], with more likely yet to be characterized.

EftM-catalyzed trimethylation of EF-Tu may act to protect EF-Tu from toxin systems that induce persister formation, and further, would explain the benefit of EftM down-regulation in a human host. If this were true, we would expect PAO1 to have a lower rate of persister formation, and therefore overall worse long-term survival in water, than a strain deleted for EftM. Conversely, trimethylation of EF-Tu may act to induce persister formation by stalling translation or complexing with ribosomes, rendering them ineffective. In this case, we would expect PAO1 to survive better long-term due to increased persister formation over PAO1Δ*eftM.*

To test this, I monitored viability of PAO1 and PAO1Δ*eftM* in water over 10 days at either 25°C (to assess for differences mediated by EftM), or at 37°C (as a control). There was no significant growth over the 10 days, as expected in water lacking nutrient sources. However, there was no significant decrease in viability

for either of the strains or temperatures tested (**Figure 2**). Additionally, PAO1 showed no significant difference from PAO1Δ*eftM* in regards to the minimum inhibitory concentration required for killing by amikacin, aztreonam, cefepime, doripenem, imipenem, piperacillin-tazobacteram, ticarcillin-claulate, tobramycin, colistin, ceftazidime, levofloxacin, meropenem, ciprofloxacin, or gentamicin (data not shown; performed by Dr. Sara Satola). While this does not eliminate the possibility that EftM has a role in persister formation, we can, from these data, conclude that EftM does not have an impact on long-term survival of *P. aeruginosa* in water.

An alternative explanation for EF-Tu K5me^3 could be to function in long-term protection of the N-terminus of EF-Tu from degradation. Set7/9 is a methyltransferase similar to EftM in that it methylates the N-terminus (lysine 4) of Histone 3, a eukaryotic protein[14]. Set7/9 can methylate other proteins, especially transcription factors; methylation of these proteins by Set7/9 was found to have a stabilizing effect on some proteins and a de-stabilizing effect on others, as presumably the methylated amino acid's surrounding sequence context determines the type of effector recruited to the methylated protein[15].

Since EF-Tu is required for translation, and translation is required for cellular division and population growth, I assessed re-growth of PAO1 after long-term incubation in stationary phase. If EF-Tu K5me^3 protects the N-terminus, I would expect the long-term cellular pool of EF-Tu to be maintained at higher levels, and presumably exit faster from stationary phase. Conversely, if methylation recruits proteases, I would expect PAO1Δ*eftM* to exit stationary

phase first. Experimental conditions included 24 hours of growth at 25°C in LB with shaking, static incubation for five days, and back-dilution and resumption of aerated growth with monitoring. On the first trial (**Figure 3, darker colors**) PAO1Δ*eftM* appeared to exit lag phase faster than the complemented strain, implying that K5me3 is a target for EF-Tu degradation. The second replicate, however (**Figure 3, lighter colors**) showed well-paired exit from stationary phase. Purified recombinant EF-Tu stored at -20°C for approximately two years appeared to lose just the N-terminus from just the unmethylated species (unpublished observation), which seems to point to methylation as a protective mechanism. The prospect of further investigation into this hypothesis is intriguing. Exit from long-term stationary phase has many affiliated variables; perhaps future studies should focus on timed incubations of recombinant purified EF-Tu with EF-Tu-depleted cellular lysates to track stability of the EF-Tu N-terminus.

Serum sensitivity

Normal human serum plays a role in host antimicrobial defense through the complement system: triggering of the complement cascade can lead to innate killing by formation of a membrane attack complex, which compromises the integrity of the gram-negative bacterial outer membrane. Complement also activates other cells such as leukocytes and endothelial cells to respond to microbial invasion[16]. The classical pathway of complement activation can utilize antibody to initiate the cascade[17]. As EF-Tu is predominantly unmethylated at 37°C, when pre-existing antibody to bacterial EF-Tu would generated, EftM-

mediated trimethylation of EF-Tu may in part impair recognition of complement initiation. Alteration of the outer membrane of *P. aeruginosa* by trimethylation on EF-Tu could also potentially impact initial protein deposit, and therefore activation, in the mannan-binding lectin pathway or the alternative pathway.

I purchased pooled normal human serum (NHS) to assess the impact EftM-catalyzed EF-Tu trimethylation has on recognition and killing by complement. Initial studies focused on PAO1 (data not shown); however, PAO1 is highly intrinsically resistant to complement-mediated killing, and is therefore not an ideal system for assessing more subtle phenotypes. PA14, conversely, is more sensitive to complement. I chose to grow my stains at 25°C so that EftM would be active and have time to trimethylate the cellular pool of EF-Tu prior to challenge with normal human serum. As seen in **Figure 4**, PA14 WT showed a reduction from ~$2x10^5$ CFU/mL to ~$5x10^3$ CFU/mL after a 60-minute incubation with 50% normal human serum (representing a 25% survival). PA14 *eftM*::tn, however, showed a much less dramatic reduction of ~$1.3x10^5$ CFU/mL to ~$8.8x10^4$ CFU/mL, a 67% survival. When strains of PA14 *eftM*::tn restored with either the thermo-instable (PAO1) or stable (PAHM4) versions of EftM were tested, I saw an intermediate phenotype to that of WT and *eftM*::tn; both strains showed a reduction from the inoculum of ~$1.3x10^5$ CFU/mL down to ~$5x10^4$ CFU/mL, representing a survival of 37% and 42%, respectively.

Analysis of these data overall show no statistically significant difference in sensitivity to NHS, dependent on EftM status. However, while not statistically significant, it is intriguing that EftM generally appears to be increasing sensitivity

of *P. aeruginosa* PA14 to complement. Perhaps the presence of the transposon (containing a gentamicin marker) in PA14 *eftM*::tn and the two complemented strains is impacting these results, and removal of the marker would restore PA14 *eftM*::tn+*eftM* to WT levels. If the presence of EftM does increase sensitivity to NHS-mediated killing, this could explain the function of down-regulating EftM during the course of infection.

Future studies should focus on testing PA14 and clean, markerless derivates for serum sensitivity. Tests with strains pre-grown at 25°C should reveal PA14 and both complements to exhibit comparable survival. Conversely, tests with strains pre-grown at 37°C should show WT, deletion, and +$eftM_{PAO1}$ to exhibit the same phenotype, with +$eftM_{PAHM4}$ retaining EftM activity (and presumably enhanced NHS sensitivity).

EF-Tu lysine 5 trimethylation functionally mimics the phosphorylcholine decoration several other respiratory pathogens add to their outer membrane. Phosphorylcholine has been shown to increase sensitivity to complement mediated killing through enhanced recruitment of C-reactive protein, a protein important in antibody-independent classical complement activation[18]. C-reactive protein is an acute phase protein, meaning it is most likely not present at appreciable levels in healthy normal human serum, but is increased in response to inflammation and tissue necrosis[19]. Preliminary studies with PAO1 (not shown) included trials where C-reactive protein added to NHS, with inconclusive results. However, repeating these studies with PA14 may reveal an enhanced difference in survival between those with EftM compared to those without.

Proteomic analysis of secreted proteins

EF-Tu is an elongation factor that delivers charged tRNA to the ribosome during translation and contributes to proofreading of the growing peptide chain[20]. During exponential phase growth it is the most abundant protein in the cell, accounting for 6-13.5% of total cellular protein and outnumbering ribosomes 8-14 to one[21]. EF-Tu's function in translation is essential for bacterial cells[22]; however, post-translational methylation can alter this function[23]. We have previously studied the proteome of PAO1, PA14, and PAHM4 with and without EftM to assess the impact of Lysine 5 methylation on the steady-state proteome, with no significant differences observed (**Chapter III**). However, this study was performed on cells that were grown in LB, pelleted, and washed with saline (PBS) to remove traces of LB (a peptide-based media) that might interfere with mass spectrometry identification. This analysis therefore did not include secreted proteins. As EF-Tu is itself translocated to the outer leaflet of the outer membrane by an unknown mechanism, and is additionally involved in the export of the toxin Tse6 through type VI secretion[24], we investigated the secretome of *P. aeruginosa* for differences mediated by EftM trimethylation status.

I grew PAO1Δ*eftM* and PAO1Δ*eftM* + $eftM_{PAO1}$ (**Table 1**) in lysogeny broth (LB) with shaking at 25°C until mid-exponential phase of growth, OD_{600}=0.8-0.9. Whole cells were pelleted, and then the supernatants filtered to remove any remaining cells. Next I used trichloroacetic acid (TCA) to precipitate proteins from the media, which were subsequently identified with label-free quantitation mass spectrometry by the Emory Proteomics Core (Duc Duong; Eric Dammer).

Samples were grown in biological triplicate, and analysis included two sterile LB control samples “grown” and precipitated in the same manner as the bacterial samples.

The results of this study reveal 64 candidate *P. aeruginosa* proteins that were significantly higher or lower with $p<0.05$ in one strain over the other, as well as not being detected in the LB negative controls. 16 of the 64 candidates had a 2-fold change or greater (**Table 2**), making them interesting candidates for further study. In addition, there was one candidate (PA0922) that had a complete absence in the deletion strain and LB control, but was detected in all three biological triplicates of the complement strain (**Table 2**). Interestingly, most of the candidate proteins are known or predicted to be localized to the cytoplasm[25]. Only one, ExoT, is actually secreted (via the type III secretion system), while four others have no prediction. Given the emergence of moonlighting functions for several proteins, these cytoplasmic candidates cannot be strictly eliminated as contamination. Rho, PA5139, and PA0922 are of particular interest for future studies given the large fold-change observed.

Preliminary follow-up studies were initiated examining relative Rho abundance in the whole-cell lysates of PAO1, PAO1Δ*eftM,* and PAO1Δ*eftM* + $eftM_{PAO1}$ by Western immunoblot (data not shown); however, no differences were observed. One interpretation is that EftM does not alter the abundance of Rho within the cell, but rather impacts the ability of Rho to be secreted. This would be congruent with our observations of no significant differences in cellular proteins (**Chapter III**) with regard to EftM status. The role of Rho once secreted, and the

benefit of EftM repressing Rho export, is less clear. Alternatively, these data could be irreproducible and should be verified before any large study is undertaken.

Part II: Timing of EftM Activity

K5me^3 correlates with total cellular EF-Tu levels

While it is well defined that EF-Tu is robustly trimethylated on lysine 5 at 25°C but not 37°C, the production and accumulation of the EftM protein itself is harder to study. Attempts at Western immunoblotting whole-cell lysates with an α EftM antibody or an α FLAG antibody for the tagged complemented strain were previously unsuccessful at resolving protein above the background noise level (data not shown), presumably due to EftM's inherently low steady-state levels. To determine if EftM is constitutively produced at 25°C, or if EftM is produced at a specific phase of growth, I monitored EF-Tu K5me^3 accumulation over the course of a normal growth curve of lag phase, exponential phase, and stationary phase.

I grew PAO1 overnight at 37°C, then back-diluted to OD_{600}=0.05. The back-diluted culture was then split in two, with one half allowed to resume growth at 37°C and the other switched to 25°C. By growing the starter culture at 37°C, cellular EF-Tu would largely be unmethylated; therefore, early density time-points at 25°C would only show newly produced EftM activity, and not residual accumulation from the overnight growth. The growth curves of PAO1 at 25°C and 37°C (**Figure 5; Left panels**) both have a clearly defined lag, exponential, and

stationary phases. The overall growth rate of 25°C is lower than 37°C, as expected. Equivalent cell numbers were collected from various densities, then were measured for relative Di/Trimethyl Lysine densitometry. When relative densitometry (with 100% set as 25°C mid-exponential phase) was plotted against culture density (**Figure 5; Right panels**), consistent trimethylation is observed throughout exponential phase. Strikingly, the 25°C culture exhibits close to 100% trimethylation density at the earliest time-point assessed. This implies that EftM is immediately produced upon the switch to 25°C, and quickly acts on the existing pool of EF-Tu. There also appears to be a decline in densitometry observed upon transition to stationary phase. As EF-Tu levels are down-regulated during stationary phase[26], this is expected.

RhlR and PvdS do not impact EftM expression

While the promoter and transcription start site for EftM have now been identified (see **Chapter III**), little more is known about *eftM* regulation. There are no currently defined activators or repressors; however, by utilizing the upstream sequence for the gene[25], we can predict which elements may bind. Analyzing the *eftM* upstream region with Virtual Footprint[27] revealed several predictions as to what may bind the regulatory region of *eftM.*

One such predicted binding protein is Fur. Fur, or ferric uptake regulator, is a central regulator of iron-regulated genes. When bound to Fe(II), Fur binds and represses transcription of its target genes; when iron is low, Fur is released and transcription proceeds[28]. There is a predicted Fur binding site ~68 bp upstream from the *eftM* ATG start codon, which interestingly happens to overlap

with the -35 of the promoter. We therefore hypothesized that under iron-rich conditions, Fur could potentially bind and compete with the *eftM* sigma factor, preventing production of EftM.

To test this hypothesis, I performed a Western blot for αDi/Trimethyl Lysine, a read-out of EftM activity, to proxy the production of EftM under iron-rich and iron-deplete conditions. I chose to grow PAO1 and PAO1Δ*eftM* (as a control for nonspecific bands) on blood agar as my iron-rich media and *Pseudomonas* isolation agar (PIA), a mixture of gelatin, potassium sulfate, magnesium chloride, Irgasan, glycerol, and agar[29] as my low-iron condition. If *eftM* is a Fur-regulated gene, we would expect to see higher levels of trimethylation from PIA-grown samples than those from blood agar because without Fe(II), Fur will not be able to bind and repress *eftM* transcription.

As seen in **Figure 6**, the levels of trimethylation observed at both 25°C and 37°C appear consistent between samples grown on blood agar compared those grown on PIA. It is possible that blood agar might not have enough free iron to be a true “high iron” medium, and for rigor, minimal media with defined amounts of exogenous iron could serve as an alternative. However, this study implies that Fur does not bind upstream and regulate the production of EftM.

A second predicted regulatory binding site for *eftM* is RhlR. There are two acyl-homoserine lactone based quorum-sensing systems in *P. aeruginosa*. RhlR is the response regulator for one of these systems, and responds to *N*-butanoyl-HSL (C4-HSL) synthesized by RhlI[30]. *eftM* has a predicted RhlR binding site spanning 44 bp upstream to 28 bp upstream of the *eftM* start codon; this

positioning would obstruct the confirmed -10 promoter region (**Chapter III**). While *eftM* has not been identified in transcriptome studies for quorum-induced genes[30], transcription of *eftM* is inherently low and therefore below the limit of detection for most global assessments. To directly test the hypothesis that RhlR binds and regulates *eftM*, I utilized a PAO1 *rhlR* transposon mutant strain for altered EF-Tu trimethylation. I grew PAO1 *rhlR*::tn at either 25°C or 37°C and collected samples at lag (OD_{600}=0.13-0.15), mid-exponential (OD_{600}=0.77-1.33), or stationary phase (overnight), then assessed relative trimethylation by Western immunoblot (**Figure 7**). Low-density samples were included as a control; since RhlR is induced by RhlI's signal at high quorum density, we would only expect to see altered trimethylation at higher densities, the condition under which RhlR's activity would be missed. As expected, low densities look the same as the PAO1 wild-type control (right-hand side). The higher density samples, however, also looked the same as the PAO1 control, implying that RhlR does not regulate *eftM*. This finding is congruent with the consistent trimethylation observed throughout the growth curve in **Figure 5**; should RhlR be activating *eftM*, we would have observed an increase in trimethylation abundance later in the growth curve, not immediately as is actually observed. Altogether these data imply that *eftM* is not quorum-sensing regulated.

An upstream transcriptional regulator does not impact *eftM*

EftM's thermoregulation is not commonly encountered amongst virulence factors; most are up-regulated at 37°C, whereas *eftM* (PA4178) is up-regulated at 25°C. A near chromosomal upstream neighbor, PA4175 (*prpL*) is also

transcriptionally thermo-regulated in the same manner. The next nearest neighbor is PA4174: it is a 34.3 kDa probable transcriptional regulator of unknown function in the same chromosomal orientation as *eftM* and *prpL* (+ strand). We thought this clustering of genes with unusual thermoregulation (i.e. up at 25°C, down at 37°C), coupled with the close proximity of an unknown transcriptional regulator, was a coincidence worth investigating.

To evaluate the impact of PA4174 on EftM production, I utilized a transposon mutant to measure relative EF-Tu K5me^3 accumulation by Western immunoblot. This strain was evaluated at both low and high density and compared to corresponding wild-type control strains. As shown in **Figure 8**, PA4174 does not appear to impact *eftM* expression. Additionally, the PA4174 transposon mutant did not have altered *prpL* levels as revealed by RT-qPCR (data not shown). Overall, while the regulon of PA4174 remains a mystery, it seems unlikely that *eftM* would be amongst the genes controlled.

Chromosomal context is not important for *eftM* expression

The bacterial chromosome is not simply a line of DNA in the cell. There is organized structure to how the chromosome is arranged in the cytosolic space, largely mediated by binding of structuring proteins. Some, like the histone-like protein H-NS, can promote filaments or bends in the DNA, which bring distant regions in close proximity[31]. There are other histone-like proteins beyond H-NS; the histone-like protein HU is widely distributed amongst bacteria, with the *P. aeruginosa* homolog named *hupB.* HU binds DNA without sequence specificity[32], but with a preference for forks, nicks, and overhangs[33]. Therefore, chromosomal

context (upstream and downstream neighbors) may be important to consider for a gene without precisely elucidated regulation because surrounding DNA sequence can impact accessibility and secondary structure of the promoter.

I previously demonstrated that I could complement an *eftM* deletion while retaining temperature regulation by inserting a copy of *eftM* with 500 bp of upstream sequence ($P_{eftM(500)}$) at an ectopic location in the chromosome (**Chapter III**). However, it was not known if 500 bp (which extends into the upstream neighbor of *eftM*) was necessary for this phenotypic maintenance. To investigate this, I constructed two more complementation strains with 250 bp of upstream sequence and just 100 bp of upstream sequence in the same fashion as the original complementation strain. When assessed for EftM activity by Western immunoblot (**Figure 9**), a clear retention of EftM activity and thermoregulation is observed, indicating that 100 bp is sufficient for *eftM* expression and thermoregulation. This information will allow future studies to hone in on the location of regulatory elements controlling *eftM* expression.

Part III: Pili and the creation of isogenic strains

Motility is not altered by EftM

One physiological role of methyltransferases is signal relay in chemotaxis pathways. Chemosensory two-component systems are at the core of motility[34]; these systems sense extracellular signals and propagate a complicated cascade in prokaryotes. One of the most well studied examples of this system is the CheA (chemotaxis) system from *E. coli. E. coli* has four methyl-accepting chemotaxis

proteins that span the cell membrane as dimers[35]. The soluble, cytoplasmic histidine kinase CheA receives signal from methyl-accepting chemotaxis proteins by way of the intermediate protein CheW. This signal induces a trans-autophosphorylation of the dimeric CheA[36]. The new phosphate group on CheA is then competed for by two response regulators, one of which (CheY) controls flagellar motor switching and the other of which (CheB) controls adaptation of chemoreceptors. Phosphorylated CheB can both deamidate and demethylate the transmembrane methyl-accepting chemotaxis proteins, and when CheB deamidates glutamine to glutamate, methyl-accepting chemotaxis proteins become targets for methylation by the methyltrasferase CheR[36]. Overall when signal is present, CheB is phosphorylated, active, and demethylates chemotaxis proteins, which induces the cell to respond to signal. The constitutive methyltransferase CheR then methylates the chemotaxis protein, which "resets" the protein and allows for continuous monitoring and response to signal[37].

P. aeruginosa has four separate chemosensory pathways, some of which control flagella like the example from *E. coli* described above, and one of which controls pili-mediated twitching motility[34]. I investigated the possibility that EftM could be acting in a motility-based chemotaxis pathway by assessing the motility of PAO1 and PA14 compared to their derivative mutants; if EftM was acting in one of these chemosensory pathways, I would expect to see lower motility in the mutant strains.

I first evaluated twitching motility of PA14, PA14 *eftM*::tn, and the two complemented mutants. Strains were compared to a mutant of *pilC* as a negative

control, as this strain is impaired for twitching. To control for subtle plate-to-plate differences in variables such as moisture content, all five strains were evaluated on a single agar plate, with tests performed in biological quintuplicate. These data (**Figure 10A**) imply that there is no influence of EftM on twitching motility.

I also evaluated swimming motility, a flagella-based motility, for defects caused by loss of EftM. I evaluated the same strains (with the exception of the control strain being changed to a *fliC* transposon mutant) for swim zones in 0.2% agar media. One of the complement strains tested (PA14 *eftM*::tn +*eftM*$_{PAHM4}$) contains a thermo-stable version of EftM, which allows for assay performance at 37°C as well as 25°C. When cultures were allowed to swim for 24 hours at 37°C (**Figure 10B**) or 49 hours at 25°C (**Figure 10C**), no apparent difference in swim motility was observed for any strain except the *fliC* negative control.

Most published motility studies are performed at 37°C, when the contribution by EftM could be missed. These studies presented here were performed at 25°C, and from these data it appears EftM does not play a role in *P. aeruginosa* chemotaxis and motility. Given the well-defined nature of the CheR pathway, it seems unlikely that EftM would be influencing this system. However, *P. aeruginosa* has several other less-defined systems that could be impacted by EftM. It is possible that EftM's role is specialized and limited in response to a chemoattractant not tested under the specific conditions I used for these studies.

Pili levels are different between PAO1 and PAO1Δ*eftM*

Type IV pili are polymerized protein fibers on the surface of a variety of bacteria and archea. These appendages are multifunctional, with roles in

adherence to biotic and abiotic surfaces, twitching motility, modulation of biofilm architecture, competence and conjugation, and secretion[38]. Type IVa pili, specifically, are composed of PilA as the major pilin subunit. PilB is the putative pilin polymerase, PilT the depolymerase, PilQ is the secretin for the complex, and the PiliMNOP proteins are the alignment system that ensures proper pilus positioning[39]. Pili were a key point of focus for several EftM studies outside of the scope of this current work. We initially hypothesized that EftM was directly or indirectly up-regulating the expression of pili proteins, and set out to test this hypothesis though Western immunoblotting for several pili subunit proteins. While ultimately from these studies we concluded that EftM did not impact pili production, these studies revealed a valuable insight: PAO1Δ*eftM* (**Table 1**) is not isogenic to PAO1.

To expand upon these data, PAO1, PAO1Δ*eftM*, and PAO1Δ*eftM* + $eftM_{PAO1}$ (**Table 1**) were utilized for the αPil protein Western blotting studies. PAO1Δ*eftM* was previously created from PAO1 by using homologous recombination to replace ~230 bp of the *eftM* coding sequence with a gentamicin cassette, which was afterwards removed using the *cre-lox* system[4]. I subsequently complemented this deletion strain with the native *eftM* promoter and coding sequence, in single copy, at the ectopic chromosomal Tn7 attachment site to create PAO1Δ*eftM* + $eftM_{PAO1}$ (**Chapter III**).

To assess the relative levels of PilA, B, M, O, Q, and T from these three strains, I grew each to mid-exponential phase of growth (OD_{600}=0.8) in LB with rotation. I then harvested the same number of CFU from each sample and

analyzed an equivalent cell volume by Western immunoblotting. To ensure a linear range of detection, I ran undiluted samples (UD), a 1:2 dilution of the cellular lysate, and a 1:4 dilution for each sample. I also included the appropriate transposon mutant as a negative control for each immunoblot.

The results from these Western blots are striking (**Figure 11**). PAO1Δ*eftM* and PAO1Δ*eftM* + $eftM_{PAO1}$ are very well matched in terms of pili protein densitometry. However, the wild-type strain seems to contain a lower amount of PilA, B, M, O, and Q. These observations were confirmed by mass spectrometry analysis of whole-cell lysates (**Chapter III**): the deletion strain and its isogenic complement are well-matched but have a statically significant and reproducible augmentation of pili levels over the parental wild-type strain.

PAO1Δ*eftM* was created by mating PAO1 with *E. coli*. One well-defined role for pili is in conjugation; pili assist in attaching the mating pairs of bacteria, facilitate the transfer of genetic material, and bring mating pairs in close contact[40]. Closer contacted pairs were found to be more efficient at transferring genetic material than well-separated pairs[40]. Perhaps, then, the conjugation event creating PAO1Δ*eftM* was performed under unintentionally strenuous conditions, and stochastic pili-enhanced mutants were in tighter contact with *E. coli*. This would make these mutants more likely to receive the antibiotic marker, and would therefore yield better survival under subsequent antibiotic selection. Additionally, during the construction of PAO1Δ*eftM* the plasmid used to remove the gentamicin marker was cured by three successive passages in LB broth. An

alternative hypothesis explaining how pili were altered is that repeated passage unintentionally selected for enhanced pili production.

The motility studies presented in **Figure 10** were performed with PA14, not PAO1. It stands to reason that were this experiment repeated with PAO1, the augmented pili found in PAO1Δ*eftM* would confer an enhanced twitching phenotype, especially given that biofilm production was altered (**Figure 1**).

The last pilus protein not yet mentioned is PilT, the depolymerization or retraction pilus. As seen in the bottom panel of **Figure 11**, PilT appears to be largely enhanced in PAO1Δ*eftM* and restored to low wild-type levels in PAO1Δ*eftM* + $eftM_{PAO1}$. The band observed in **Figure 11** is slightly larger than the molecular weight of PilT (38.0 kDa). Further investigation revealed that PilT is actually a faint band just under the 37 kDa marker, and not the prominent band seen in the middle of the blot. This unidentified protein was, therefore, cross-reacting with the αPilT antibody (a reagent generated in rabbits against recombinant, his-tagged PilT protein purified from *E. coli*). We were curious to elucidate the identity of this cross-reactive band. Only two proteins are known to be different between strains with compared to those without EftM: the first is the presence/absence of EftM itself, and the second is presence/absence of $K5me^3$ on EF-Tu. Our cross-reactive band is too big to be EftM, and therefore was either cross-reacting with the N-terminus of EF-Tu, or was revealing the identity of a new protein differentially impacted by EftM. We were confident this band was EftM-dependent; it disappeared in the complement strain at 25°C but was seen in

the lysates of all three samples when grown at the EftM-inactivating temperature of 37°C (data not shown).

The prominent band's identity was investigated through immune-precipitation and mass spectrometry (data not shown). Preliminary results indicated the cross-reactive band to be EF-Tu. To confirm, I performed a series of Western immunoblots to prove cross-reactivity of the antibody. Utilizing EF-Tu purified from PAO1 (methylated) or PAO1Δ*eftM* (unmethylated), I ran a 10% acrylamide gel with 50 ng of each protein in quintuplicate. One replicate was Coomassie stained to ensure equal loading of methylated and unmethylated EF-Tu (**Figure 12**). Each of the remaining four replicates was immunoblotted with a different antibody. First, I blotted with αEF-Tu raised against the N-terminus to confirm the identity of the purified proteins and to show that the N-terminus of the protein was intact. Next I blotted with αHis antibody to show preservation of the C-terminus containing my 6x His tag. Third I performed an αTrimethyl Lysine western blot to demonstrate that the purified methylated protein was methylated. These first three blots, along with the Coomassie-stained gel, establish that I have relatively equal amounts of EF-Tu, that the EF-Tu is fully in tact, and that it is not contaminated with other proteins. The last blot performed was with αPilT. As clearly seen in **Figure 12**, the unmethylated protein reacts strongly with the αPilT antibody, while the methylated protein does not.

Together these results point to the N-terminus of EF-Tu cross-reacting with our αPilT antibody. When K5 is methylated by EftM, the cross-reaction is largely blocked, explaining the low abundance of the band in wild-type and

complemented strains. Ironically, EftM was discovered when an antibody raised against phosphorylcholine cross-reacted with EF-Tu K5me[3].

Creation of isogenic EftM strains and *in vivo* significance

The information on pili abundance revealed in the Western blots seen in **Figure 11,** as well as in the whole-cell proteome (**Chapter III**), called into question the significance of EftM as an adhesin. Previous studies on the virulence of EftM demonstrated that purified methylated EF-Tu bound oropharyngeal and bronchoepithelial cells almost 2-fold more efficiently over unmethylated EF-Tu[4]; however, the *in vivo* murine infections may have been performed with a deletion strain altered for pili production. As pili are a known adhesin themselves[41], this prompted further investigation into the efficacy of EftM as a virulence factor.

I first created my own set of isogenic strains. Starting with PAO1, I used allelic recombination to delete the entire *eftM* coding sequence, in contrast to the partial deletion seen in PAO1Δ*eftM.* Additionally, I introduced the recombination vector through electroporation instead of conjugation. After recombining out the gentamicin marker, I had a clean, markerless *eftM* gene deletion with only an *FRT* scar left behind (PAO1Δ*eftM* SAM, also known as PASP124). I then complemented this strain with the PAO1 and PAHM4 alleles of *eftM*.

To confirm successful construction of an isogenic set, I first performed a Western immunoblot for αTrimethyl Lysine. **Figure 13A** shows the pattern typically observed with our classic strain series; high methylation at 25°C and low methylation at 37°C, no methylation at either temperature in the deletion mutant,

and elevated methylation at 37°C in a PAHM4-complemented strain. The newly constructed strains seen in **Figure 13B** show a seemingly identical pattern, confirming successful strain construction. I also performed an αPilA Western immunoblot (not shown) and observed equal levels of PilA amongst the newly constructed strains.

These strains were subsequently used by Dr. Dina Moustafa from my laboratory to infect BALB/c mice in a similar manner as previously published[4]. To directly compare these new strains with prior studies, nasal washes and lung homogenates were evaluated for bacterial recovery, while survival of a separate set of mice was monitored over 96 hours. The nasal washes of the mice after 24 hours (**Figure 14A**) were well paired between the wild-type and complement, and showed a statistically significant reduction in CFU/mL for PAO1Δ*eftM* SAM. The bacterial load enumerated from the lungs (**Figure 14B**) showed the same trend, with PAO1Δ*eftM* SAM found in significantly lower quantities. Finally, survival curves for 96-hour infections show increased survival of mice infected with PAO1Δ*eftM* (**Figure 14C**).

Altogether these data demonstrate that the original EftM virulence phenotype observed[4] is reproducible. EftM is catalyzing a modification on EF-Tu that is most likely allowing for better colonization during the initial stages of infection, which leads to higher CFU recovery from the nose and lungs and subsequent increased mortality of the mice. In addition to confirming these previous findings with new, isogenic strains, here we show for the first time that the phenotype observed in mice can be complemented. The inclusion of this

complement strain further strengthens our confidence in the significance of EftM as a virulence factor during infection.

Concluding Statements

EftM is an intriguing *P. aeruginosa* methyltransferase with many open questions. The first published report of EftM was in 2008, just ten years ago. In this short period of time the protein has been biochemically characterized as a SAM-dependent methyltransferase with an unusually low T_m; studied in multiple models and routes of infection; been genetically investigated, with the promoter and transcription start site defined; and, as shown here, had the preliminary platform laid for a wide range of phenotypic impacts EftM may have on the cell. While these phenotypic studies presented herein are largely negative results, these questions were important to address and present to prevent a duplication of effort in the future.

Several of the studies presented here do show promise for future investigation. Of particular note is the serum sensitivity data presented in **Figure 4**. EftM's predominant associated phenotype is in functionally mimicking the phosphoryl choline modification added to the outer surface of several other pathogens. These other pathogens use phosphorylcholine to engage the platelet activating factor receptor of epithelial cells. However, phosphorylcholine also increases recruitment of C-reactive protein to the bacterial surface, which enhances complement-mediated killing. Rigorous investigation of K5me^{3}'s impact on C-reactive protein recruitment will be informative regardless of result

discovered: if K5me^3 enhances complement-mediated clearance, this points to the significance of EftM being thermoregulated (e.g. the modification is seen during the initial stages of infection and help initial attachment, but is removed during longer or chronic infection to avoid immune effectors). Alternatively, if K5me^3 does not enhance complement-mediated killing, than a benefit to this system over the more widely-observed phosphorylcholine modification will have been revealed.

A second area warranting further investigation is in alternative model systems to mammals. It is intriguing that the N-terminus of EF-Tu is recognized as a PAMP in *Arabidopsis*[42], and tempting to speculate that K5me^3 could act to block recognition. The data presented in **Figure 12** highlights the strong potential for K5me^3 to block epitope recognition, as demonstrated by the strong cross-reaction of αPilT to unmethylated but not methylated EF-Tu. It is therefore theoretically feasible that K5me^3 would act as a protective mechanism during plant infection.

Overall, the data presented here are a strong foundation for future EftM studies. EftM is relevant to several aspects of microbial physiology, including gene regulation, post-translational modification, response to temperature, and virulence. With such great strides being made in only 10 years of study with this enzyme, it is exciting to speculate what could be uncovered in the next few years with work building on the phenotypic studies presented here.

Materials and Methods

Western Immunoblotting

Unless indicated, all Western immunoblots were performed as follows: strains were grown overnight in 3 mL lysogeny broth (LB) with rotation. The following morning, starter culture density was read and the samples were back-diluted to OD_{600}=0.05 in 3 mL fresh LB. Samples were allowed to resume growth at their respective overnight temperature (either 25°C or 37°C as indicated) until mid-exponential phase (OD_{600}=0.8). A culture volume containing the number of cells equivalent to 1 mL at OD_{600}=1 was pelleted by centrifugation, and then pellets were resuspended in 100 µl Laemmli buffer. Samples were boiled for 5 minutes prior to loading 10 µl into a 10% acrylamide gel (Biorad). Samples were separated by SDS-PAGE, then transferred to PVDF membrane at 100 V for one hour. After transfer, membranes were blocked for one hour in PBST+5% milk except for αDi/Trimethyl Lysine, αTrimethyl Lysine, and αHis, which were blocked in PBST+5% BSA. Membranes were washed and incubated in primary antibody overnight. The next morning, membranes were washed with PBST 3x, then incubated in appropriate secondary for one hour. After another 3x wash with PBST, membranes were exposed with Pierce ECL Western Blotting Substrate (ThermoFisher), and imaged on a ChemiDoc MP Imaging System. Monoclonal rabbit αDi/Trimethyl Lysine: Upstate Biotechnology, Inc (discontinued). Monoclonal rabbit αTrimethyl Lysine: ImmuneChem ICP0601. All polyclonal rabbit αPil protein antibodies were a kind gift from Dr. Lori Burrows (McMaster

University). Monoclonal mouse αEF-Tu: mAb 900, Hycult Biotech. Monoclonal mouse αHis:THE^{TM} His Tag antibody, GenScript.

Biofilm assay

PAO1 and derivatives, PA14 and derivatives, mPAO1 transposon mutants, and PA14 Sad36 (**Table 1**) were utilized for studies. 3 mL LB cultures were grown overnight at 25°C with rotation. The next morning strains were back-diluted to OD_{600}=0.05 in fresh LB, and 200 µl of each strain was added to eight separate wells of a pegged-lid 96-well plate. The plate was sealed with parafilm to retain moisture, then incubated static for 24 hours at 25°C. The pegs were washed 3x with water, allowed to air dry for 5 minutes, then transferred to a plate with 0.1% crystal violet for a five minute staining incubation. Pegs were again washed 3x with water, then biofilms dissolved in 200 µl methanol per well for five minutes. Samples were then read at OD570 using a BioTek plate reader.

Water survival

PAO1 and PAO1Δ*eftM* were grown overnight at 37°C with rotation. Cultures were back-diluted to 10^6 CFU/mL in water, divided into 1 mL aliquots, and incubated at either 25°C or 37°C static in the dark. 1 mL aliquots were removed at periodic intervals from Day 0 to Day 10 and enumerated by plating serial dilutions for CFU determination.

Exit from stationary phase

PAO1Δ*eftM* and PAO1Δ*eftM* + $eftM_{PAO1}$ were grown in 5 mL LB with rotation at 25°C for 24 hours. After growth, cultures were left static at 25°C for five additional days. Subsequently the cultures were vortexed to disrupt aggregates, density

measured, and cultures were back-diluted to OD_{600}=0.05 in 200 mL fresh LB in a 1 L flask. Cultures were then allowed to resume growth at 25°C with rotation. Samples were monitored every 30 minutes for OD_{600}, and results plotted as a function of time.

Serum sensitivity

Serum sensitivity assays were performed with strain PA14 and derivatives (**Table 1**). Overnight cultures were grown at 25°C, then back-diluted in the morning and grown until mid-exponential phase (OD_{600}=0.8). After measuring density, all cultures were diluted to an assay starting inoculum of 1x10^5 CFU/mL when mixed 50:50 with either 100 µl normal human serum, 100 µl heat-inactivated serum, or 100 µl PBS. Cells were incubated with serum in a 1.5 mL eppendorf tube with rotation at 37°C for one hour, then immediately serially plated for survival on LA.

Proteomics of secreted proteins

Overnight cultures of PAO1Δ*eftM* and PAO1Δ*eftM* + $eftM_{PAO1}$ were back-diluted to OD_{600}=0.05 in LB and grown at 25°C with shaking until mid-exponential phase (OD_{600}=0.8). Samples were centrifuged for 15 minutes at 4°C and 4,000g, then supernatants were filtered through a 0.45 µm low protein-binding filter. 100 mL filtered supernatants were incubated with 20 mL 100% trichloroacetic acid (TCA) at 4°C with rotation overnight in a glass bottle. The next morning samples were centrifuged for 30 minutes at 3,500 g and 4°C. The media/TCA supernatant was removed and pelleted proteins resuspended in 4 mL cold acetone to wash, then centrifuged again. This was repeated one additional time; the final pellet was

resuspended in 50 µl Tris-urea, then stored at -20°C until analysis by Duc Duong and Eric Dammer of the Emory Proteomics Core (see **Chapter III** for details).

Time-course of EF-Tu K5me^3

An overnight culture of PAO1 Spain grown at 37°C was back-diluted to OD_{600}=0.05 in a total volume of 50 mL, then split into two 25 mL cultures. One was incubated at 25°C, the other at 37°C, and both monitored at regular intervals for OD_{600}. Sample volumes equivalent to 1 mL of an OD_{600}=1 culture were collected at periodic intervals for Western blotting with an anti-DiTrimethyl Lysine antibody. Densitometry analysis was performed using Image Lab 4.0 by setting the reactivity of the 25°C OD_{600}=0.61 sample (mid-log) as 100%.

Twitching motility

PA14 and derivatives were utilized, with PA14 *pilC*::tn as a negative control. Strains were struck out from freezer stocks onto LA and incubated at 37°C overnight. Exactly 25 mL of LA+1% agar plates were allowed to cool for 75 minutes, then inoculated with single colonies from the overnight plates by stabbing a toothpick containing the colony through the plate. After inoculation at 25°C for 72 hours, the media was carefully removed using forceps. Petri dishes were stained with 0.1% crystal violet for 2 minutes, then rinsed with DI water. Twitching zones were measured in mm. All five strains were inoculated into separate zones of the same plate.

Swimming motility

LA plates containing exactly 20 mL of 0.2% agar were allowed to cool for one hour, then inoculated with a single 5 µl drop of an overnight culture of bacteria

grown at either 25°C or 37·C. Plates were then incubated at their respective temperatures for 24 hours (37°C) or 49 hours (25°C), at which time swim zones were measured.

Cloning

PAO1Δ*eftM* Sam was constructed by amplifying 1000 bp upstream and 1000 bp downstream of *eftM,* along with an FRT-flanked gentamicin cassette. Fragments were seamlessly fused to pEX18Tc using isothermal assembly, transformed into *E. coli* DH5a, and selected for on LA+gent10. Plasmids were checked by Sanger Sequencing, then introduced to PAO1 Spain by electroporation and selection on LA+gent60 µg/mL. After successful merodiploid confirmation, the disrupted gene version was selected for by swabbing colonies for isolation on LA+10% sucrose+gent60 µg/mL. *eftM*::gent colonies were then electroporated with the helper plasmid pFLP2 to excise the gentamicin marker, selected for on LA+carb300 µg/mL, then counterselected on LA+10% sucrose to remove the plasmid. Successful replacement of *eftM* with an *FRT* scar was confirmed by Sanger sequencing from the upstream and downstream regions of *eftM*, as well as successful restoration of carbenicillin and gentamicin susceptibility,

Mouse infections, performed by Dr. Dina Moustafa

All animal procedures were conducted according to the guidelines of the Emory University Institutional Animal Care and Use Committee (IACUC), under approved protocol number DAR-2003421-042219BN. The study was carried out in strict accordance with established guidelines and policies at Emory University School of Medicine, and recommendations in the Guide for Care and Use of

Laboratory Animals of the National Institute of Health, as well as local, state, and federal laws.

Ten-to twelve-week old female BALB/c mice were obtained from Jackson Laboratories (Bar Harbor, ME). Mice were housed under specific pathogen free (SPF) conditions and were fed ad libitum; mice were given one week of acclimation before the experiments were initiated. PAO1, PAO1Δ*eftM* SAM, and isogenic complements were grown on *Pseudomonas* Isolation Agar (PIA) for 16-18 h at 25°C and were suspended in PBS to an OD_{600} of 0.5, corresponding to ~10^9 CFU/mL. Inocula were adjusted spectrophotometrically to obtain the desired dose in a volume of 20 µL.

BALB/c mice were anesthetized intraperitoneally with 200 µl of ketamine (6.7 mg/ml) and xylazine (1.3 mg/ml) in a 0.9% saline solution prior to infection, and were intranasally instilled with 20 µl (10 µl per nostril) ~ $2x10^7$ colony forming units (CFU) P. aeruginosa strain PAO1 or isogenic mutants. For colonization experiments, mice were euthanized at 24 hours post- infection by CO_2 asphyxiation, and whole lungs were collected aseptically, weighed, and homogenized in 1 mL of PBS. Nasal washes (NW) were obtained by flushing 1 mL of PBS through the nasal passage using an 18-G catheter placed at the oropharyngeal opening. Tissue homogenates and NW were serially diluted and plated on PIA and CFU determinations. For survival experiments, mice were closely monitored for up to 4 days post infection. Mice that became morbid with ruffled fur, shaking, unresponsive to touch, unable to move, and unable to obtain food and water were humanely euthanized by CO_2. Comparison of number of

viable bacteria obtained in lung homogenates was determined with one-way ANOVA. Survival curves were compared using a log rank test. Analysis was conducted using GraphPad Prism 6.0 software

Table 1. Strain List

ID	Genotype	Reference
PAO1	*P. aeruginosa* PAO1	Barbier, Owings *et al* 2013
PAO1Δ*eftM*	PAO1 *eftM* Δ255-487	Barbier, Owings *et al* 2013
PAO1Δ*eftM* + $eftM_{PAO1}$	PAO1Δ*eftM att*Tn7::$P_{eftM(500bp)}$-$eftM_{PAO1}$-FLAG	Chapter III
PAO1ΔeftM + P_{250}-*eftM*	PAO1Δ*eftM att*Tn7::$P_{eftM(250bp)}$-$eftM_{PAO1}$-FLAG	This study
PAO1ΔeftM + P_{100}-*eftM*	PAO1Δ*eftM att*Tn7::$P_{eftM(100bp)}$-$eftM_{PAO1}$-FLAG	This study
PAO1Δ*eftM* + $eftM_{PAHM4}$	PAO1Δ*eftM att*Tn7::P_{eftM}-$eftM_{PAHM4}$-FLAG	Chapter III
PAO1Δ*eftM* SAM	PAO1 *eftM*::*FRT.* Full gene deletion. aka PASP124	This study
PAO1Δ*eftM* SAM + P_{500}-eftM	PAO1Δ*eftM* SAM *att*Tn7::$P_{eftM(500bp)}$-$eftM_{PAO1}$-FLAG	This study
PAO1Δ*eftM* SAM + P_{100}-eftM	PAO1Δ*eftM* SAM *att*Tn7::$P_{eftM(100bp)}$-$eftM_{PAO1}$-FLAG	This study
PAO1Δ*eftM* SAM + $P_{PAHM4(500)}$-eftM	PAO1Δ*eftM* SAM *att*Tn7::P_{eftM}-$eftM_{PAHM4}$-FLAG	This study
PAO1 *pilT*::tn	PW1729; phoAwp06q3H07	Held, Ramage *et al* 2012
PAO1 *pilA*::tn	PW8621; lacZwp08q4E01	Held, Ramage *et al* 2012
PAO1 *pilB*::tn	PW8623; lacZbp01q4G07	Held, Ramage *et al* 2012
PAO1 *pilM*::tn	PW9474; phoAwp09q1B02	Held, Ramage *et al* 2012
PAO1 *pilO*::tn	PW9469; phoAbp01q4A05	Held, Ramage *et al* 2012
PAO1 *pilQ*::tn	PW9466; phoAbp03q3F02	Held, Ramage *et al* 2012
PAO1 *rhlR*::tn	PW6882; laczbp03q2b10	Held, Ramage *et al* 2012
PA14	*P. aeruginosa* PA14	Rahme, Stevens *et al.* 1995
PA14 *eftM*::tn	PA14_08970::MAR2xT7	Liberati *et al.* 2006
PA14 *eftM*::tn + $eftM_{PAO1}$	PA14 *eftM::*tn *att*Tn7::P_{eftM}-$eftM_{PAO1}$-FLAG	Chapter III
PA14 *eftM*::tn + $eftM_{PAHM4}$	PA14 *eftM::*tn *att*Tn7::P_{eftM}-$eftM_{PAHM4}$-FLAG	This study
PA14 Sad36	Surface Attachment Defective mutant (*flgK*::tn*)*	O'Toole, Kolter 2002
PA14 *pilC*::tn	PAMr_nr_mas_06_2:G11 ID 34276	Liberati *et al.* 2006
PA14 *fliC*::tn	PAMr_nr_mas_07_3:A8 ID 36424	Liberati *et al.* 2006
PA14_09910::tn	PAMr_nr_mas_09_4:E1 ID 41345	Liberati *et al.* 2006

	Locus	Description	Fold Change	*p*-value
1	PA5239	transcription termination factor **Rho**	-11.85	3E-06
2	PA5139	hypothetical protein	9.33	7E-07
3	PA0647	hypothetical protein	-4.76	0.0001
4	PA4253	50S ribosomal protein L14 **RplN**	-3.88	0.009
5	PA0767	GTP-binding protein **LepA**	3.22	3E-05
6	PA0639	conserved hypothetical protein	-3.19	3E-59
7	PA0044	exoenzyme T **ExoT**	-2.87	0.043
8	PA1493	sulfate-binding protein of ABC transporter **CysP**	2.67	0.013
9	PA3763	phosphoribosylformylglycinamidine synthase **PurL**	-2.55	7E-59
10	PA5201	conserved hypothetical protein	-2.53	0.0003
11	PA4855	phosphoribosylamine-glycine ligase **PurD**	-2.45	0.017
12	PA4764	ferric uptake regulation protein **Fur**	2.42	0.025
13	PA5275	conserved hypothetical protein	2.41	0.003
14	PA4333	probable fumarase	-2.22	0.0005
15	PA5243	delta-aminolevulinic acid dehydratase **HemB**	2.21	0.039
16	PA2582	hypothetical protein	2.16	0.027
17	PA0922	hypothetical protein	N/A**	N/A

Table 2: Proteins with >2-fold change in culture supernatants.

Supernatants from mid-exponential phase cultures of PAO1Δ*eftM* and PAO1Δ*eftM* + $eftM_{PAO1}$ grown at 25°C (n=3) were precipitated by trichloroacetic acid (TCA). Pelleted proteins were identified and quantified by label-free mass spectrometry. Those with a 2-fold difference or larger between the mean of one sample compared to the mean of the other sample, and a *p*-value of <0.05, are listed.

Positive fold change = detection is higher in the *eftM*-complemented strain.

Negative fold change = detection is higher in the *eftM* deletion strain.

** = detected in all three biological replicates of the complement strain only.

Pink; cytoplasmic protein. Green; cytoplasmic membrane protein. Yellow; Periplasmic protein. Blue; Secreted protein. White; unknown.

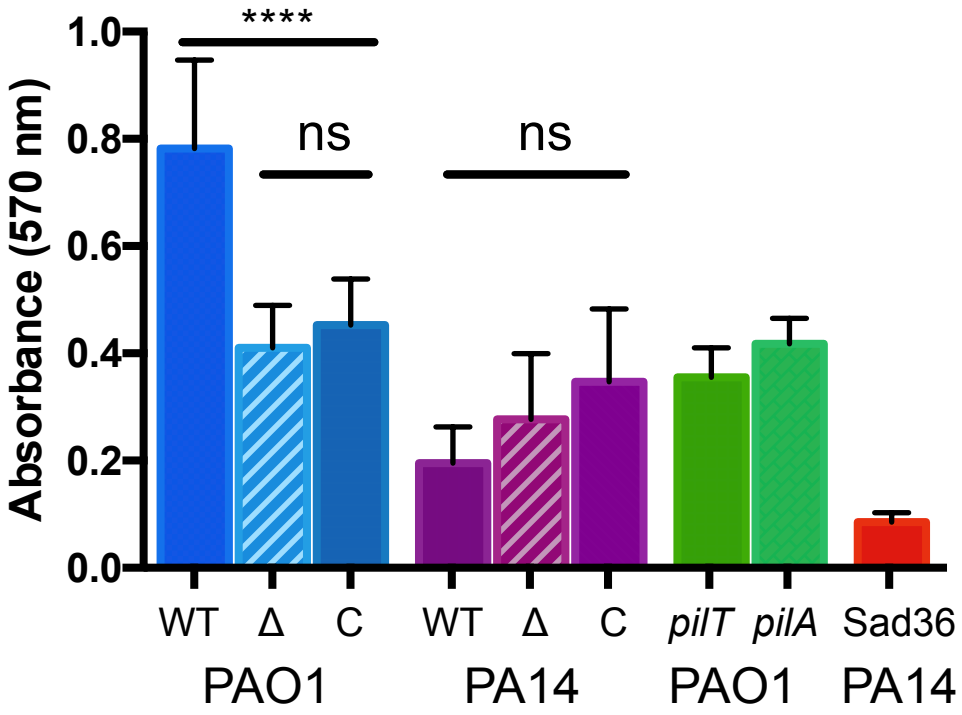

Figure 1: EftM does not appear to alter biofilm production after static 24 hour growth at 25°C.

PAO1, PAO1Δ*eftM*, PAO1Δ*eftM* + $eftM_{PAO1}$, PA14, PA14 *eftM*::tn, PA14 *eftM*::tn + $eftM_{PAO1}$, PAO1 *pilT*::tn, PAO1 *pilA*::tn, and PA14 Sad36 (surface attachment defective) were assessed for relative biofilm mass. Biofilm was allowed to form from standardized inputs with static incubation at 25°C. After 24 hours, biofilms were stained with crystal violet, dissolved, and read by absorbance at 570 nm. Intensity of crystal violet correlates with biofilm mass. Absorbance was plotted as an average and error bars as standard deviation of the mean. Significance was determined by one-way ANOVA with Tukey multiple comparisons analysis. N=8.

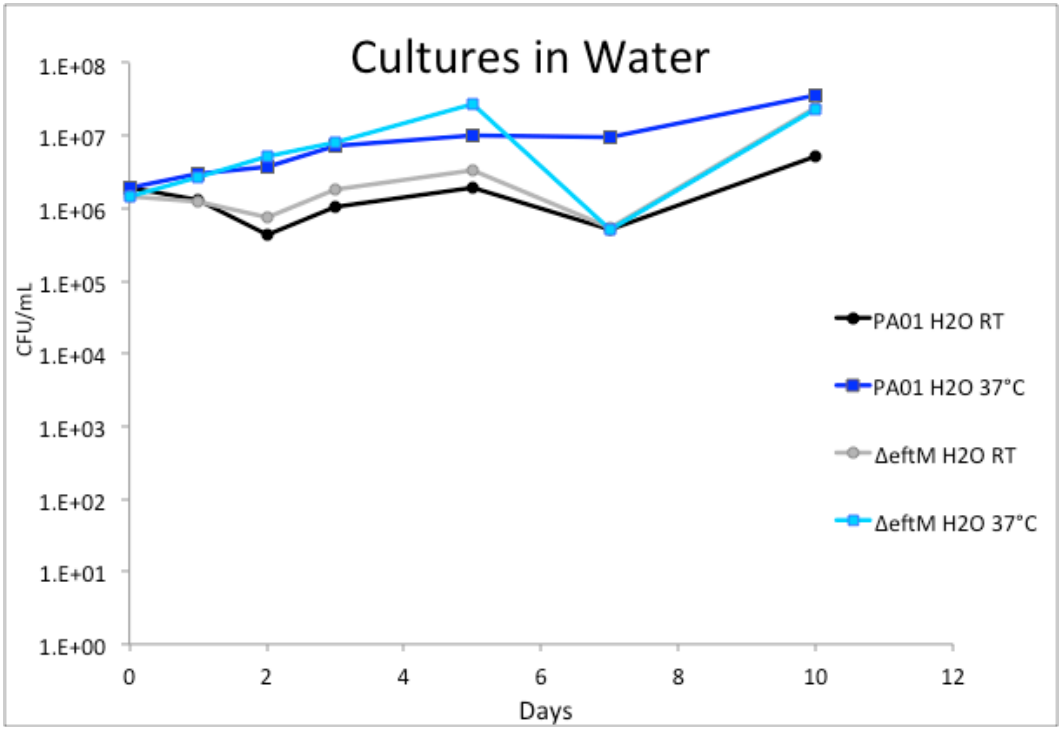

Figure 2: Contribution of EftM to long-term survival in water.

PAO1 and PAO1Δ*eftM* were grown overnight at 37°C with rotation. Cultures were back-diluted to 10^6 CFU/mL in water, divided into 1 mL aliquots, and incubated at either 25°C or 37°C static in the dark. 1 mL aliquots were removed at periodic intervals from Day 0 to Day 10 and enumerated by plating serial dilutions for CFU determination. N=1.

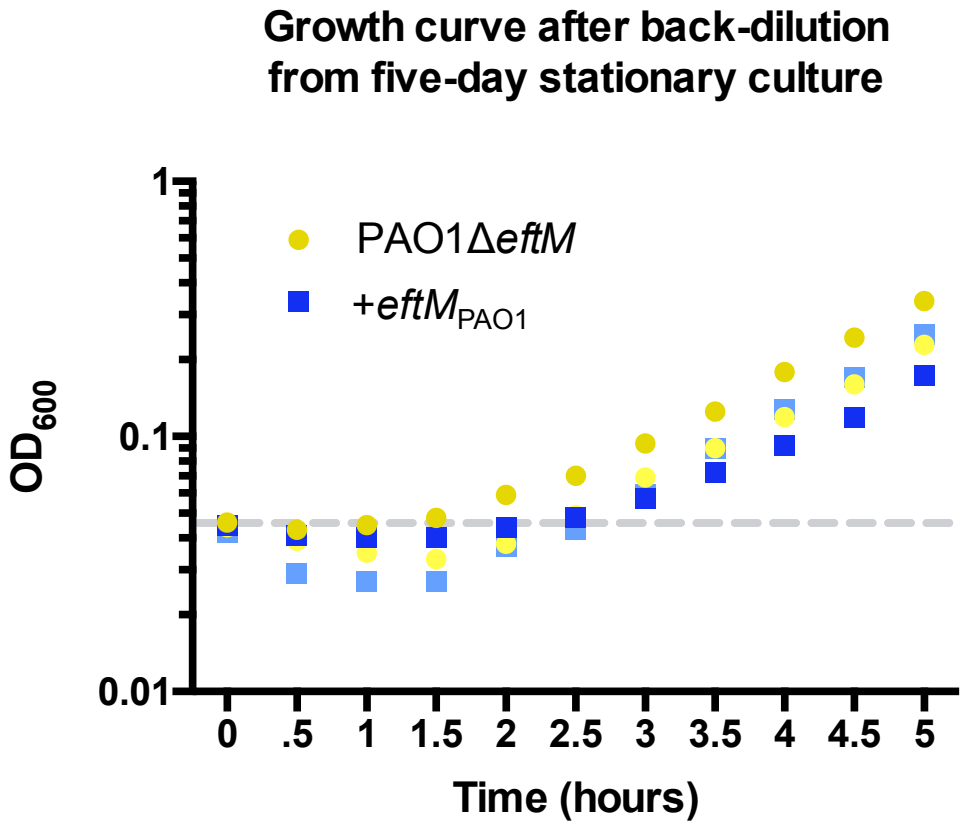

Figure 3: Exit from long-term stationary phase.

PAO1Δ*eftM* and PAO1Δ*eftM* + *eftM*$_{PAO1}$ were grown for 24 hours with rotation, then incubated static for five days at 25°C. After back-dilution, cells were allowed to resume growth with shaking and were monitored for OD_{600} ever 30 minutes. Light colors are one replicate, and darker colors a second. N=2.

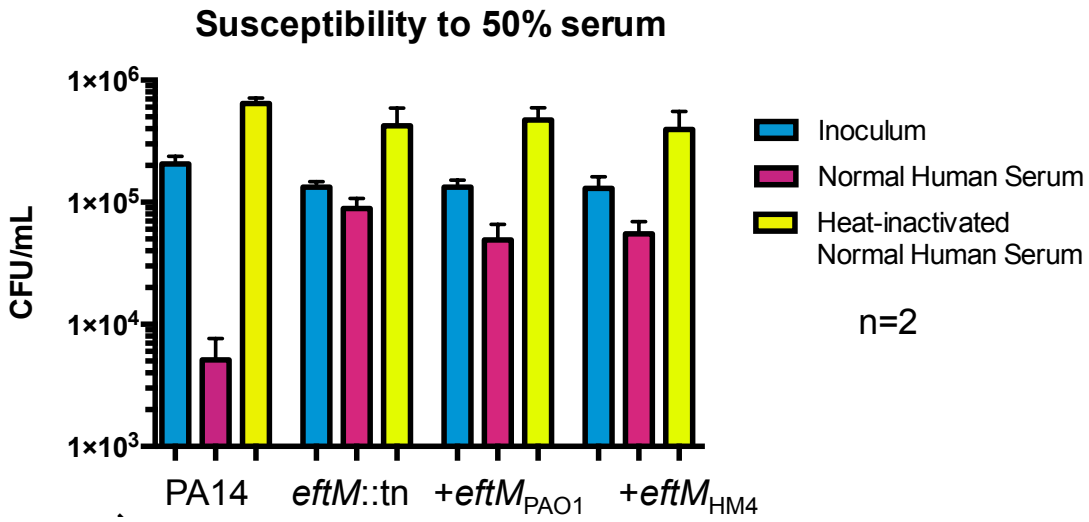

Figure 4: Survival of PA14 and derivatives after one hour incubation with 50% normal human serum.

PA14, PA14 *eftM*::tn, PA14 *eftM*::tn + $eftM_{PAO1}$, and PA14 *eftM*::tn + $eftM_{PAHM4}$ were grown to mid-exponential phase at 25°C, then back-diluted to a final concentration of $1x10^5$ CFU/mL in 50% normal human serum or heat-inactivated normal human serum. After 60 minutes at 37°C with rotation, samples were enumerated for bacterial survival. Results are represented as mean CFU/mL with error bars representing standard deviation of the mean. N=2.

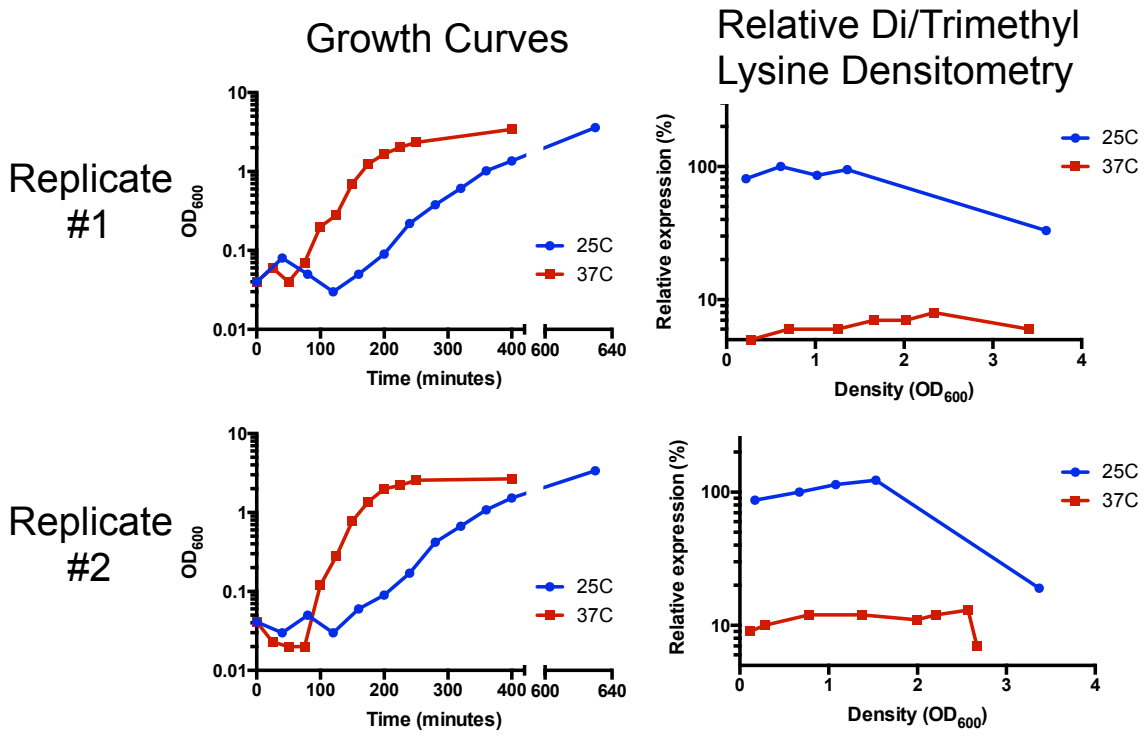

Figure 5: Trimethylation of EF-Tu appears consistent throughout growth phase.

PAO1 was grown overnight at 37°C, then back-diluted to OD_{600}=0.05. The back-diluted culture was split into two aliquots with one allowed to resume growth at 37°C and the second switched to 25°C. At periodic intervals samples were assessed for OD_{600}, which are shown plotted as a function of time on the left-hand panels. Cell volumes equivalent to 1 mL of an OD_{600}=1 culture were also collected at periodic intervals, harvested by centrifugation, and resuspended in Laemmli buffer. After analysis by αDi/Trimethyl Lysine western immunoblotting, relative densitometry was plotted as a function of OD_{600}. Reactivity observed from the 25°C OD_{600}=0.61 sample was set as 100%. N=2.

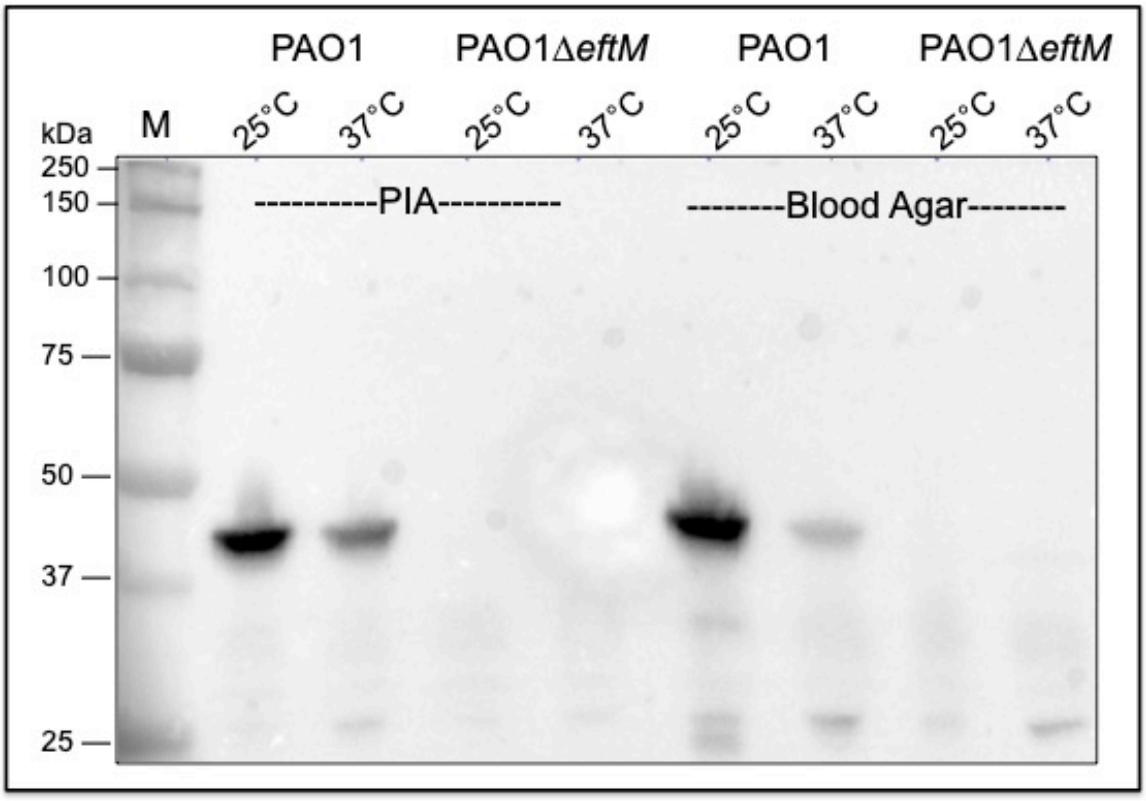

Figure 6: αDi/Trimethyl Lysine Western blot of bacteria grown on various media.

PAO1 and PAO1Δ*eftM* were grown on Pseudomonas Isolation Agar (PIA; low iron) or Blood Agar plates (high iron) at either 25°C for ~48 hours or 37°C for ~16 hours. After growth, colonies were swabbed into sterile PBS and density read at OD_{600}. A standardized cell number of each was collected by centrifugation, and then pellets were resuspended in 100 µl Laemmli buffer. 10 µl samples were separated by 10% SDS-PAGE and blotted with an αDi/Trimethyl Lysine antibody.

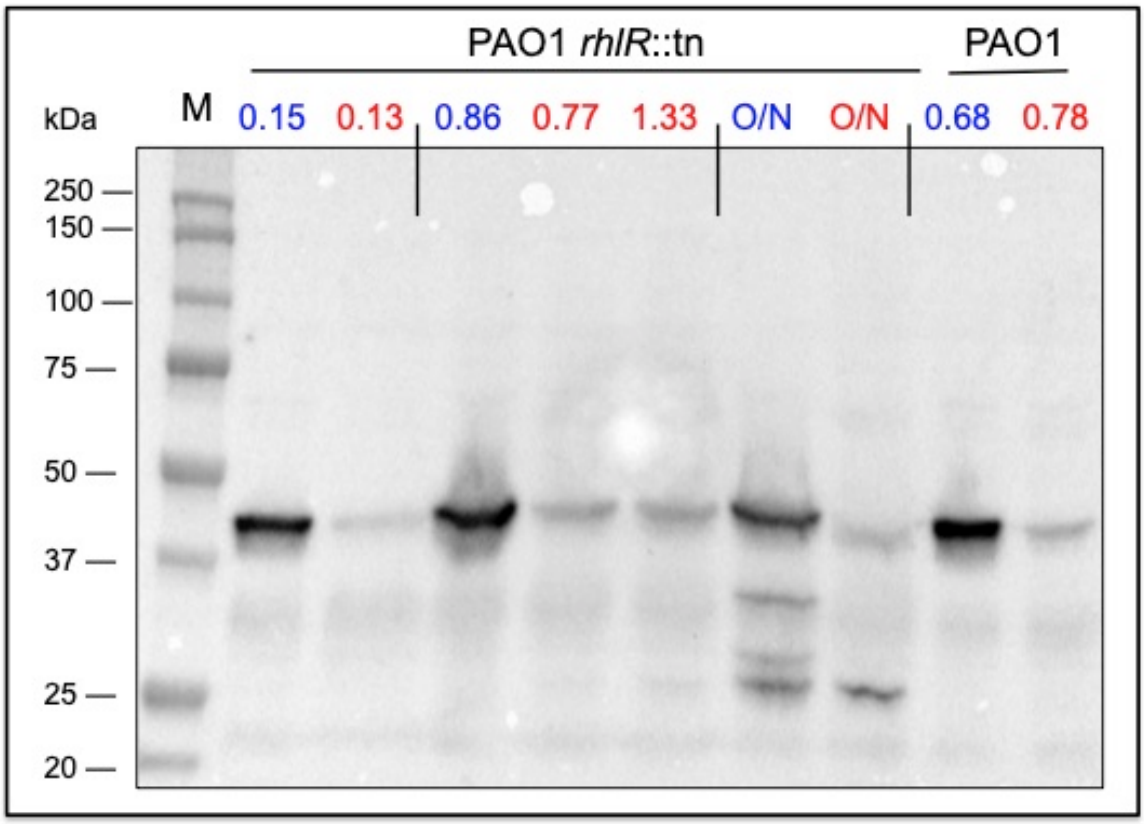

Figure 7: EftM temperature regulation in an *rhlR* mutant.

PW6882 (PAO1 *rhlR*::tn) and PAO1 were grown overnight at 37°C with rotation, then back-diluted. Samples were allowed to resume growth at either 25°C (blue) or 37°C (red) and monitored at OD_{600}. Samples equivalent to 1 mL of an OD_{600}=1 culture were collected at indicated culture densities, pelleted, and resuspended in 100 µl of 1x Laemmli. 10 µl aliquots were then blotted with an αDi/Trimethyl Lysine antibody. Right-most two lanes are controls for typical thermoregulation observed in PAO1.

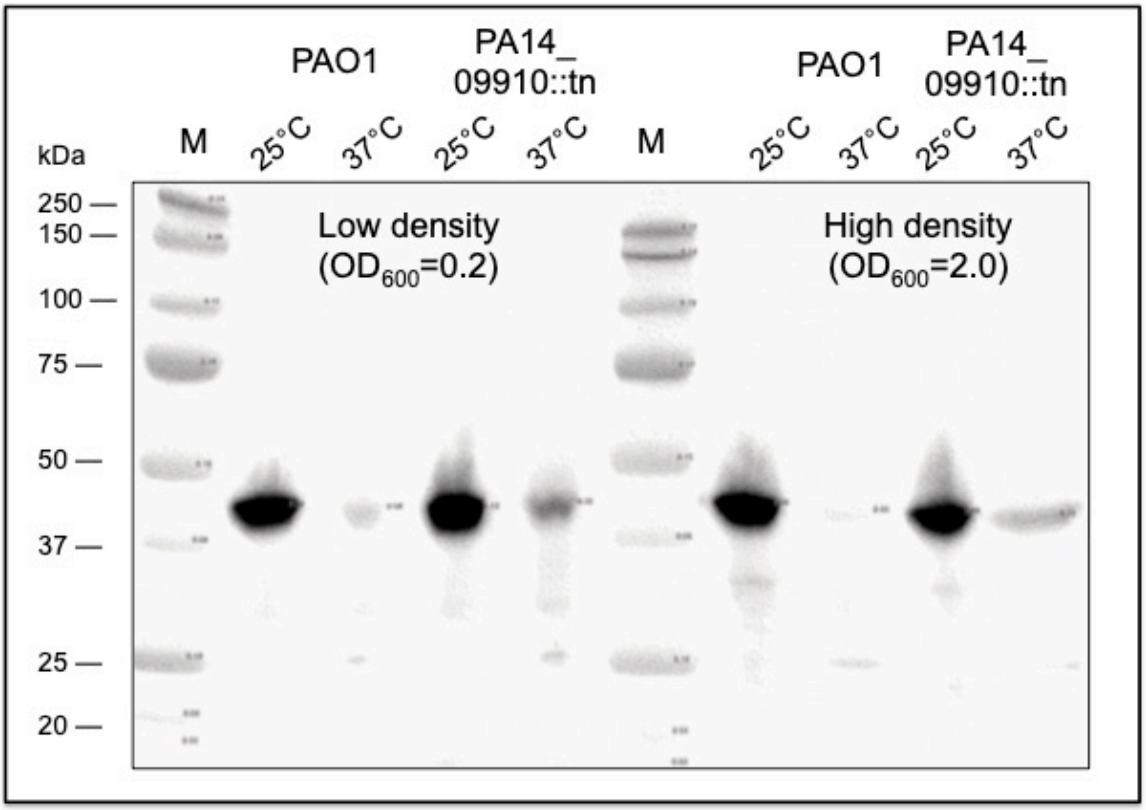

Figure 8: Comparison of EftM activity in PAO1 vs a putative transcriptional regulator transposon mutant.

PAO1 or PA14_09910::*tn* (PAO1 homolog: PA4174) were grown overnight at 25°C or 37°C, then back-diluted to OD_{600}=0.05, allowed to continue growing, and collected at OD_{600}=0.2 or 2.0 by pelleting a 1 mL OD_{600}=1.0 equivalent. Pellets were resuspended in 100 µl Laemmli buffer and Western blotted according to standard protocol with separation on a 10% acrylamide gel and blotting with an αDi/Trimethyl Lysine antibody.

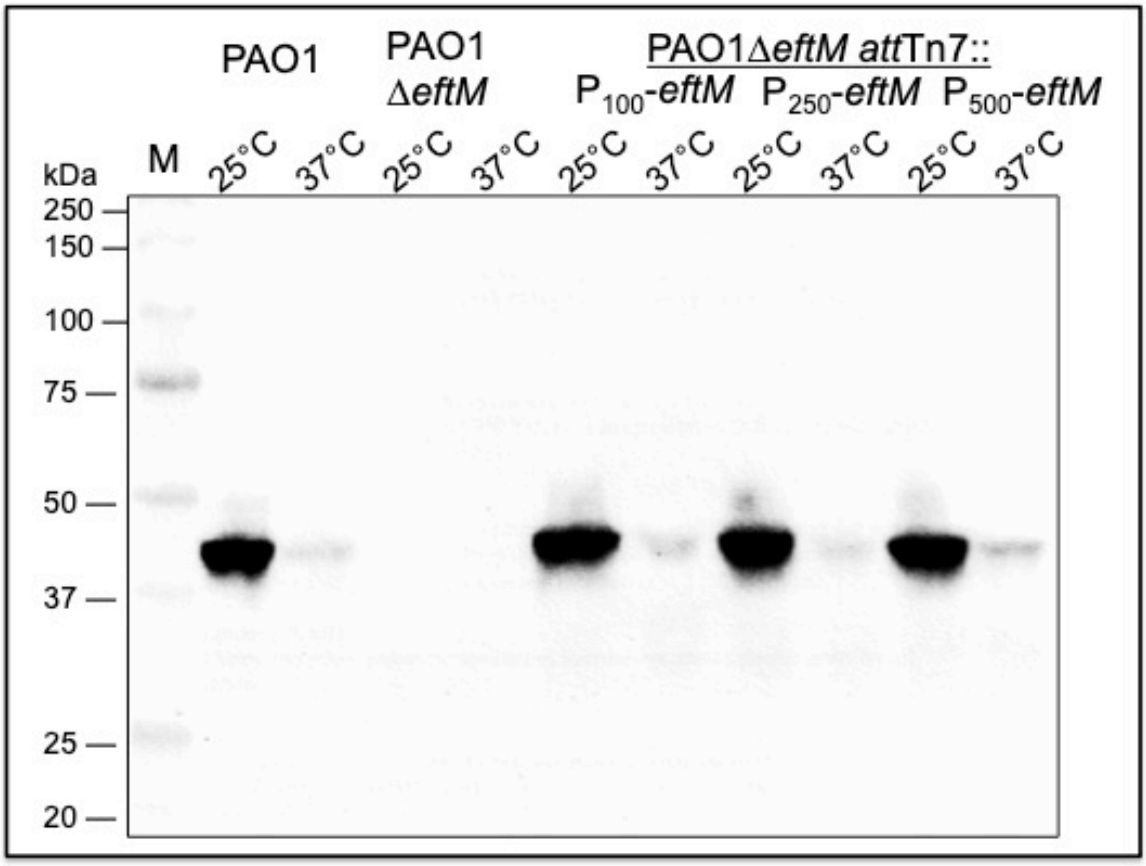

Figure 9: chromosomal context does not impact *eftM* expression.

PAO1, PAO1Δ*eftM*, PAO1Δ*eftM* + $eftM_{PAO1}$, PAO1Δ*eftM* + P_{250}-$eftM_{PAO1}$, and PAO1Δ*eftM* + P_{100}-$eftM_{PAO1}$ were utilized. Strain P_{500} contains 500 bp of sequence upstream of the *eftM* ATG start codon as *eftM*'s promoter region, while P_{250} contains 250 bp, and P_{100} contains just the 100bp intergenic region. Strains were incubated at 37°C overnight with rotation. In the morning, cultures were back-diluted to OD_{600}=0.05, split, and incubated at either 25°C or 37°C. Once cultures reached OD_{600}=0.5-0.8, a 1 mL OD_{600}=1 equivalent was collected, pelleted, and resuspended in 100 µl Laemmli buffer. 15 µl of each sample was separated by SDS-PAGE and blotted with an αDi/Trimethyl Lysine antibody.

A

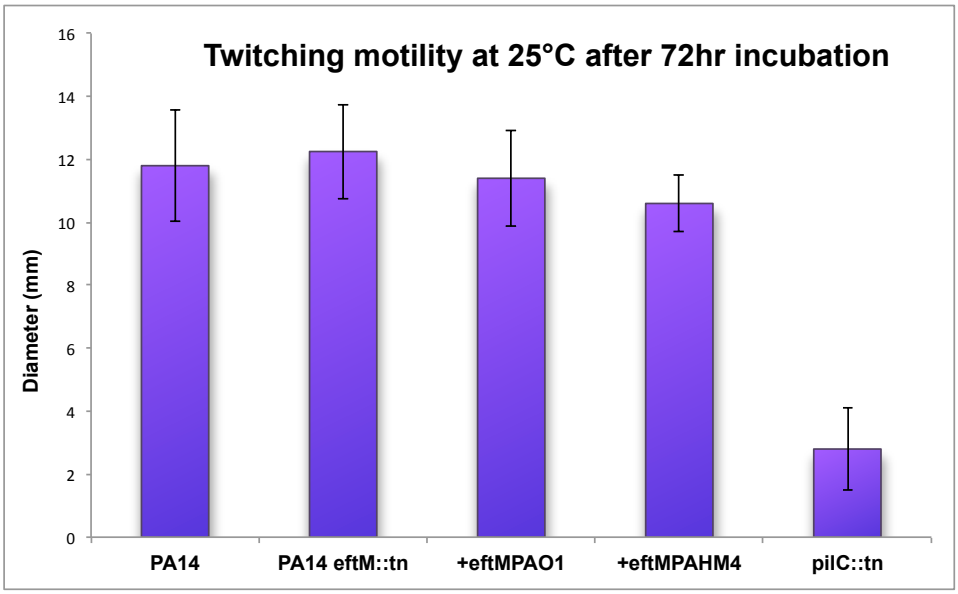

B

37°C

PA14 *eftM*::tn +*eftM*$_{PAO1}$ +*eftM*$_{HM4}$ *fliC*::tn

C

25°C

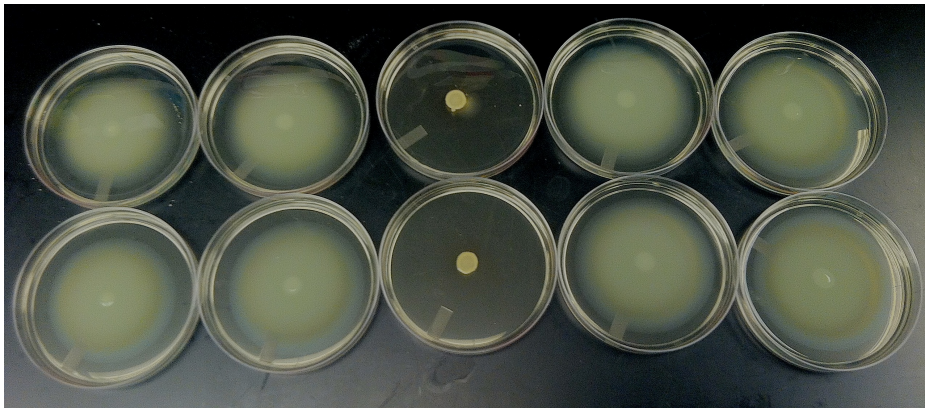

PA14 *eftM*::tn *fliC*:::tn *eftM*::tn+*eftM*$_{PAO1}$ +*eftM*$_{HM4}$

Figure 10: EftM does not appear to impact twitching or swimming based motility.

A: PA14 and derivatives were stabbed into 1% agar plates, then assessed for pili-based twitching motility after three days of growth at 25°C. After 72 hours, media was removed and the polystyrene plate was stained with crystal violet to reveal the diameter of twitching zone. Diameters were plotted as an average and standard deviation for each strain (n=5).

B: 0.2% agar swim plates were inoculated with a single 5 µl drop of each indicated strain grown overnight at 37°C. After 24 hours of growth at 37°C in a humidified incubator, plates were photographed.

C: 0.2% agar swim plates were inoculated with a single 5 µl drop of each indicated strain grown overnight at 25°C. After 49 hours of growth at 25°C in a humidified incubator, plates were photographed.

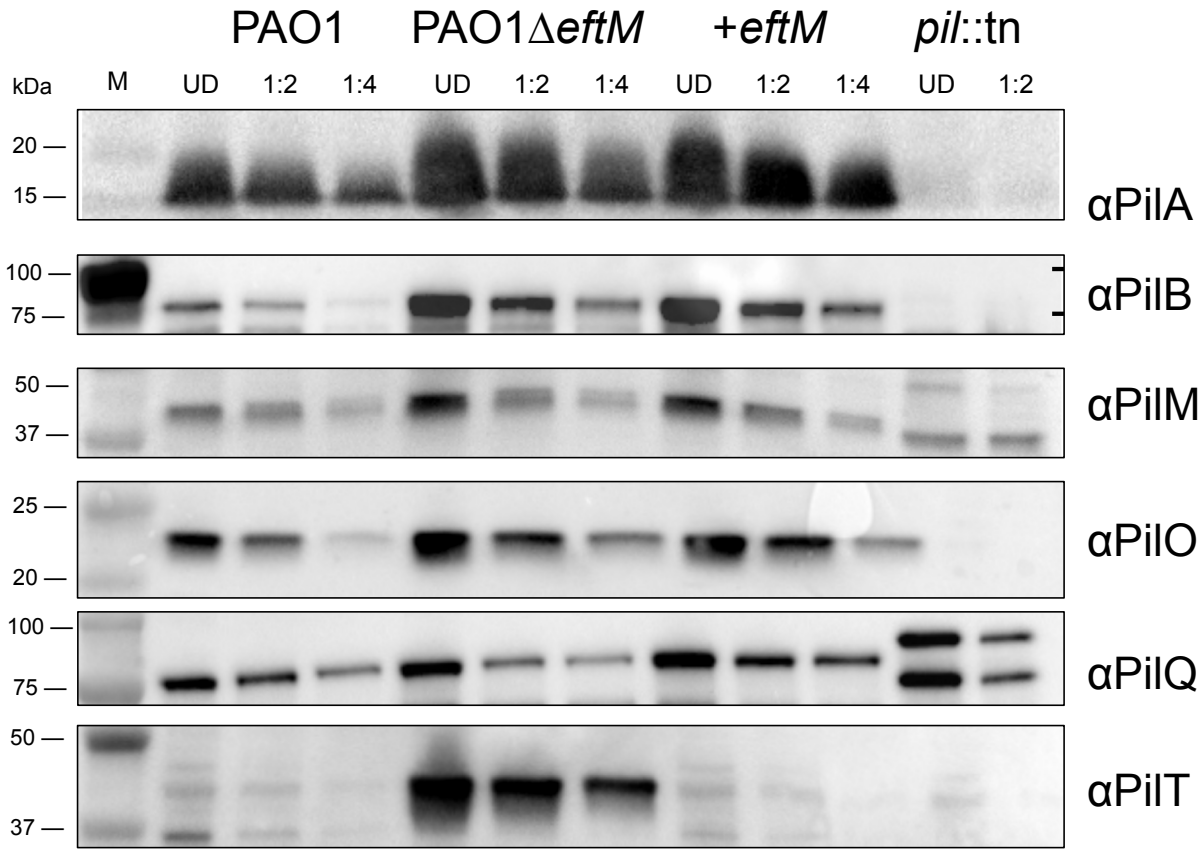

Figure 11: Pili were altered during construction of PAO1Δ*eftM.*

PAO1, PAO1Δ*eftM,* PAO1Δ*eftM* + $eftM_{PAO1}$, and appropriate transposon mutant control strains (see Table 1) were grown to OD600=0.8 with rotation in LB, at which time a 1mL of OD_{600}=1 equivalent collected by centrifugation. Pellets were resuspended in 100 µl of Laemmli buffer. 10 µl of each sample (UD), 10 µl of a 1:2 dilution of this sample (1:2), or 10 µl of a 1:4 dilution (1:4) were separated by SDS-PAGE, then blotted with the indicated αPil antibody (kind gifts from Dr. Lori Burrows). Blots are representative of multiple replicates.

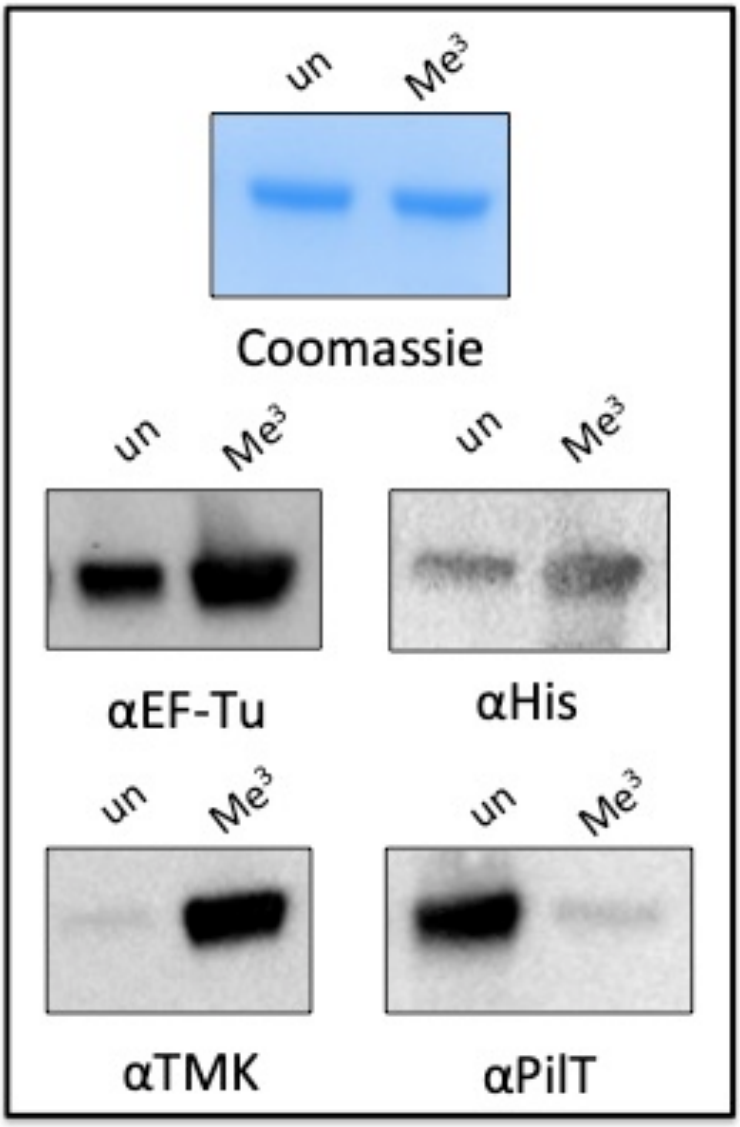

Figure 12: αPilT strongly cross-reacts with unmethylated, but not methylated, EF-Tu.

C terminally tagged (6x-his) EF-Tu was purified from PAO1ΔeftM (unmethylated protein) or its isogenic complement PAO1Δ*eftM* + $eftM_{PAO1}$ (methylated protein). 50 ng of each were separated by SDS-PAGE in quintuplicate, then either stained or immunoblotted with the indicated antibody.

A

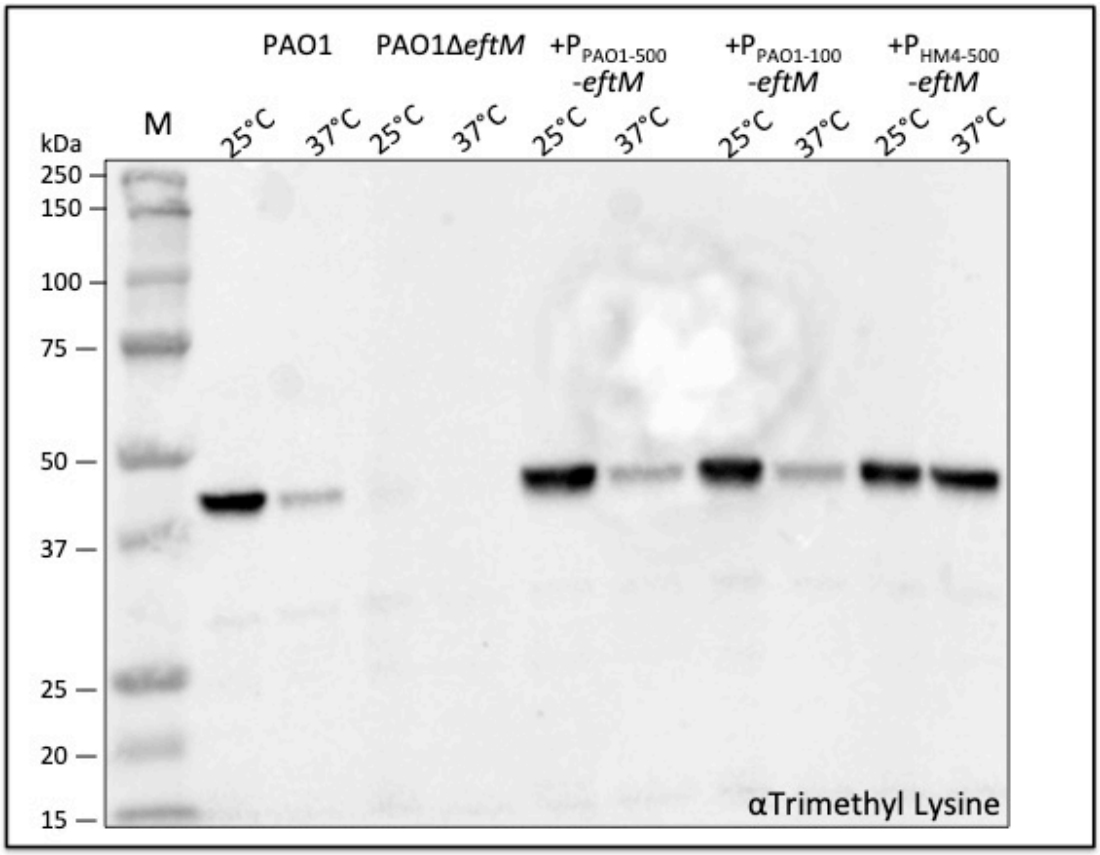
PAO1
PAO1Δ*eftM*
+P PAO1-500 -*eftM*
+P PAO1-100 -*eftM*
+P HM4-500 -*eftM*
M
25°C
37°C
kDa
250
150
100
75
50
37
25
20
15
αTrimethyl Lysine

B

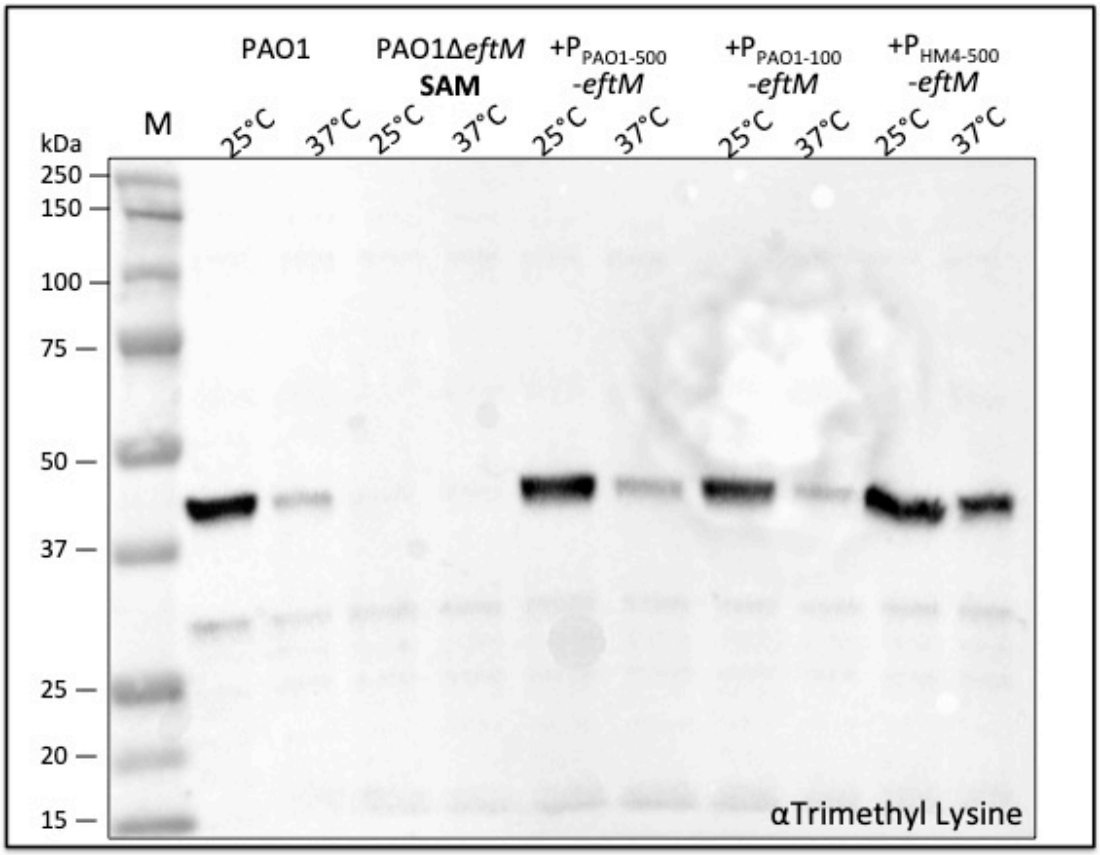
PAO1
PAO1Δ*eftM*
SAM
+P PAO1-500 -*eftM*
+P PAO1-100 -*eftM*
+P HM4-500 -*eftM*
M
25°C
37°C
kDa
250
150
100
75
50
37
25
20
15
αTrimethyl Lysine

Figure 13: A newly constructed, full *eftM* deletion is phenotypically similar to the previously-characterized deletion strain.

A: PAO1, PAO1Δ*eftM* (partial deletion; see **Table 1**), and isogenic complementation strains are analyzed for αTrimethyl Lysine reactivity at 25°C and 37°C.

B: PAO1, PAO1Δ*eftM* SAM (full deletion; see **Table 1**), and isogenic complementation strains are analyzed for αTrimethyl Lysine reactivity at 25°C. This newly constructed strain set shows the same trend as the well-characterized strains from (A).

A

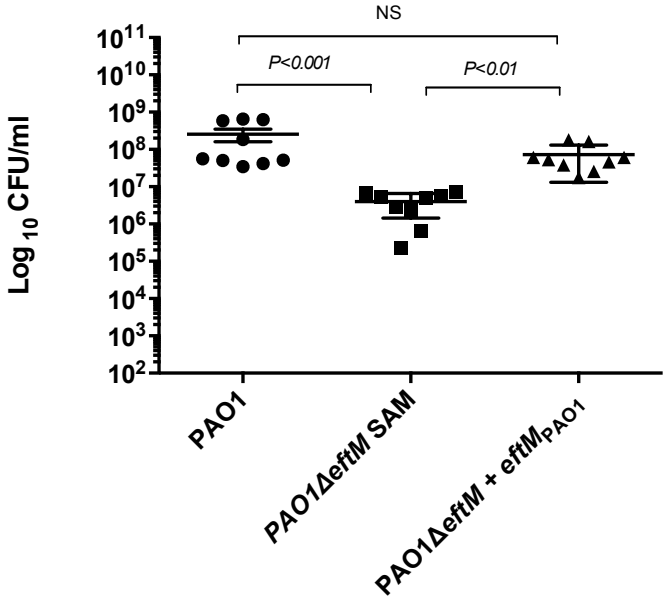
NS
P<0.001
P<0.01
Log 10 CFU/ml
PAO1
PAO1ΔeftM SAM
PAO1ΔeftM + eftMPAO1

B

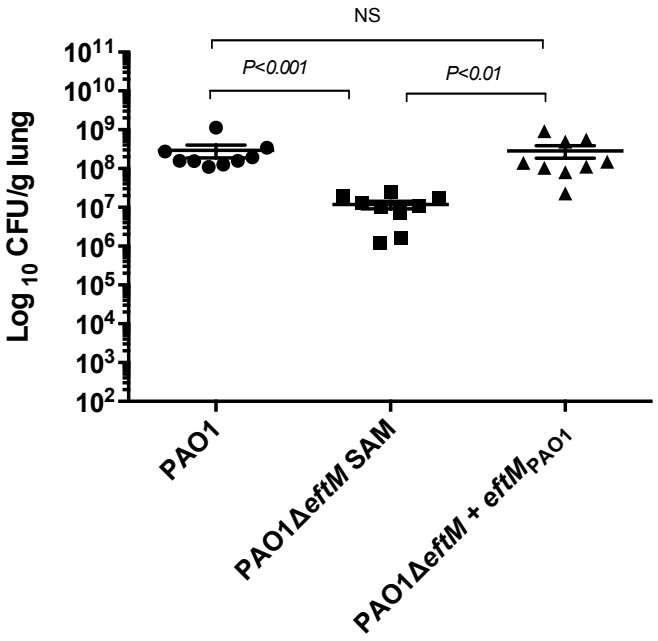
NS
P<0.001
P<0.01
Log 10 CFU/g lung
PAO1
PAO1ΔeftM SAM
PAO1ΔeftM + eftMPAO1

C

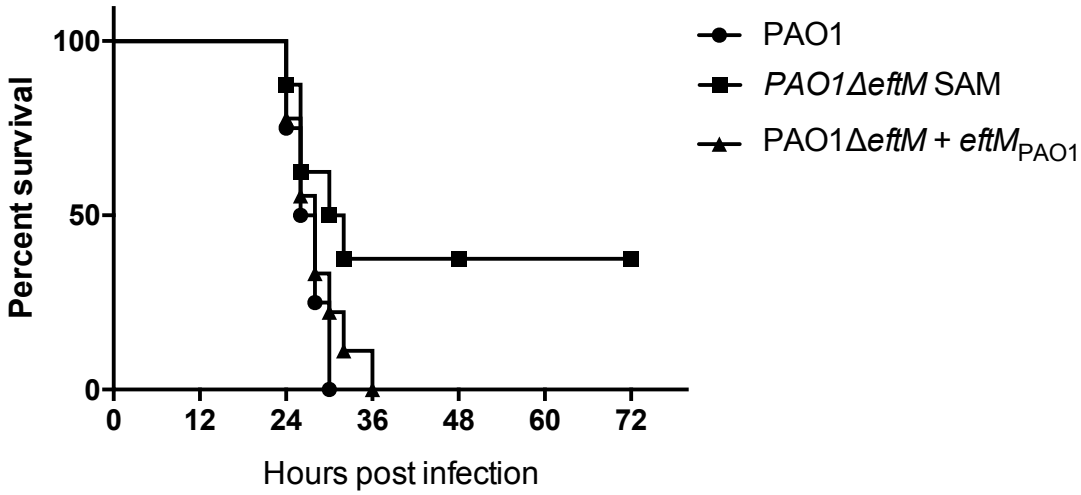
Percent survival
Hours post infection
PAO1
PAO1ΔeftM SAM
PAO1ΔeftM + eftMPAO1

Figure 14: Survival and recovery of bacteria with and without EftM in a murine model of infection.

BALB/c mice were infected intranasally with PAO1, PAO1Δ*eftM* SAM, or PAO1Δ*eftM* SAM + $eftM_{PAO1}$.

A: Bacterial load in the nasal wash of mice 24 hours after infection with the indicated *P. aeruginosa* strains. N=9.

B: Bacterial load in the lungs of mice 24 hours after infection with the indicated *P. aeruginosa* strains. N=9.

C: Survival curves over 72 hours for mice infected intranasally with ~$2x10^7$ CFU of the indicated strains. N=8.

1 Spiers, A. J., Buckling, A. & Rainey, P. B. The causes of Pseudomonas diversity. *Microbiology* **146 (Pt 10)**, 2345-2350, doi:10.1099/00221287-146-10-2345 (2000).

2 LaBauve, A. E. & Wargo, M. J. Growth and laboratory maintenance of Pseudomonas aeruginosa. *Curr Protoc Microbiol* **Chapter 6**, Unit 6E 1, doi:10.1002/9780471729259.mc06e01s25 (2012).

3 Owings, J. P. *et al.* Pseudomonas aeruginosa EftM Is a Thermoregulated Methyltransferase. *J Biol Chem* **291**, 3280-3290, doi:10.1074/jbc.M115.706853 (2016).

4 Barbier, M. *et al.* Lysine trimethylation of EF-Tu mimics platelet-activating factor to initiate Pseudomonas aeruginosa pneumonia. *MBio* **4**, e00207-00213, doi:10.1128/mBio.00207-13 (2013).

5 Clark, S. E. & Weiser, J. N. Microbial modulation of host immunity with the small molecule phosphorylcholine. *Infect Immun* **81**, 392-401, doi:10.1128/IAI.01168-12 (2013).

6 Rasamiravaka, T., Labtani, Q., Duez, P. & El Jaziri, M. The formation of biofilms by Pseudomonas aeruginosa: a review of the natural and synthetic compounds interfering with control mechanisms. *Biomed Res Int* **2015**, 759348, doi:10.1155/2015/759348 (2015).

7 Skariyachan, S., Sridhar, V. S., Packirisamy, S., Kumargowda, S. T. & Challapilli, S. B. Recent perspectives on the molecular basis of biofilm formation by Pseudomonas aeruginosa and approaches for treatment and biofilm dispersal. *Folia Microbiol (Praha)* **63**, 413-432, doi:10.1007/s12223-018-0585-4 (2018).

8 Deziel, E., Comeau, Y. & Villemur, R. Initiation of biofilm formation by Pseudomonas aeruginosa 57RP correlates with emergence of hyperpiliated and

highly adherent phenotypic variants deficient in swimming, swarming, and twitching motilities. *J Bacteriol* **183**, 1195-1204, doi:10.1128/JB.183.4.1195-1204.2001 (2001).

9 O'Toole, G. A. & Kolter, R. Flagellar and twitching motility are necessary for Pseudomonas aeruginosa biofilm development. *Mol Microbiol* **30**, 295-304 (1998).

10 Lewis, K. Persister cells. *Annu Rev Microbiol* **64**, 357-372, doi:10.1146/annurev.micro.112408.134306 (2010).

11 Mulcahy, L. R., Burns, J. L., Lory, S. & Lewis, K. Emergence of Pseudomonas aeruginosa strains producing high levels of persister cells in patients with cystic fibrosis. *J Bacteriol* **192**, 6191-6199, doi:10.1128/JB.01651-09 (2010).

12 Sala, A., Bordes, P. & Genevaux, P. Multiple toxin-antitoxin systems in Mycobacterium tuberculosis. *Toxins (Basel)* **6**, 1002-1020, doi:10.3390/toxins6031002 (2014).

13 Wood, T. L. & Wood, T. K. The HigB/HigA toxin/antitoxin system of Pseudomonas aeruginosa influences the virulence factors pyochelin, pyocyanin, and biofilm formation. *Microbiologyopen* **5**, 499-511, doi:10.1002/mbo3.346 (2016).

14 Wang, H. *et al.* Purification and functional characterization of a histone H3-lysine 4-specific methyltransferase. *Molecular cell* **8**, 1207-1217 (2001).

15 Yang, X. D., Lamb, A. & Chen, L. F. Methylation, a new epigenetic mark for protein stability. *Epigenetics* **4**, 429-433 (2009).

16 Bugla-Ploskonska, G., Kiersnowski, A., Futoma-Koloch, B. & Doroszkiewicz, W. Killing of Gram-negative bacteria with normal human serum and normal bovine serum: use of lysozyme and complement proteins in the death of Salmonella strains O48. *Microb Ecol* **58**, 276-289, doi:10.1007/s00248-009-9503-2 (2009).

17 Sarma, J. V. & Ward, P. A. The complement system. *Cell Tissue Res* **343**, 227-235, doi:10.1007/s00441-010-1034-0 (2011).

18 Weiser, J. N. *et al.* Phosphorylcholine on the lipopolysaccharide of Haemophilus influenzae contributes to persistence in the respiratory tract and sensitivity to serum killing mediated by C-reactive protein. *J Exp Med* **187**, 631-640 (1998).

19 Gewurz, H., Mold, C., Siegel, J. & Fiedel, B. C-reactive protein and the acute phase response. *Adv Intern Med* **27**, 345-372 (1982).

20 Noel, J. K. & Whitford, P. C. How EF-Tu can contribute to efficient proofreading of aa-tRNA by the ribosome. *Nat Commun* **7**, 13314, doi:10.1038/ncomms13314 (2016).

21 Furano, A. V. Content of elongation factor Tu in Escherichia coli. *Proc Natl Acad Sci U S A* **72**, 4780-4784 (1975).

22 Abdulkarim, F., Tuohy, T. M., Buckingham, R. H. & Hughes, D. Missense substitutions lethal to essential functions of EF-Tu. *Biochimie* **73**, 1457-1464 (1991).

23 Van Noort, J. M. *et al.* Methylation in vivo of elongation factor EF-Tu at lysine-56 decreases the rate of tRNA-dependent GTP hydrolysis. *Eur J Biochem* **160**, 557-561 (1986).

24 Whitney, J. C. *et al.* An interbacterial NAD(P)(+) glycohydrolase toxin requires elongation factor Tu for delivery to target cells. *Cell* **163**, 607-619, doi:10.1016/j.cell.2015.09.027 (2015).

25 Winsor, G. L. *et al.* Enhanced annotations and features for comparing thousands of Pseudomonas genomes in the Pseudomonas genome database. *Nucleic Acids Res* **44**, D646-653, doi:10.1093/nar/gkv1227 (2016).

26 Chang, D. E., Smalley, D. J. & Conway, T. Gene expression profiling of Escherichia coli growth transitions: an expanded stringent response model. *Mol Microbiol* **45**, 289-306 (2002).

27 Munch, R. *et al.* Virtual Footprint and PRODORIC: an integrative framework for regulon prediction in prokaryotes. *Bioinformatics* **21**, 4187-4189, doi:10.1093/bioinformatics/bti635 (2005).

28 Ochsner, U. A. & Vasil, M. L. Gene repression by the ferric uptake regulator in Pseudomonas aeruginosa: cycle selection of iron-regulated genes. *Proc Natl Acad Sci U S A* **93**, 4409-4414 (1996).

29 King, E. O., Ward, M. K. & Raney, D. E. Two simple media for the demonstration of pyocyanin and fluorescin. *J Lab Clin Med* **44**, 301-307 (1954).

30 Schuster, M., Lostroh, C. P., Ogi, T. & Greenberg, E. P. Identification, timing, and signal specificity of Pseudomonas aeruginosa quorum-controlled genes: a transcriptome analysis. *J Bacteriol* **185**, 2066-2079 (2003).

31 Atlung, T. & Ingmer, H. H-NS: a modulator of environmentally regulated gene expression. *Mol Microbiol* **24**, 7-17 (1997).

32 Bonnefoy, E. & Rouviere-Yaniv, J. HU, the major histone-like protein of E. coli, modulates the binding of IHF to oriC. *The EMBO journal* **11**, 4489-4496 (1992).

33 Kamashev, D. *et al.* Comparison of histone-like HU protein DNA-binding properties and HU/IHF protein sequence alignment. *PLoS One* **12**, e0188037, doi:10.1371/journal.pone.0188037 (2017).

34 Garcia-Fontana, C. *et al.* High specificity in CheR methyltransferase function: CheR2 of Pseudomonas putida is essential for chemotaxis, whereas CheR1 is involved in biofilm formation. *J Biol Chem* **288**, 18987-18999, doi:10.1074/jbc.M113.472605 (2013).

35 Falke, J. J. & Hazelbauer, G. L. Transmembrane signaling in bacterial chemoreceptors. *Trends Biochem Sci* **26**, 257-265 (2001).

36 Wadhams, G. H. & Armitage, J. P. Making sense of it all: bacterial chemotaxis. *Nat Rev Mol Cell Biol* **5**, 1024-1037, doi:10.1038/nrm1524 (2004).

37 Perez, E., West, A. H., Stock, A. M. & Djordjevic, S. Discrimination between different methylation states of chemotaxis receptor Tar by receptor methyltransferase CheR. *Biochemistry* **43**, 953-961, doi:10.1021/bi035455q (2004).

38 Giltner, C. L., Nguyen, Y. & Burrows, L. L. Type IV pilin proteins: versatile molecular modules. *Microbiol Mol Biol Rev* **76**, 740-772, doi:10.1128/MMBR.00035-12 (2012).

39 Burrows, L. L. Pseudomonas aeruginosa twitching motility: type IV pili in action. *Annu Rev Microbiol* **66**, 493-520, doi:10.1146/annurev-micro-092611-150055 (2012).

40 Ou, J. T. & Anderson, T. F. Role of pili in bacterial conjugation. *J Bacteriol* **102**, 648-654 (1970).

41 Pizarro-Cerda, J. & Cossart, P. Bacterial adhesion and entry into host cells. *Cell* **124**, 715-727, doi:10.1016/j.cell.2006.02.012 (2006).

42 Kunze, G. *et al.* The N terminus of bacterial elongation factor Tu elicits innate immunity in Arabidopsis plants. *Plant Cell* **16**, 3496-3507, doi:10.1105/tpc.104.026765 (2004).

Investigation into the mechanism of transcriptional thermoregulation for the *Pseudomonas aeruginosa* virulence factor PrpL

Samantha M. Prezioso[1,2], Kathryn A. MacGillivray[2,4], Joanna B. Goldberg[2,3,4]

[1]Microbiology and Molecular Genetics (MMG) Program, Graduate Division of Biological and Biomedical Sciences, Emory University, Atlanta, GA 30322, USA.

[2]Division of Pulmonology, Allergy/Immunology, Cystic Fibrosis and Sleep, Department of Pediatrics, Emory University School of Medicine, Atlanta, GA 30322, USA.

[3]Emory Antibiotic Resistance Center, Atlanta, GA 30322, USA.

[4]Emory+Children's Center for Cystic Fibrosis and Airway Disease Research, Atlanta, GA 30322, USA.

Introduction

A species of significant medical importance, *Pseudomonas aeruginosa* is a gram-negative, metabolically flexible opportunistic pathogen. For people with the genetic condition cystic fibrosis, a positive respiratory culture for *P. aeruginosa* is correlated with an increased risk of death, decreased predicted forced expiratory volume in one second (FEV_1), and an increased risk of hospitalization for acute respiratory exasperations[1]. One weapon *P. aeruginosa* utilizes in infection of these patients, amongst many other types of infections, is an arsenal of proteases. Proteases are enzymes that hydrolyze peptide bonds within peptides and proteins[2]. In cystic fibrosis patients specifically, several proteases can be detected in the lung: elastase (LasB), alkaline protease, PasP, and protease IV[3]. Protease IV is important for many reasons, one of which is its ability to degrade surfactant proteins, which lowers the human surfactant host defense and propagates acute lung injury[4].

Protease IV is also known as PrpL for PvdS-regulated endoprotease, lysyl class[5] and is a 26 kDa serine protease that is secreted from *P. aeruginosa*[6]. The protein is initially translated as a single 48 kDa peptide which, based on its amino acid sequence, is suggested to be secreted through the type II secretion system. Following transport to the periplasm, the signal peptide at the N-terminus is cleaved to form a 45 kDa protein, with a second independent self-cleavage event occurring again at the N-terminus to form the mature 26 kDa protein[7] prior to release to the extracellular space. The cleaved propeptide released from the N-terminus during the second round of periplasmic processing stays non-covalently

associated with the mature PrpL until after extracellular secretion, presumably to inhibit activity while still inside the *P. aeruginosa* cell. This propeptide is later degraded by the quorum-sensing regulated protease LasB (elastase), which releases enzymatically active PrpL[7].

Regulation of the expression of the *prpL* gene is even more complex. *prpL* is thought to be regulated by the iron-dependent alternative sigma factor PvdS[5], and was shown to be strongly (~15-fold) increased in a PvdS-overexpression strain compared to a wild-type strain, but is 1.4-fold down-regulated with a non-significant *p*-value in a *pvdS*-deletion strain when compared to wild-type[8]. *prpL* is quorum sensing-regulated, with *prpL* transcription up-regulated in response to the two *P. aeruginosa* N-acyl-homoserine lactone quorum-sensing molecules[9-12], the signaling molecules for the Las and Rhl systems. While regulated by the Las or Rhl quorum sensing molecules, the upstream regulatory region of *prpL* is likely not directly bound by LasR[13]. *prpL* is 5-fold down-regulated in the absence of a transcriptional regulator, PA2449, which has a role in glycine metabolism and pyocyanin biosynthesis[14]. This may be direct regulation, or could alternatively be indirect through PA2449 impacting quorum-sensing pathways. Interestingly, *prpL* is also controlled by the histone-like nucleoid structuring proteins (H-NS) MvaT/MvaU, as evidenced by microarray of a wild-type vs *ΔmvaT* strain[15] and ChIP-on-chip to identify direct MvaT and MvaU binding targets[16]. MvaT and MvaU share little sequence similarity to the *E. coli* H-NS protein, yet are classified as *hns*-like proteins based on ability to functionally complement an *hns*-mutant strain of *E.*

coli[17]. Overall the known regulation of *prpL* is complex, with multiple distinct regulatory systems impacting transcription of this protease.

One layer of *prpL* regulation that has been observed, but for which the mechanism has not been elucidated, is the impact of temperature on transcription. Several studies investigating the global transcriptional changes of *P. aeruginosa* in response to a temperature shift of 22-25°C to 37°C have noted transcriptional up-regulation of *prpL* at the lower temperature by RNA-seq[18,19] and microarray[20]. Yet, the mechanism mediating this up-regulation remains a mystery. None of those regulatory factors listed above are themselves temperature responsive. Furthermore, the majority of genes in the regulons of these aforementioned regulators are not impacted by temperature[18], thus excluding these regulatory networks as the mechanism responsible for controlling *prpL* thermo-responsivity. Therefore we suggest that the temperature regulation of expression of *prpL* will be informative not only for this important virulence factor, but may also potentially shed light on a novel regulation pathway for other thermo-regulated genes important in infection.

Results

Steady-state *prpL* mRNA and PrpL protein are thermoregulated independently of PvdS.

prpL has previously been reported to be up-regulated in response to lower temperature[18-20]. However, there is currently no known mechanism mediating this effect. First I sought to establish thermoregulation under our standard laboratory conditions as a foundation for studying this system. To do so, I utilized RT-qPCR to compare mid-exponential steady-state levels of mRNA from PAO1 at 25°C and compared them to 37°C (**Figure 1A**). The results of this analysis demonstrate a ~10-fold up-regulation of steady-state transcript levels at 25°C compared to 37°C, in line with previous observations. Temperature changes lead to differences in growth rates and gene expression. Therefore as a control for all applicable studies, *rpoD* was chosen for its expression stability to ensure samples are appropriately matched[21]. When probed from the same samples analyzed above, *rpoD* showed no significant difference as expected (**Figure 1A**).

As *prpL* has been reported to be transcribed from a PvdS-dependent promoter[5], I next investigated this alternative sigma factor's involvement in thermoregulation of transcription. I performed the same RT-qPCR analysis of *prpL* and *rpoD,* this time from a PAO1 transposon mutant strain in which *pvdS* was disrupted (PW5085)[22], grown and collected in the same manner as the wild-type PAO1. Despite the absence of the only described sigma factor for this gene, *prpL* transcription was unaffected, implying the potential for a second sigma factor to be

driving transcription. Further, temperature regulation between the 25°C and 37°C samples was maintained (**Figure 1A**), indicating that temperature regulation is PvdS-independent.

The differences in steady-state levels of mRNA established above do not guarantee that protein output will different between our 25°C and 37°C-grown samples. To confirm that the differences observed in **Figure 1A** were reflected in secreted protein levels, and not just transcript levels, I performed Western immunoblotting from culture supernatants to assess levels of mature 26 kDa protein. Since PrpL is a secreted protease, supernatants from an equivalent number of cells were collected from wild-type PAO1 grown at 25°C and 37°C. These supernatants were concentrated 20-fold, then analyzed by Western immunoblotting with an antibody specific for PrpL (**Figure 1B**). This analysis revealed that protein levels were higher at 25°C than 37°C. Further accumulation of PrpL, but with a maintenance of temperature regulation, is additionally observed from overnight stationary samples. This indicates that thermoregulation is not just contained to mid-exponential phase, and that thermoregulation is likely not impacted by quorum regulation.

Temperature regulation of *prpL* is mediated from the upstream intergenic DNA.

prpL has a large, 534 bp intergenic region between the start codon of its coding sequence (CDS) and its closest upstream neighbor (PA4174). To begin to elucidate the mechanism conferring thermoregulation to steady-state mRNA levels

of *prpL,* I constructed a series of reporter fusions. These constructs seamlessly fuse *prpL* upstream DNA to a promoterless *lacZ,* and retain the original spacing of the promoter and ribosomal binding site to the ATG start codon. This construct was then inserted in the ectopic chromosomal CTX attachment site[23], where production and enzymatic activity of LacZ was used to measure relative promoter strength. The reporter strain with 500 bp of upstream DNA (representative of the entire intergenic region) showed a maintenance of 10x up-regulation at 25°C compared to 37°C (**Figure 2A**), indicating that the mechanism mediating transcriptional thermoregulation is contained in that intergenic region of DNA, but is not dependent on the greater chromosomal topographical context (i.e. upstream and downstream neighbors). This is important because *prpL* is regulated by MvaT and MvaU, which rely on DNA curvature for oligimerization on the target double-stranded DNA. 10-fold up-regulation of the promoter reporter is consistent with the 10-fold up-regulation in mRNA steady-state levels observed in **Figure 1A**, implying that thermoregulation of this chromosomal region can be studied outside of the larger chromosomal context.

When the 500 bp promoter fragment was cut down to just the 200 bp proximal to the CDS, thermoregulation was unaffected (**Figure 2A**), indicating that the entire intergenic region is not necessary for thermoregulation. An *rpoD* reporter, constructed in the same fashion as *prpL*, was utilized as a control. Additional *prpL* reporters were constructed which contained 96 bp down to 70 bp of upstream sequence; however, results of these studies were difficult to interpret as there was read-through transcription from an upstream CTX element promoting

LacZ production. The 500 bp and 200 bp reporters mentioned above were checked by 5'RACE, which confirmed that the only transcription of *lacZ* from these strains was from a native *prpL* promoter.

The results from these reporter fusions therefore indicate that our mechanism is contained to the 200 bp proximal to the start of the CDS, while the results from the RT-qPCR study indicate that transcription is PvdS-independent. Therefore, to investigate further the promoter driving transcription under my standard conditions, I performed 5'RACE with 25°C-harvested mRNA to determine the mRNA transcription start site (TSS). While several TSSs have been previously reported, a unique TSS under my test conditions may enable a prediction of the PvdS-independent promoter. These results of 5'RACE from 25°C-harvested mRNA (**Figure 2B**), however, show a TSS roughly consistent with one of the TSSs reported previously[18]. Of interest, though, were dual peaks underneath the assay-added poly-C tail. This "read-through" from the sequencing trace may indicate the presence of additional mRNA transcripts with a distal TSS (**Figure 3B**). This TSS2 prediction is less accurate than TSS1, as dual peaks underneath the prominent sequenced base has lower resolution; however, TSS2 appears to be congruent with an additional TSS prediction previously reported[5].

MvaT and MvaU are involved in thermoregulating *prpL*

5'RACE did not help elucidate the promoter and/or transcription factors driving transcription under our standard growth conditions due to the discovery of multiple transcription start sites in close proximity. As an alternative approach to

finding the thermoregulator, I performed a DNA pull-down assay using the proximal 200 bp sequence upstream from the *prpL* start codon as bait to isolate any proteins binding to this region of DNA. I incubated this biotinylated DNA bait with soluble proteins from PAO1 grown to mid-exponential phase at either 25°C or 37°C, then analyzed the results by Coomassie-staining elutions separated by SDS-PAGE. The results show the isolation of different proteins when the lysates were prepared from 25°C-grown cultures (blue arrows) compared to when the lysates were prepared from 37°C-grown cultures (red arrows; **Figure 3A**). Subsequent mass-spectrometry identification of these proteins (**Figure 3B**) revealed binding of two known transcriptional regulators, MvaT and MvaU. Other proteins identified were TopA, or DNA Topoisomerase; PA1348, a hypothetical protein with no known function or homologues; and keratin, which is human contamination presumably overwhelming the signal of the actual protein observed in **Figure 3A.** This contamination was most likely introduced during the mass spectrometry analysis, since the silver stain of pre-treated samples seen in **Figure 3A** shows a sharp band, while keratin contamination is typically more diffuse[24].

One limitation of DNA pull-down assays is that they will not be able to identify potential thermoreguatory elements that are not proteins, such as small RNAs; therefore, as a complementary approach, I simultaneously undertook a transposon mutagenesis approach to identify thermoregulatory factors of *prpL*. The same strain utilized in **Figure 2A** (PAO1, with 200 bp of *prpL* promoter seamlessly fused to *lacZ* and inserted at the CTX attachment site) was mutagenized with the mariner transposon contained on pSAM_DTc[25]. After plating on x-gal-containing

media, colonies were isolated which showed dysregulation of the normal color observed for the parental strain. These mutants were then mapped for their transposon insertions (**Figure 3C**). Most of the mutants identified were those containing alterations to the outer membrane (ex. GalU) or metabolism (ex. DavD, DavT), known caveats to this type of approach. LasR was identified as well; quorum-sensing is known to regulate *prpL*, but as shown in **Figure 1**, does not impact temperature regulation. Regardless, identification of a known regulator gave us confidence in these data. Lastly, as with **Figure 3B**, MvaT was identified as regulating *prpL.* While it has been previously reported that MvaT and MvaU bind upstream and regulate *prpL*[16]*,* it has not been previously uncovered to have an implication in the thermoregulatory phenotype of *prpL*.

To assess the involvement of MvaT and MvaU in thermoregulating *prpL*, I acquired a set of mutant strains in MvaT, MvaU, and a double mutant from the laboratory of Dr. Simon Dove[16]. The loss of both MvaT and MvaU is lethal; however, there is a wide option of suppressor mutations possible which will permit growth in the absence of these two proteins[26], an unknown combination of which allowed for the double mutant presented here to survive. These strains received the same reporter construct previously used, containing 200 bp upstream of *prpL* fused to *lacZ*, at the CTX attachment site. When assessed by β-galactosidase assay, the single MvaT or MvaU mutants showed the wild-type phenotype of ~10x up-regulation at 25°C, consistent with the known overlapping regulons of MvaT and MvaU[27]. However, when both proteins were deleted, ablation of temperature

responsivity was observed, strongly implicating MvaT and MvaU as being involved in the thermoregulatory scheme for *prpL*.

Discussion

PrpL is an important protease that can degrade a wide variety of substrates during infection. While recognized by multiple groups to be highly thermoregulated, the mechanism governing this temperature responsiveness has yet to be elucidated. Regulation of *prpL* is complex; yet, when these other regulatory mechanisms are disrupted, we still see a conservation of thermoregulation. For example, one system regulating *prpL* is the quorum-sensing system. The Western blot of mid-exponential vs stationary culture supernatants presented in **Figure 1B** clearly shows strong up-regulation at 25°C over 37°C, regardless of growth phase. Of note regarding **Figure 1B** is the ~17 kDa band observed underneath the mature PrpL protein. This band has been previously observed and is reported to share amino acid sequence to PrpL, appears after sample storage, and the presence of the band does not lead to a decrease in total protease activity[28]. This secondary band is most likely the propeptide of PrpL[7], which stays non-covalently associated with the mature protease until degradation by LasB, another quorum-regulated protease. Another known layer of *prpL* regulation is an iron-based response. The RT-qPCR presented in **Figure 1A,** however, shows no difference between wild-type PAO1 grown in a high-iron media (LB) vs a PAO1 transposon mutant in which the alternative sigma factor PvdS, a Fur-and iron-regulated sigma factor, is disrupted. Altogether these data imply that temperature is completely independent and unaffected by these two other layers of regulation.

The final additional layer of known *prpL* regulation is by *Pseudomonas hns*-like family members. H-NS family members are widely distributed amongst gram-

negative bacteria, and MvaT and MvaU are *P. aeruginosa* members of the *hns*-like family, despite sharing little sequence similarity to the *E. coli* H-NS. This layer of regulation does not appear to be independent of our temperature-regulated phenotype, as observed by the ablation of temperature responsivity in an *mvaT/mvaU* double mutant in **Figure 4.** This is interesting because H-NS is generally thought to repress at lower temperatures, while higher temperature can alleviate repression by H-NS. Not only is our observed thermoregulation in the opposite direction, but unlike H-NS, MvaT and MvaU generally thought to be insensitive to temperature. The lack of sequence similarity between H-NS and MvaU/T may explain why, despite performing the same DNA-binding function, H-NS is sensitive to temperature while MvaT is not intrinsically sensitive to temperature change[29].

If MvaT and MvaU alone were the sole themoregulatory element mediating our thermoresponsive phenotype, we would expect the entire regulon of MvaT and MvaU to be thermoregulated in the same manner as *prpL*. However, cross-referencing the list of MvaT and MvaU-regulated genes[16] with those temperature regulated in the same manner as *prpL*[18] produces very little overlap, suggesting that MvaT and MvaU alone cannot be directly responsible for the phenotype observed with *prpL*. While MvaT and MvaU are therefore not known to thermoregulate in this manner, other H-NS proteins have been investigated for this possibility. These proteins have been shown to have an accessory protein, or an anti-repressor, that alleviates repression by H-NS or *hns*-like proteins at the permissive temperature. We therefore hypothesize this may be the case for *prpL*

as well. To date I have tested several transcriptional regulators that are known to be themselves transcriptionally up-regulated at 25°C, the rationale being that an anti-repressor at 25°C would itself need to be more abundant at 25°C. I tested the four known transcriptional regulators identified through RNA-seq[20] to be 3.8-10.5x up-regulated at 25°C: PA0527, PA0535, PA3006, and PA3341. When assessed by β-galactosidase assay with my standard 200bp-promoter reporter, I saw no difference in thermoresponsivity. However, there are at least 16 other untested genes identified in the RNA-seq as being higher at 25°C that are either hypothetical/putative regulators or have a helix-turn-helix DNA binding motif (PA0200, PA1289, PA1404, PA1789, PA2143, PA2174, PA2190, PA2384, PA2485, PA2753, PA3572, PA3905, PA4139, PA4359, PA4577, PA4877).

This work to date has established the pervasiveness of *prpL* thermoregulation under a variety of conditions, and has implicated MvaT/U binding as a component of this thermoregulatory mechanism. Future work will focus on identifying the anti-repressor of MvaT/U at 25°C. A directed approach can be utilized, by leveraging tools and pipelines already in place, to continue screening the 16 regulators mentioned above as being up-regulated at 25°C. Additionally, the transposon mutagenesis discussed in **Figure 3C** can be modified to be higher-throughput. One limitation to the screen we used here is that the color dysregulation observed on x-gal was subtle and subjective. Since we now hypothesize that we are looking for an anti-repressor, transposon mutagenesis in our target gene will confer a constitutively repressed reporter. If we swap *lacZ* for *sacB* as our reporter, and plate on sucrose, we may be able to perform a high-

throughput screen to identify surviving mutants. Two copies of the *sacB* reporter will be necessary to prevent an overabundance of *sacB* transposon mutant colonies, but should colonies survive, this may make progress on identifying the anti-repressor. Alternatively, a tagged MvaT strain can be constructed (PAO1Δ*mvaT att*Tn7::*mvaT*-FLAG), grown at 25°C, and immunoprecipitated using an αFLAG antibody. This may reveal protein binding partners of MvaT, and therefore our anti-repressor. Each of these potential approaches have caveats and pitfalls; however, identifying our anti-repressor would represent a large step forward in understanding MvaT/MvaU function in *Pseudomonas.* Long-term goals would include performing RNA-seq on an anti-repressor mutant to identify all genes impacted by our newly characterized transcriptional regulator, thus revealing an entirely new regulon important in *Pseudomonas aeruginosa* virulence.

Material and Methods

Strains

P. aeruginosa PAO1 was utilized as a wild-type strain for all studies. PAO1 *pvdS*::tn is PW5085; lacZbp03q1H07 from the PAO1 transposon mutant library[22]. PAO1Δ*mvaT,* PAO1Δ*mvaU,* and PAO1 Δ*mvaU* Δ*mvaT* were a kind gift from Dr. Simon Dove[26].

RNA isolation and RT-qPCR

Cultures were incubated at 25°C or 37°C in Luria-Bertani broth (LB) with rotation until exponential phase of growth (OD_{600}=0.8). After harvesting, RNA was isolated with a MasterPure RNA Purification Kit (Epicentre) according to manufacturer's instructions. Residual contaminating DNA was removed with TURBO DNase (ThermoFisher). Purified isolated RNA was converted to cDNA with TaqMan Reverse Transription reagents (Invitrogen) with random hexamers and analyzed with FastStart Universal SYBR Green Master (Rox; Roche) on a Roche LightCycler 96. Primers utilized are as follows: *prpL* 5' GTCAACCGTCCCTACTGGAG 3' and 5' GAGTCGGCGAAATACGATACCT 3'; *omlA* 5' AAAATCGACATCCAGCAAGG 3' and 5' GGTCGCTGTCGTTGAAGAAC 3'; and *rpoD*[21] 5' GGG CGA AGA AGG AAA TGG TC 3' and 5' CAG GTG GCG TAG GTG GAG AA 3'. CT values were normalized to the internal control gene *omlA.* Significance was determined by two-way ANOVA with Sidak multiple comparisons analysis (GraphPad Prism version 6.0).

Cloning

Reporter strains were constructed through isothermal assembly of promoter fragments, a promoterless *lacZ* cassette, and miniCTX1[23]. Primers utilized to amplify P_{prpL} are as follows: TGGATCCCCCGGGCTGCAGGAGTAATGGTAAGCGGCCAGGGCTCTA for $P_{prpL(500bp)}$ and TGGATCCCCCGGGCTGCAGGTGGTAGAGAGAGCAATCCAACATCAAT for $P_{prpL(200bp)}$, both with reverse primer TCATGGTCATGAATCGACTCCTTCAGTTTTTTGGGA. Primers utilized for P_{rpoD} are as follows: TGGATCCCCCGGGCTGCAGGCCTTGAAAAGCAGTTCTTCGAC and TCATGGTCATAACACCCTATCCACTGAAGGT. Reporter constructs were confirmed through Sanger sequencing, then introduced into the appropriate strain background through electroporation and selection on LA+tetracycline 100 µg/mL. After selection for integrants, the tetracycline cassette was removed by electroporation with pFLP2[30] and counterselection on LA+10% sucrose prior to utilization. Final strains are designated PAO1 *att*CTX::$P_{prpL-500}$-*lacZ,* PAO1 *att*CTX::$P_{prpL-200}$-*lacZ*, and PAO1 *att*CTX::P_{rpoD}-*lacZ* respectively.

Western Immunoblotting

PAO1 wild-type was grown to mid-exponential phase or allowed to grow overnight at 25°C or 37°C in LB with rotation. A volume equivalent to 2 mLs of an OD_{600}=1 culture was collected and whole cells were spun out by centrifugation. Supernatants were then concentrated 20-fold to 50 µl in a 10k filter unit, mixed with 50 µl of 2x Laemmli buffer, boiled, and 20 µl was loaded in each lane of a 10% polyacrylamide gel. After separation by SDS-PAGE and transfer to PVDF, the

membrane was blocked with PBST+5% milk; incubated overnight at 4°C with αPrpL-1 (generated to AA117-130; a kind gift from Zhenyu Cheng[31]); and secondary antibody αRabbit IgG HRP before exposure with Pierce ECL substrate.

Beta-galactosidase Assays

Reporter strains were grown in LB at 25°C or 37°C to mid-exponential phase for collection. 1 mL of culture was centrifuged, media removed, and pellets were resuspended in 1 mL Z buffer (60 mM sodium phosphate dibasic, 40 mM sodium phosphate monobasic, 10 mM potassium chloride, 1 mM magnesium sulfate, 50 mM β-mercaptoethanol, pH 7.0). 200 µl of resuspended cells were added to 800 µl Z buffer, 100 µl chloroform, and 50 µl 0.1% SDS. Mixtures were vortexed and incubated at 30°C for 10 minutes. Reactions were started by addition of 200 µl of 4 mg/mL ortho-nitrophenyl-β-galactoside and timed until the development of a yellow color, at which point 400 µl of 1 M sodium carbonate was added to terminate the reaction. Cell debris was removed by centrifugation and the sample supernatant was read at 420 nm. Miller units were calculated as follows: $(1{,}000 \times A_{420}) / (\text{reaction time in minutes} \times \text{cell suspension volume in mL} \times OD_{600})$. Significance was determined by two-way ANOVA with Sidak multiple comparisons analysis (GraphPad Prism version 6.0).

5’ Rapid Amplification of cDNA Ends (5’RACE)

mRNA was isolated as described above from strain PAO1 grown at 25°C. 5’RACE was performed as per manufacturer’s instructions using the 5’RACE System for Rapid Amplification of cDNA Ends, version 2.0 (Thermo Fisher). Briefly mRNA was converted to cDNA using ThermoScript Reverse Transcriptase (Invitrogen) with

Gene Specific Primer 1 (GCGTTGGGGTTGGCGAAG) and the addition of betaine. Then the 3'end of the cDNA was tailed with a poly-C tail, and the resulting cDNA amplified with betaine using primer CCTGGAGCACGGCGACGT before Sanger sequencing for the junction between the 5'untranslated region (UTR) and the poly-C tail.

DNA Pull-Down

The general method used is as previously described[32]. Briefly, 60 ug of DNA probe was amplified using oligonucleotides [BIO]-TGGTAGAGAGAGCAATCCAACATCAAT and GAATCGACTCCTTCAGTTTTTTGGGA (Eurofins). PCR product was cleaned and concentrated using a DNA purification kit (NEB Monarch). PAO1 was grown to mid-log phase at either 25°C or 37°C with rotation, at which time cells were pelleted. Re-suspended pellets were sonicated to lyse the cells and centrifuged to collect soluble proteins. To prepare the magnetic beads (Invitrogen Dynabeads M280 Streptavidin), 200 µl of beads were transferred to a microcentrifuge tube, storage solution removed, and beads washed three times with assay buffer. Washed beads and DNA probe were co-incubated with rotation for 30 minutes two times to saturate beads, then probe-labeled beads were mixed with 375 µl of soluble lysate mixed with salmon sperm DNA as a non-specific competitor. After incubation beads were washed 5x and eluted with buffer containing 1 M sodium chloride. Samples were analyzed by Silver Staining.

Mass Spectrometry Identification, performed by Kendrick Labs, Inc.

Samples were lyophilized, re-dissolved in 20 µl SDS Sample Buffer, and heated in a dry bath at 95°C for 10 minutes prior to loading. SDS-PAGE was performed[33] using a 10% acrylamide slab gel (125 mm length x 150 mm width x 0.7 mm thickness) overlaid with a 25 mm stacking gel. Electrophoresis was performed using 15 mAmp/gel for about 3.5 hours at which time the bromophenol blue front had migrated to the end of the slab gel. The gel was stained with Coomassie blue, destained in 10% acetic acid until a clear background was obtained, then dried between cellophane sheets.

Gel bands of interest were extracted and washed in high purity, high performance liquid chromatography HPLC grade water, dehydrated, cut into small pieces, and destained by incubating in 50 mM ammonium bicarbonate, 50 mM ammonium bicarbonate/50% acetonitrile, and 100% acetonitrile under moderate shaking, followed by drying in a speed-vac concentrator. The gel bands were then rehydrated with 50 mM ammonium bicarbonate. This procedure was repeated twice. The gel bands were then rehydrated in 50 mM ammonium bicarbonate containing 10 mM DTT and incubated at 56°C for 45 minutes. The DTT solution was then replaced by 50 mM ammonium bicarbonate containing 100 mM Iodoacetamide for 45 minutes in the dark, with occasional vortexing. The gel pieces were then re-incubated in 50 mM ammonium bicarbonate/50% acetonitrile, and 100% acetonitrile under moderate shaking, followed by drying in speed-vac concentrator. The dry gel pieces were then rehydrated using 50 mM ammonium bicarbonate containing 10 ng/mL trypsin and incubated overnight at 37°C under low shaking. The resulting peptides were extracted twice with 5% formic acid/50

mM ammonium bicarbonate/50% acetonitrile and once with 100% acetonitrile under moderate shaking. Peptide mixture was then dried in a speed-vac, solubilized in 20 mL of 0.1% formic acid/2% acetonitrile.

The extracted peptide mixture was analyzed by reversed phase nanoliquid chromatography (LC) and MS (LC-MS/MS) using a NanoAcuity UPLC (Micromass/Waters, Milford, MA) coupled to a Q-TOF Xevo G2 mass spectrometer (Micromass/Waters, Milford, MA), according to published procedures[34]. Briefly, the peptides were loaded onto a 100 mm x 10 mm NanoAquity BEH130 C18 1.7 mm UPLC column (Waters, Milford, MA) and eluted over a 60 minute gradient of 2-80% organic solvent (ACN containing 0.1% FA) at a flow rate of 400 nL/min. The aqueous solvent was 0.1% FA in HPLC water. The column was coupled to a Picotip Emitter Silicatip nano-electrospray needle (New Objective, Woburn, MA). MS data acquisition involved survey MS scans and automatic data dependent analysis (DDA) of the top six ions with the highest intensity ions with the charge of 2+, 3+ or 4+ ions. The MS/MS was triggered when the MS signal intensity exceeded 250 counts/second. In survey MS scans, the three most intense peaks were selected for collision-induced dissociation (CID) and fragmented until the total MS/MS ion counts reached 10,000 or for up to 6 seconds each. Calibration was performed for both precursor and product ions using 1 pmol GluFib (Glu1-Fibrinopeptide B) standard peptide with the sequence EGVNDNEEGFFSAR and the monoisotopic doubly-charged peak with m/z of 785.84.

Transposon Mutagenesis

100 µl of overnight-cultured PAO1 *att*CTX::$P_{prpL(200bp)}$-*lacZ* was added to 100 µl overnight *E. coli* DH5α pSAM_DTc[25] and 800 µl warm LB. The sample was gently pelleted and washed with 1 mL warm LB, then repelleted and resuspended in 30 µl warm LB. The entire sample was spotted onto a warm LA plate and incubated at 37°C for 7 hours. After 7 hours, the entire bacterial spot was resuspended in 500 µl LB, then plated in 100 µl aliquots on LA containing spectinomycin 25 µg/mL, tetracycline 100 µg/mL, and x-gal 60 µg/mL. After incubation at the indicated temperature, colonies showing color dysregulation were isolated. To map transposon insertions, genomic DNA was prepared from candidate colonies, digested with SalI, and ligated into pUC19. Plasmids were transformed into DH5α and selected for those receiving the transposon by plating on tetracycline 10 µg/mL. Sanger-sequencing of the resulting plasmid from a primer specific for the transposon (GATGACGATGAGCGCATTGTTAGATTTCAT) was used to reveal the junction between the transposon sequence and the transposon-disrupted gene. Half of the mutants presented were mapped by Kathryn MacGillivray.

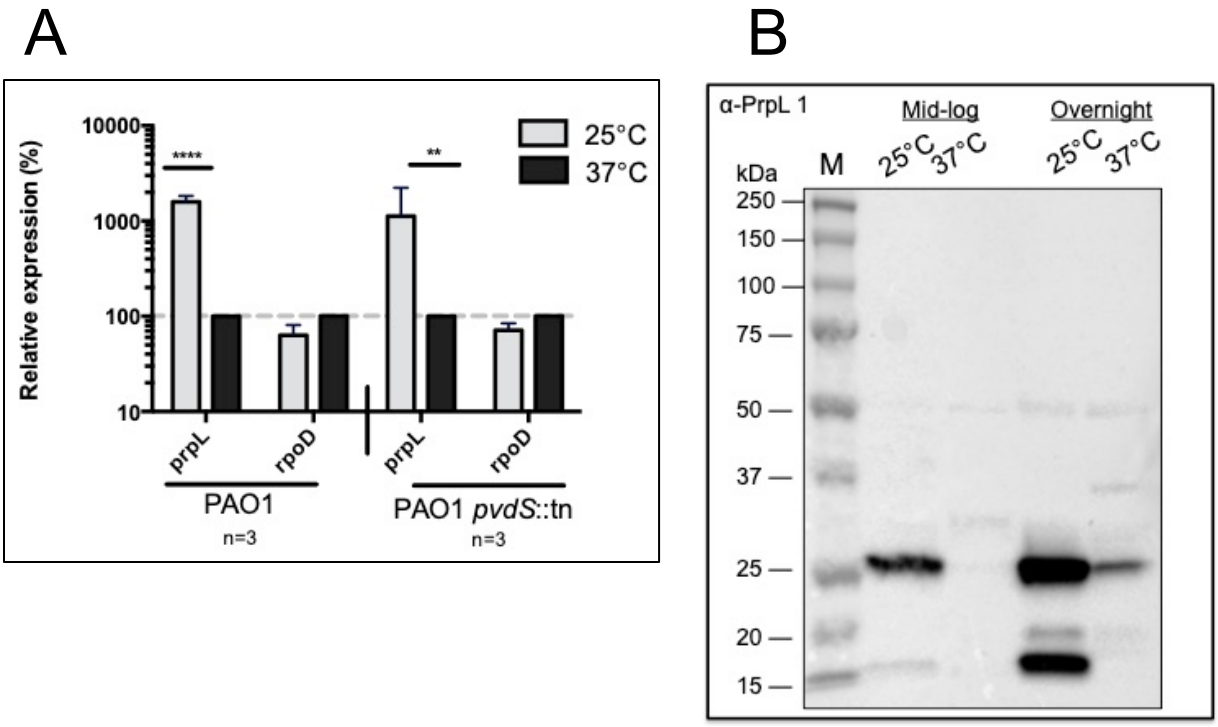

Figure 1: *prpL* is thermoregulated and independent of PvdS.

Panel A: RT-qPCR was utilized to assess steady-state mRNA levels from mid-exponential PAO1 or a PAO1 *pvdS* transposon mutant. CT values for *prpL* were first normalized to *omlA* as an internal control, then each temperature pair was compared by setting 37°C as 100%. *rpoD* was evaluated in the same manner as a control for no change in response to temperature. Error bars represent standard deviation of the mean. Significance was determined by two-way ANOVA with Sidak multiple comparisons analysis. N=3.

Panel B: Differences in transcript levels are manifested as differences in PrpL protein abundance in cell supernatants. PAO1 was grown to mid-exponential phase or overnight at 25°C or 37°C. A standardized cell number was collected and whole cells were spun out. Supernatants were then concentrated 20-fold to a standard volume in a 10k filter unit and 20 µl was loaded in each lane. After separation by SDS-PAGE, samples were blotted with an αPrpL antibody.

A

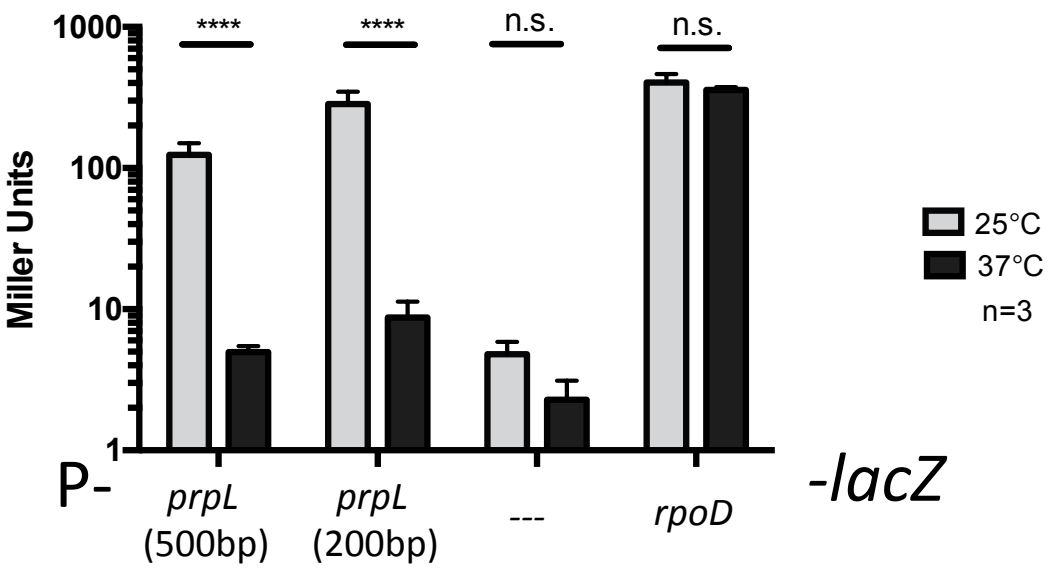
1000
100
10
1
Miller Units
****
****
n.s.
n.s.
25°C
37°C
n=3
P-
prpL
(500bp)
prpL
(200bp)
---
rpoD
-lacZ

B

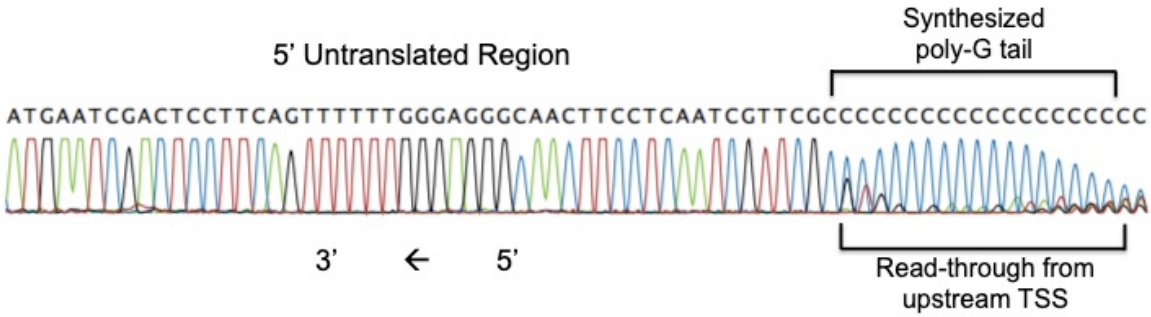
5' Untranslated Region
Synthesized
poly-G tail
ATGAATCGACTCCTTCAGTTTTTTGGGAGGGCAACTTCCTCAATCGTTCGCCCCCCCCCCCCCCCCCCC
3'
←
5'
Read-through from
upstream TSS

C


-200 bp (intergenic)
TGGTAGAGAGAGCAATCCAACATCAATGGCAAGTGAAGG
AAATAGCTATCTATTCTGCTATCCACAAACGCTTCTTCATATT
Predicted PvdS -35
TAATAGCTAGCAGAAACGAATATAAAAAATATTTGAACGACT
TSS 1&2
(Wilderman
et al.)
TSS 2
(Prezioso)
TSS 1
(Prezioso)
Predicted PvdS -10
CCGTCACACCTGCATATCTTTCGCCACGCGAACGATTGAG
5'URT (Wurtzel et al.)
GAAGTTGCCCTCCCAAAAAACTGAAGGAGTCGATTCATG
prpL

Figure 2: Temperature regulation of *prpL* is mediated from the upstream intergenic DNA.

Panel A: β-galactosidase assays establishing that temperature regulation is at the level of transcription initiation; the responsible element is within 200 nucleotides of the translation start codon. Nucleotide sequences of varying length were seamlessly fused to a promoterless *lacZ* gene with the *prpL* ATG start codon being the point of fusion. Constructs were integrated into the *P. aeruginosa* PAO1 genome at the CTX attachment site and extraneous sequence excised through FRT excision. Reporter strains were grown in LB to mid-log phase at either 25°C or 37°C and β-galactosidase assays were performed. A promoterless *lacZ* construct was included as a control for background transcription, and *rpoD* was included as a control for no temperature regulation. Error bars represent standard deviation of the mean. Significance was determined by two-way ANOVA with Sidak multiple comparisons analysis. N=3.

Panel B: 5'RACE of *prpL* on the PAO1 wild-type strain. mRNA was collected during mid-exponential growth in LB at 25°C. Samples were DNase treated, then mRNA was transcribed to cDNA using ThermoScript Reverse Transcriptase. 5'RACE was performed using ThermoFisher 5'RACE kit. Data was analyzed by Sanger Sequencing.

Panel C: Diagram of the 200 bp upstream from the ATG coding sequence start. Transcription Start Sites (TSS) observed from (B) are notated in black. TSSs observed by Wilderman *et al.*[5] are annotated in orange. The 5'Untranslated Region (5'UTR) observed by Wurtzel *et al*[18]*.* is written in pink. PvdS binding site in blue

was predicted based on consensus sequence presented by Swingle *et al*[35] and Schulz *et al*[8].

A

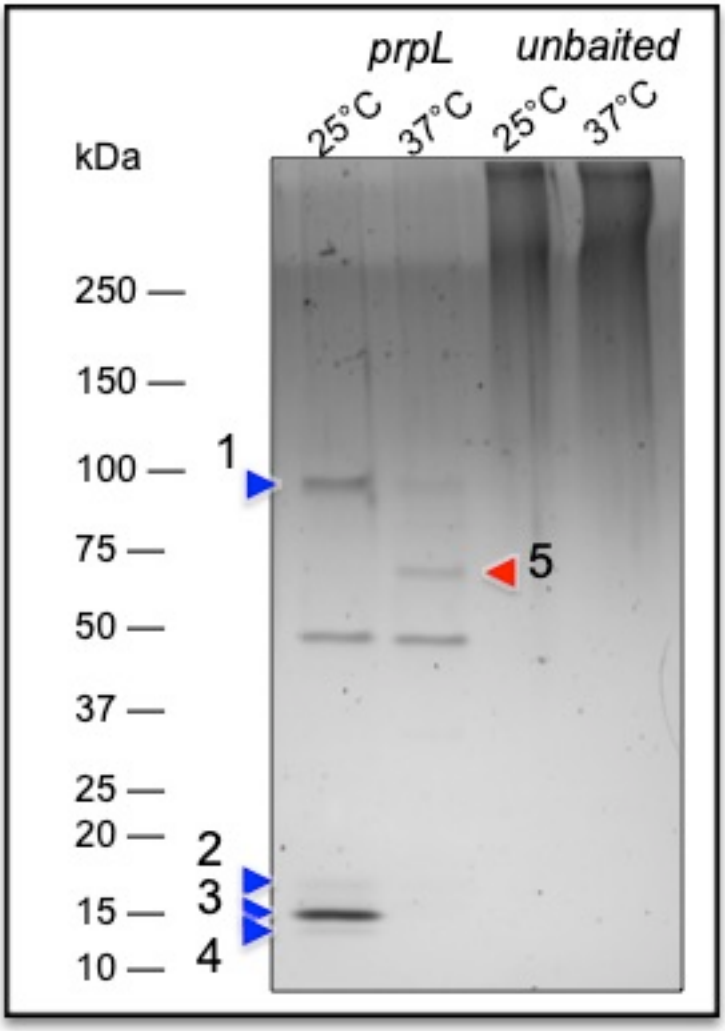

B

Band number	Lysate temperature	Protein size	Protein name	Locus	Gene function
1	25°C	98.3 kDa	TopA	PA3011	DNA Topoisomerase I
2	25°C	24.7 kDa	-	PA1348	hypothetical
3	25°C	14.2 kDa	MvaT, P16 subunit	PA4315	H-NS-like protein
4	25°C	13.4 kDa	MvaU	PA2667	H-NS-like protein
5	37°C	~65 kDa	Keratin	N/A	Contamination

C

Identity	Gene function	Condition IDed
GalU	LPS/Outer Membrane Integrity	Blue, 48 hrs at 37°C
MtnA	5-methylthioribose-1-phosphate isomerase	Blue, 48 hrs at 37°C
ShaA	Sodium/Ion Transport (cytoplasmic membrane)	Blue, 48 hrs at 37°C
ShaC	Sodium/Ion Transport (cytoplasmic membrane)	Blue, 48 hrs at 37°C
GalU	LPS/Outer Membrane Integrity	Blue, 48 hrs at 37°C
MvaT	**Histone-like structuring protein**	**Blue, 48 hrs at 37°C**
DavD	Redox, metabolism; aldehyde dehydrogenase	White, 48 hrs at 37°C
DavT	Redox, metabolism; aldehyde dehydrogenase	White, 48 hrs at 37°C
LasR	Quorum Sensing	White, 48 hrs at 37°C
DppB	Dipeptide ABC Transporter Permease	Lighter, 96 hrs at 25°C
YchF	Hypothetical (ATP/GTP binding protein?)	Lighter, 96 hrs at 25°C
DeaD	Probable ATP-Dependent RNA Helicase	Lighter, 96 hrs at 25°C

Figure 3: Confirmation that MvaT and MvaU bind *prpL* under our experimental conditions.

Panel A: DNA pull-down for transcription factors bound to *prpL*. The 200 nt upstream of the *prpL* ATG start codon was PCR amplified using a forward primer with biotin covalently attached at the 5' end. This DNA bait was co-incubated with the soluble fraction of PAO1 whole cell lysates collected after mid-exponential growth in LB at either 25°C or 37°C. Bound proteins were washed eight times and eluted with 1M NaCl. Eluted samples were buffer exchanged to remove salt and analyzed by separation on a 4-20% SDS-PAGE gel followed by silver staining. The four 25°C bands denoted by blue arrows, and the one 37°C band denoted by the red arrow, were extracted from a parallel coomassie-stained gel and analyzed by mass spectrometry for protein identification.

Panel B: Candidate bands were analyzed by mass spectrometry and mapped through comparison with the PAO1 genome sequence accessible at pseudomonas.com. Numbers correlate with arrow numbers denoted in Panel A. Panel C: Candidate proteins identified through transposon mutagenesis screen. The PAO1 *att*CTX::P_{prpL}-*lacZ* reporter strain was mutagenized and plated on x-gal-containing media to identify colonies dysregulated for color production in the manner indicated.

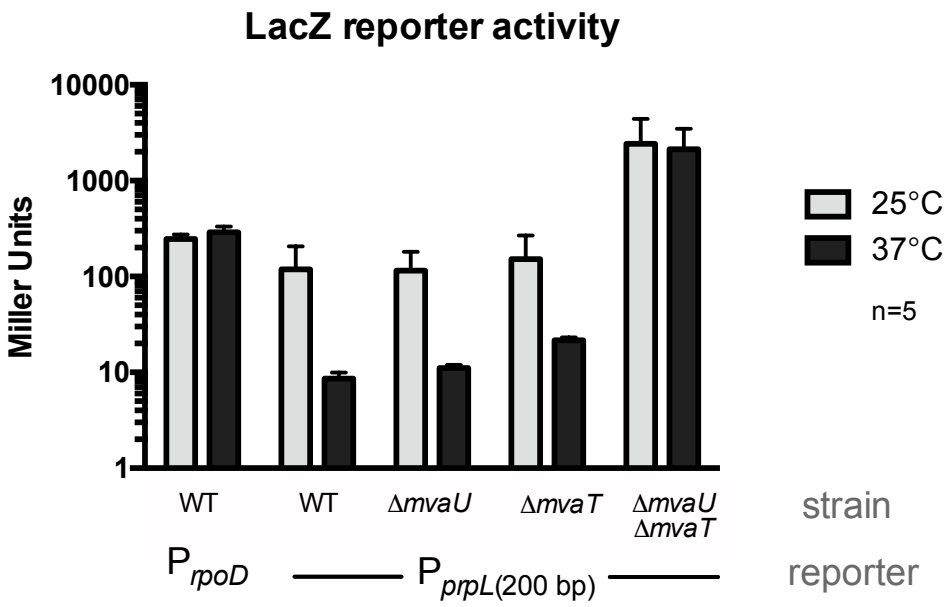

Figure 4: MvaT/U are involved in thermoregulating *prpL*.

β-galactosidase assay of a *prpL* reporter construct in various wild-type or deletion strains. Reporter strains were grown in LB to mid-log phase at either 25°C or 37°C and β-galactosidase assays were performed. *rpoD* was included as a control for no temperature regulation. N=5.

1 Emerson, J., Rosenfeld, M., McNamara, S., Ramsey, B. & Gibson, R. L. Pseudomonas aeruginosa and other predictors of mortality and morbidity in young children with cystic fibrosis. *Pediatr Pulmonol* **34**, 91-100, doi:10.1002/ppul.10127 (2002).

2 Lopez-Otin, C. & Bond, J. S. Proteases: multifunctional enzymes in life and disease. *J Biol Chem* **283**, 30433-30437, doi:10.1074/jbc.R800035200 (2008).

3 Upritchard, H. G., Cordwell, S. J. & Lamont, I. L. Immunoproteomics to examine cystic fibrosis host interactions with extracellular Pseudomonas aeruginosa proteins. *Infect Immun* **76**, 4624-4632, doi:10.1128/IAI.01707-07 (2008).

4 Malloy, J. L., Veldhuizen, R. A., Thibodeaux, B. A., O'Callaghan, R. J. & Wright, J. R. Pseudomonas aeruginosa protease IV degrades surfactant proteins and inhibits surfactant host defense and biophysical functions. *Am J Physiol Lung Cell Mol Physiol* **288**, L409-418, doi:10.1152/ajplung.00322.2004 (2005).

5 Wilderman, P. J. *et al.* Characterization of an endoprotease (PrpL) encoded by a PvdS-regulated gene in Pseudomonas aeruginosa. *Infect Immun* **69**, 5385-5394 (2001).

6 Elliott, S. *et al.* Isolation and characterization of the structural gene for secreted acid phosphatase from Schizosaccharomyces pombe. *J Biol Chem* **261**, 2936-2941 (1986).

7 Oh, J., Li, X. H., Kim, S. K. & Lee, J. H. Post-secretional activation of Protease IV by quorum sensing in Pseudomonas aeruginosa. *Sci Rep* **7**, 4416, doi:10.1038/s41598-017-03733-6 (2017).

8 Schulz, S. *et al.* Elucidation of sigma factor-associated networks in Pseudomonas aeruginosa reveals a modular architecture with limited and function-specific crosstalk. *PLoS Pathog* **11**, e1004744, doi:10.1371/journal.ppat.1004744 (2015).

9 Schuster, M., Lostroh, C. P., Ogi, T. & Greenberg, E. P. Identification, timing, and signal specificity of Pseudomonas aeruginosa quorum-controlled genes: a transcriptome analysis. *J Bacteriol* **185**, 2066-2079 (2003).

10 Arevalo-Ferro, C. *et al.* Identification of quorum-sensing regulated proteins in the opportunistic pathogen Pseudomonas aeruginosa by proteomics. *Environ Microbiol* **5**, 1350-1369 (2003).

11 Wagner, V. E., Bushnell, D., Passador, L., Brooks, A. I. & Iglewski, B. H. Microarray analysis of Pseudomonas aeruginosa quorum-sensing regulons: effects of growth phase and environment. *J Bacteriol* **185**, 2080-2095 (2003).

12 Conibear, T. C., Willcox, M. D., Flanagan, J. L. & Zhu, H. Characterization of protease IV expression in Pseudomonas aeruginosa clinical isolates. *Journal of medical microbiology* **61**, 180-190, doi:10.1099/jmm.0.034561-0 (2012).

13 Gilbert, K. B., Kim, T. H., Gupta, R., Greenberg, E. P. & Schuster, M. Global position analysis of the Pseudomonas aeruginosa quorum-sensing transcription factor LasR. *Mol Microbiol* **73**, 1072-1085, doi:10.1111/j.1365-2958.2009.06832.x (2009).

14 Lundgren, B. R. *et al.* Gene PA2449 is essential for glycine metabolism and pyocyanin biosynthesis in Pseudomonas aeruginosa PAO1. *J Bacteriol* **195**, 2087-2100, doi:10.1128/JB.02205-12 (2013).

15 Vallet, I. *et al.* Biofilm formation in Pseudomonas aeruginosa: fimbrial cup gene clusters are controlled by the transcriptional regulator MvaT. *J Bacteriol* **186**, 2880-2890 (2004).

16 Castang, S., McManus, H. R., Turner, K. H. & Dove, S. L. H-NS family members function coordinately in an opportunistic pathogen. *Proc Natl Acad Sci U S A* **105**, 18947-18952, doi:10.1073/pnas.0808215105 (2008).

17 Tendeng, C., Soutourina, O. A., Danchin, A. & Bertin, P. N. MvaT proteins in Pseudomonas spp.: a novel class of H-NS-like proteins. *Microbiology* **149**, 3047-3050, doi:10.1099/mic.0.C0125-0 (2003).

18 Wurtzel, O. *et al.* The single-nucleotide resolution transcriptome of Pseudomonas aeruginosa grown in body temperature. *PLoS Pathog* **8**, e1002945, doi:10.1371/journal.ppat.1002945 (2012).

19 Termine, E. & Michel, G. P. Transcriptome and secretome analyses of the adaptive response of Pseudomonas aeruginosa to suboptimal growth temperature. *Int Microbiol* **12**, 7-12 (2009).

20 Barbier, M. *et al.* From the environment to the host: re-wiring of the transcriptome of Pseudomonas aeruginosa from 22 degrees C to 37 degrees C. *PLoS One* **9**, e89941, doi:10.1371/journal.pone.0089941 (2014).

21 Savli, H. *et al.* Expression stability of six housekeeping genes: A proposal for resistance gene quantification studies of Pseudomonas aeruginosa by real-time quantitative RT-PCR. *J Med Microbiol* **52**, 403-408, doi:10.1099/jmm.0.05132-0 (2003).

22 Jacobs, M. A. *et al.* Comprehensive transposon mutant library of Pseudomonas aeruginosa. *Proc Natl Acad Sci U S A* **100**, 14339-14344, doi:10.1073/pnas.2036282100 (2003).

23 Hoang, T. T., Kutchma, A. J., Becher, A. & Schweizer, H. P. Integration-proficient plasmids for Pseudomonas aeruginosa: site-specific integration and use for engineering of reporter and expression strains. *Plasmid* **43**, 59-72, doi:10.1006/plas.1999.1441 (2000).

24 Ochs, D. Protein contaminants of sodium dodecyl sulfate-polyacrylamide gels. *Anal Biochem* **135**, 470-474 (1983).

25 Roux, D. *et al.* A putative lateral flagella of the cystic fibrosis pathogen Burkholderia dolosa regulates swimming motility and host cytokine production. *PLoS One* **13**, e0189810, doi:10.1371/journal.pone.0189810 (2018).

26 Castang, S. & Dove, S. L. Basis for the essentiality of H-NS family members in Pseudomonas aeruginosa. *J Bacteriol* **194**, 5101-5109, doi:10.1128/JB.00932-12 (2012).

27 Vallet-Gely, I., Donovan, K. E., Fang, R., Joung, J. K. & Dove, S. L. Repression of phase-variable cup gene expression by H-NS-like proteins in Pseudomonas aeruginosa. *Proc Natl Acad Sci U S A* **102**, 11082-11087, doi:10.1073/pnas.0502663102 (2005).

28 Engel, L. S., Hill, J. M., Caballero, A. R., Green, L. C. & O'Callaghan, R. J. Protease IV, a unique extracellular protease and virulence factor from Pseudomonas aeruginosa. *J Biol Chem* **273**, 16792-16797 (1998).

29 Winardhi, R. S. *et al.* Higher order oligomerization is required for H-NS family member MvaT to form gene-silencing nucleoprotein filament. *Nucleic Acids Res* **40**, 8942-8952, doi:10.1093/nar/gks669 (2012).

30 Hoang, T. T., Karkhoff-Schweizer, R. R., Kutchma, A. J. & Schweizer, H. P. A broad-host-range Flp-FRT recombination system for site-specific excision of chromosomally-located DNA sequences: application for isolation of unmarked Pseudomonas aeruginosa mutants. *Gene* **212**, 77-86 (1998).

31 Cheng, Z. *et al.* Pathogen-secreted proteases activate a novel plant immune pathway. *Nature* **521**, 213-216, doi:10.1038/nature14243 (2015).

32 Jutras, B. L., Verma, A. & Stevenson, B. Identification of novel DNA-binding proteins using DNA-affinity chromatography/pull down. *Curr Protoc Microbiol* **Chapter 1**, Unit1F 1, doi:10.1002/9780471729259.mc01f01s24 (2012).

33 Burgess-Cassler, A., Johansen, J. J., Santek, D. A., Ide, J. R. & Kendrick, N. C. Computerized quantitative analysis of coomassie-blue-stained serum proteins separated by two-dimensional electrophoresis. *Clin Chem* **35**, 2297-2304 (1989).

34 Darie, C. C. *et al.* Identifying transient protein-protein interactions in EphB2 signaling by blue native PAGE and mass spectrometry. *Proteomics* **11**, 4514-4528, doi:10.1002/pmic.201000819 (2011).

35 Swingle, B. *et al.* Characterization of the PvdS-regulated promoter motif in Pseudomonas syringae pv. tomato DC3000 reveals regulon members and insights regarding PvdS function in other pseudomonads. *Mol Microbiol* **68**, 871-889, doi:10.1111/j.1365-2958.2008.06209.x (2008).

Future Directions for studies of EftM and PrpL

Samantha M. Prezioso, Joanna B. Goldberg

EftM and PrpL are two *Pseudomonas aeruginosa* virulence factors in close chromosomal proximity (PA4178 and PA4175, respectively). Both are thermoregulated in a pattern typically not observed for virulence factors, with greater protein abundance at 25°C compared to 37°C. EftM is dual thermoregulated at both the transcriptional and post-translational level. *prpL,* on the other hand, is not post-translationally thermoregulated but has complex transcriptional regulation, one aspect of which is controlled by temperature. From the studies presented here, several key questions have emerged.

Paramount is understanding the full mechanism by which transcriptional thermoregulation is achieved. Progress has been made on uncovering the factors regulating EftM. Rigorous biochemical characterization using circular dichroism (CD) and differential scanning fluorimetry (DSF) has revealed a low melting temperature (T_m) of just 37°C for EftM[1], which largely accounts for the high levels of EF-Tu methylation observed at 25°C and low levels observed at 37°C. Preliminary studies leveraging a series of PAO1 and PAHM4 promoter/coding sequence chimeric complementation strains (not shown) has hinted that protein stability is a larger contributor to overall thermoregulation than the second, dual layer of thermoregulation also observed in the mRNA steady-state levels. However, transcriptional thermoregulation is still a contributing factor to the observed phenotype. Therefore this mechanism is important to elucidate, especially given that transcriptional thermoregulation appears to not be linked to protein thermoregulation (See **Chapter III, Figure 1**).

The data presented in **Chapter III** implies that this thermoregulation occurs during transcription initiation. Given the inherently low levels of *eftM* transcript (around the order of one copy of *eftM* per 100 of the housekeeping gene *omlA* at 37°C), this has proven difficult to study. Attempts at transposon mutagenesis of P_{eftM}-*lacZ* reporter strains to identify color-dysregulated mutants on x-gal were unsuccessful; transcription of *eftM* is not high enough to produce a blue pigment at 25°C. I then replaced the ribosome binding site of the native *eftM* promoter sequence with an optimized ribosome binding site, which increased reporter production but decreased the temperature response differential, thus mitigating the benefit to this construct. Future investigations into the transcriptional thermoregulator of *eftM* should be carefully designed. One option is to perform the same DNA-pull down assay presented in Chapter V, but with the *eftM* promoter sequence replacing *prpL*. This may identify protein regulators without the subjective nature of picking colonies in a transposon mutagenesis screen. If this were to be undertaken, however, we could speculate that the ratio of DNA-to-lysate would need to be optimized such that large amounts of lysate are allowed to bind *eftM*. Given the lowly expressed nature of *eftM*, it would stand to reason that transcription from this promoter is an infrequent event; subsequently, the levels of proteins mediating this transcription could be themselves lowly expressed. An interesting note regarding the *eftM* promoter is that the native *eftM* promoter does not function in *E. coli*. While EftM can be actively expressed in *E. coli*, and trimethylate endogenous *E. coli* EF-Tu, it can only do so if it is expressed from a non-native promoter (data not shown). This

implies that the sigma factor or a transcriptional activator of *eftM* is not universally conserved, and may help narrow down candidates.

An alternative approach to a DNA pull-down could be to continue studying the upstream region using the β-galactosidase pipeline in place. The smallest fragment studied to date has been 99 nucleotides of *eftM* upstream region. By creating successive truncations from the 5' end, a minimum sequence could be revealed which allows for transcription but ablates thermoregulation. This sequence could then be used to predict binding motifs, therefore leading to the regulatory element. Lastly, the thermoregulatory element moderating *eftM* could be a small RNA. To date, little has been studied regarding this possibility. However, emerging global sRNA studies could be analyzed to produce lists of candidates for directed testing.

Then again, even more unconventional work-arounds might need to be undertaken for *eftM*. For example, it could be worth investigating the expression of *eftM* in *Pseudomonas putida.* In contrast to PAO1, where the optimal growth temperature is 37°C, 30°C is the optimal growth temperature for *P. putida*[2]. *P. putida* does not appear to have an otholog of *eftM*, but presumably could still have many of the same transcription factors found in PAO1. These factors may be even more abundant in *P. putida* owing to its optimization for growth at lower temperature. Therefore, conducting studies of *eftM* in this strain may produce exaggerated phenotypes, and consequently enable a more easily discernable impact of a transposon mutagenesis screen. Overall, the inherently low levels of *eftM* create an exceptionally challenging problem for studying *eftM*

thermoregulation. Global assays such as ChIP-seq or microarrays cannot be reliably utilized, as *eftM* tends to fall below the limit of detection for these assays. The only option for studying *eftM* thermoregulation is therefore directed approaches such as those outlined above.

Future studies investigating the thermoregulation of *prpL* may be more straight-forward. Current work strongly implies that MvaT and MvaU are functioning as repressors of *prpL*, and an unknown anti-repressor is alleviating repression at 25°C. MvaT and MvaU are similar to H-NS. H-NS functions almost universally as a repressor, and has many affiliated anti-repressor proteins that modulate its gene regulatory effect. One intriguing example is the anti-repressor SlyA from *S. typhimurium* and *E. coli*. SlyA can displace H-NS from DNA, but H-NS can in turn displace SlyA when the relative abundance of the two favors H-NS[3]. While *P. aeruginosa* does not have SlyA, there is a probable transcriptional regulator in the genome (PA3341) that shares 40% identity at the N-terminus. Excitingly, PA3341 is also 4.3x transcriptionally up-regulated at 25°C compared to 37°C. This increased abundance at 25°C, combined with homology to a known H-NS-interacting protein, made PA3341 a prime candidate as the *prpL* thermoregulator. I tested this hypothesis by creating a clean deletion of PA3341 and assessing *prpL* activity by β-galactosidase assay, with the hypothesis being that deletion of an H-NH anti-repressor would lower 25°C *prpL* expression to that seen for 37°C. Unfortunately the PA3341 deletion showed no alteration in *prpL* transcriptional transcription, implying that this is not the thermoregulator for *prpL*. As mentioned earlier, though, there are 16 other putative or hypothetical DNA

binding proteins that are up-regulated at 25°C (PA0200, PA1289, PA1404, PA1789, PA2143, PA2174, PA2190, PA2384, PA2485, PA2753, PA3572, PA3905, PA4139, PA4359, PA4577, PA4877). With transposon mutants of most of these readily available, and a pipeline in place to measure *prpL* thermoregulation by β-galactosidase assay, these could easily be tested as our candidate anti-repressors.

Alternatively, the *prpL* MvaT/U anti-repressor does not itself need to show higher steady-state levels at 25°C. Temperature could simply be altering the secondary structure of a steadily-expressed pool of anti-repressor protein such that the anti-repressor is no longer able to engage MvaT and/or MvaU at 37°C. To this end, an interesting study to identify binding proteins of MvaT/U would be to immunoprecipitate MvaT. Chromatin immunoprecipitations have been undertaken with MvaT to identify target DNA binding regions[4]; however, to the best of my knowledge, no one has immunoprecipitated the MvaT protein to elucidate protein binding partners. When performed at 25°C, the temperature at which our presumptive anti-regulator engages MvaT, we may be able to isolate and identify this protein. Presumably other proteins beyond our target thermo-antirepressor would be pulled out. MvaU is known to multimerize with MvaT, and would serve as a positive control. Other anti-regulators identified, even if they are not our target anti-repressor, could further the general field of knowledge regarding MvaT/U.

Ultimately once our transcriptional thermoregulator is identified, a clean deletion mutant should be constructed. This mutant could be analyzed by RNA-

seq and compared to the parental wild-type to reveal additional members of the protein's regulon. These studies could reveal an entirely new *P. aeruginosa* thermoregulatory network mediating increased gene expression at 25°C, and will have important implications for the field of *P. aeruginosa* virulence and gene regulation. Should this target regulator never be identified, however, PA3341 could be characterized instead. Little is currently known about this regulator. We know that it is expressed at higher levels at lower temperature[5]. Additionally, the strain deleted for PA3341 appears to have a slight growth defect that preliminarily appears to be exacerbated at 25°C compared to 37°C. It would be interesting to elucidate the effect PA3341 has on transcriptional thermoregulation in *P. aeruginosa.*

Several of the studies presented in this work raise interesting questions about EftM beyond thermoregulation mechanisms. One is the greater physiological relevance of thermoregulating EftM in the first place. The serum sensitivity data presented in **Chapter IV** may begin to hint at this. EftM catalyzes a post-translational modification that mimics phosphorylcholine, which like phosphorylcholine, then increases binding to platelet activating factor receptor through molecular mimicry of platelet activating factor. The downside to phosphorylcholine surface decoration, however, is that phosphorylcholine also increases recruitment of C-reactive protein to the bacterial surface, which enhances complement-mediated killing. It will be informative to fully study serum sensitivity of *eftM* mutants, regardless of result discovered. If K5me^3 enhances complement-mediated clearance the way phosphorylcholine does, then this hints

at the significance of EftM being thermoregulated (e.g. the modification is seen during the initial stages of infection and help initial attachment, but is removed during longer or chronic infection to avoid immune effectors). Alternatively, if K5me^3 does not enhance complement-mediated killing, then an improvement of EftM over phosphorylcholine incorporation will have been revealed. Ultimately, it is exceptionally curious that an enzyme that is produced in such low levels is subjected to multiple layers of thermoregulation. It is tempting to conclude from this that there is a detriment to expressing EftM at elevated temperatures, and would greatly benefit our knowledge of EftM to elucidate this reason.

Alternatively it is possible that there is no detriment to EftM at 37°C, and only a benefit at 25°C. Therefore an additional area warranting further investigation is in alternative model systems to mammals. It is interesting that the N-terminus of EF-Tu is recognized as a PAMP in *Arabidopsis*[6], which could lead to speculation that K5me^3 blocks recognition, especially given the clear data demonstrating that K5me^3 minimizes αPilT cross-reaction with EF-Tu (**Chapter IV**). Future work carefully infecting 25°C-grown PAO1 and the newly constructed isogenic mutants (**Chapter IV**) into *Arapidopsis* could reveal an additional benefit to EftM.

One last hypothesis to the benefit of EftM has emerged during the course of my studies. Personal observations with purified, methylated EF-Tu compared to unmethylated EF-Tu have produced some speculative but intriguing theories. First, long-term storage of a batch of purified, unmethylated EF-Tu at -20°C resulted in selective loss of the first ~10 amino acids of EF-Tu. This corresponds

to the disordered N-terminus within which lysine 5 is contained. A parallel batch of methylated EF-Tu, stored in the same fashion, did not show degradation of the N-terminus. Both proteins appear to be relatively the same size when visualized by Coomassie staining, and both have intact C-termini when analyzed for the C-terminal his-tag. However, just the N-terminus was lost in the unmethylated EF-Tu. While subtle, we may be able to see this in a second, independent batch of purified EF-Tu as well: In **Chapter IV, Figure 12,** the αEF-Tu blot shows slightly higher levels of reactivity of methylated EF-Tu compared to unmethylated EF-Tu. The EF-Tu antibody's epitope is SKEKFE, corresponding to AA 3-7 in *P. aeruginosa*. Since this antibody was raised to *E. coli* EF-Tu, which is unmethylated, I typically observe slightly stronger reactivity of this antibody to fresh PAO1Δ*eftM* lysates compared to strains containing EftM; presumably EftM-catalyzed trimethylation of EF-Tu slightly impairs antibody recognition. Given this information, it is therefore even more striking that the αEF-Tu antibody is reacting stronger with the methylated purified EF-Tu in this Western blot. It is therefore tempting to speculate that methylation at the N-terminus helps preserve and protect the first few amino acids of EF-Tu, especially when EF-Tu is subjected to purification and/or long-term storage. Additional anecdotal evidence includes that after performing several rounds of EF-Tu protein purifications, I see slightly higher yields of methylated EF-Tu compared to the unmethylated EF-Tu for the same protocol. This is not drastic, and may be just a coincidence. However, given the known ability of methylation to impact protein stability, this is an aspect of EftM physiology that should be further investigated.

Temperature regulation is well recognized to be important in bacterial physiology. *P. aeruginosa* has a relatively large genome, and sensing local temperature allows for the customizing or fine-tuning of the expression of a subset of proteins which maximize their likelihood of success in their new environment. Temperature regulating a subset of genes may avoid wasteful expenditure of cellular resources, help avoid detection by immune molecules, and can maximize of colonization factors. However, studies of temperature regulation tend to focus on up-regulation of genes at 37°C, upon entry to the host. It is critical to also study the inverse, where factors are down-regulated upon entry. By studying thermoregulation of *eftM* and *prpL*, two *P. aeruginosa* proteins regulated in this manner, we create a better understanding of the utilization of these factors during infection. Further, knowledge of the mechanisms utilized by these genes may be applied to the study of other *P. aeruginosa* genes, which will in turn create an overall better understanding of the infection progression of this important and deadly opportunistic pathogen.

1 Owings, J. P. *et al.* Pseudomonas aeruginosa EftM Is a Thermoregulated Methyltransferase. *J Biol Chem* **291**, 3280-3290, doi:10.1074/jbc.M115.706853 (2016).

2 Fonseca, P., Moreno, R. & Rojo, F. Pseudomonas putida growing at low temperature shows increased levels of CrcZ and CrcY sRNAs, leading to reduced Crc-dependent catabolite repression. *Environ Microbiol* **15**, 24-35, doi:10.1111/j.1462-2920.2012.02708.x (2013).

3 Stoebel, D. M., Free, A. & Dorman, C. J. Anti-silencing: overcoming H-NS-mediated repression of transcription in Gram-negative enteric bacteria. *Microbiology* **154**, 2533-2545, doi:10.1099/mic.0.2008/020693-0 (2008).

4 Castang, S., McManus, H. R., Turner, K. H. & Dove, S. L. H-NS family members function coordinately in an opportunistic pathogen. *Proc Natl Acad Sci U S A* **105**, 18947-18952, doi:10.1073/pnas.0808215105 (2008).

5 Barbier, M. *et al.* From the environment to the host: re-wiring of the transcriptome of Pseudomonas aeruginosa from 22 degrees C to 37 degrees C. *PLoS One* **9**, e89941, doi:10.1371/journal.pone.0089941 (2014).

6 Kunze, G. *et al.* The N terminus of bacterial elongation factor Tu elicits innate immunity in Arabidopsis plants. *Plant Cell* **16**, 3496-3507, doi:10.1105/tpc.104.026765 (2004).